THESIS

DETERMINING THE IMPACT OF VOLCANIC ERUPTION ON THE DISCHARGE USING HYDROLOGICAL MODEL

Case in Code Watershed, Yogyakarta Special Province, Indonesia

Thesis submitted to the Double Degree M.Sc. Program,
Universitas Gadjah Mada and Faculty of Geo-Information Science and Earth Observation,
University of Twente in partial fulfillment of the requirement for the degree of Master of
Science in Geo-Information for Spatial Planning and Risk Management

UGM

ITC

By:
AGUS YASIN
UGM : 10/307092/PMU/06737
ITC : 027674

Supervisor :
Dr. M. PRAMONO HADI, M.Sc. (UGM)
Dr. M.W. (MENNO) STRAATSMA, (ITC)

DOUBLE DEGREE M.Sc. PROGRAMME
UNIVERSITAS GADJAH MADA
FACULTY OF GEO-INFORMATION AND EARTH OBSERVATION
UNIVERSITY OF TWENTE
2012

THESIS

DETERMINING THE IMPACT OF VOLCANIC ERUPTION ON THE DISCHARGE USING HYDROLOGICAL MODEL
Case in Code Watershed, Yogyakarta Special Province, Indonesia

Prepared by
AGUS YASIN
UGM : 10/307092/PMU/06737
ITC : 027674

was defended before the Board of Examiner
on the date 6th March 2012

Board of Examiners

Supervisor 1	ITC Examiner
Dr. M. Pramono Hadi, M.Sc.	Dr. M. (Mark) van der Meijde
Supervisor 2	External Examiner
Dr. M.W. (Menno) Straatsma	Prof. Dr. H.A. Sudibyakto, M.S.

This thesis was declared acceptable
to obtain the master degree
Date ....

Program Director of Geo-Information for
Spatial Planning and Risk Management

Prof. Dr. H.A. Sudibyakto, M.S.
NIP. 19560805 198303 1 004

Approved by
Vice Director for Academic Affairs,
Development and Cooperation

Prof. Ir. Suryo Purwono, MA.Sc., Ph.D.
NIP. 19611119 198601 1 001

Disclaimer

This document describes work undertaken as part of a program of study at the Double Degree International Program of Geo-information for Spatial Planning and Risk Management and Earth Observation, University of Twente, The Netherlands, and Universitas Gadjah Mada, Indonesia. All views and opinions expressed therein remain the sole responsibility of the author, and do not necessarily represent those of the institute.

Abstract

After Merapi eruption (October – December 2010), several conditions change as consequence of the eruption. This research analyzed the hydrologic change of the Code watershed (30 km^2) in north Yogyakarta. Therefore this research developed a hydrologic model for the watershed by means of available data and hydrological equations to predict the discharge and further simulate the extreme rainfall event to predict flood in Code river.

The research concluded that the changes related to hydrological process in Code watershed due to the eruption is mainly affected the soil. The change includes: sand fraction increased on soil texture composition, additional ash deposition of 32-41 mm on soil depth, and decreased of infiltration rates. Related with the model, statistically it has high error and low correlation of 0.46 and 0.22 for pre and post eruption model respectively. The model simulated that soil depth has the most sensitive to the discharge. It performs positive response while the other parameters tested, Ksat, porosity and maximum storage gives negative response to the discharge. In addition, the amount of discharge in the model is lower than the amount in measured discharge for the pre eruption model. Meanwhile, the post eruption model performs higher than the measured discharge.

Predicted discharge based on extreme rainfall event on 5, 20, 50 and 100 year periods gives the amount of discharge in a day reaching 2,171,967 m3/day, 2,969,264 m3/day, and 3,515,760 m3/day respectively. About 19, 29, 35 and 37 of 50 sections of Code river were prone to flood when 5, 20, 50 and 100 year extreme rainfall event occurs respectively. Sub disctrics that prone to flood are Jetis, Gondokusuman, Gedong tengah and Mergangsan.

Key words: **hydrologic model, Merapi eruption, flood, Code watershed**

Acknowledgements

Alhamdulillah, I humbly thank to Allah SWT for being so merciful in the phase of my life spend at UGM and ITC.

I express my gratitude to UGM and ITC for allowing me to take up the M.Sc course. Thanks to Pusbindiklatren Bappenas and NESO for providing financial support to compete the M.Sc course. I am also thankful to Ministry of Forestry especially BKSDA Aceh for the opportunity to pursue the M.Sc course.

I would like to thank Rector UGM, Director of Graduate School UGM, Program Director of Geo-info and its all staffs which provided me with such a wide scientific environment where I learnt a lot.

I wish to express my sincere thanks and appreciation to my UGM supervisor, Dr. Pramono Hadi. His valuable feedback, guidance and constant support received throughout the research have immensely helped me in successful completion of the research. My foremost thank goes to my ITC supervisor, Dr. Menno Straatsma for consistence support and encouragement through comment, email, and skype meeting. His in-depth knowledge in the hydrologic model has complimented the work done in this thesis.

Words are not enough to express my sincere gratitude and utmost respect to all my friends of Batch VI for the time spent with at Room 210, Geography Lab, ITC Hotel and Ayodhya. Thank you for a pleasant environment to study and the great moments lived together.

I am grateful to my parents and family for their support and care. Lastly, my special thanks to my wife Asri Puspitasari and my beloved princess Ayyilaisha Dizlila, whose motivated me to successfully complete this project.

Table of Contents

List of Figures

List of Tables

List of Graphs

List of Appendixs

List of Abbreviations

ABSCAN	Automated Baseflow Separation for Canadian datasets
ASL	Average Mean Sea Level
AWLR	Automatic Water Level Recorder
BPSDA POO	(Bureau of Water Resources Management Progo Opak Oyo)
BMKG	Badan Meteorologi, Klimatologi dan Geofisika (Bureau of Meteorology, Climatology and Geophysics)
BAPPEDA	Badan Perencanaan Pembangunan Daerah (Bureau of Regional Development)
BPTP	Balai Penelitian Teknologi Pertanian (Bureau of Agriculture Technology)
EUROSEM	European Soil Erosion Model
FAO	Food Agricultural Organization
GIS	Geographic Information System
Ksat	Saturated Hydraulic Conductivity
LAI	Leaf Area Index
LDD	Local Drainage Direction
LISEM	Limburg Soil Erosion Model
MAE	Mean Absolute Error
MA%E	Mean Absolute Percentage Error
NRCS	Natural Resources Conservation Service
PVMBG	Pusat Vulkanologi dan Mitigasi Bencana Geologi (Center of Vulcanology and Geology Disaster Mitigation)
RMSE	Root Mean Square Error
SPOT	Satellite Pour l'Observation de la Terre
SPSS	Statistical Product and Service Solutions
SWAT	Soil and Water Assessment Tool
SWC	Soil Water Characteristics
USDA	United States Department of Agriculture
USGS	United States Geological Survey
VEI	Volcanic Explosivity Index
WMO	World Meteorological Organization
WOFOST	World Food Studies

1. INTRODUCTION

The Indonesian archipelago is dotted with volcanoes (Gertisser, 2011). Charbonnier (2011) described that about 60 % of Indonesians live around 16 active volcanoes on the island of Java. There are 129 volcanoes on Java, Indonesia and one of the most active of these is Gunung Merapi ('The Fire Mountain'). The Merapi volcano (2,968m) is situated on the administrative boundary between Central Java and Yogyakarta Province. Merapi, ranks second after Semeru as the most active volcano of Indonesia and also second after Kelud in surface area at risk. The distribution of volcano in Indonesia is figured below (Figure 1-1).

Figure 1-1. Major volcanoes of Indonesia with eruptions since 1900 A.D. (USGS, 2001)

Deegan (2011) stated that Merapi is one of the most active volcanoes in Java, and represents a serious hazard by being located less than 30 km from Yogyakarta, a city with population of about 3,5 million. In addition, Boundan *et al*. (1992) stated that in historic times, small eruptions occur every 2-3 years, larger ones every 9-12 years, whereas major eruptions average 50 to 60 years interval.

Events like volcanic eruptions challenge equilibrium models of nature (Dove, 2008). According to USGS, types of volcano hazards are: volcanic gases, lahars, pyroclastic flows, lava flows, tephra (volcanic ashes), air pollution, and volcanic landslide. In term of hydrolog 1 d watershed, those hazards give any damaging impacts to the hydrological process.

Pyroclastic flows, lava flows and also gases could damage the vegetation in its surrounding. Volcanic ashes and volcanic landslide would impact soil layer while lahars give sedimentation in river channel. Gertisser (2011) explained that some hydrological monitoring after the eruption which usually been taken are detecting lahars, surveying river channel, measuring sediment on the move, and analysis of spring water.

1.1. Background

Recent eruption on Mount Merapi started from October 26th until November 2010. Some experts believe that it is the most explosive in magnitude and number of victims for over this century. The 2010 eruption is shown on Figure 1-2.

Figure 1-2. Impacted area of 2010 eruption of mount Merapi
(source : http://www.volcanodiscovery.com)

According to Ministry of Forestry (2011), the 2010 Merapi eruption has destroyed vegetation in slope of Merapi (Figure 1-2). The heavy damage as shown in red color includes 1,242 hectares. Meanwhile moderate and minor damage shown in yellow and green color are 1,208 and 2,544 hectares respectively. Those area were suffered from the pyroclastic flows.

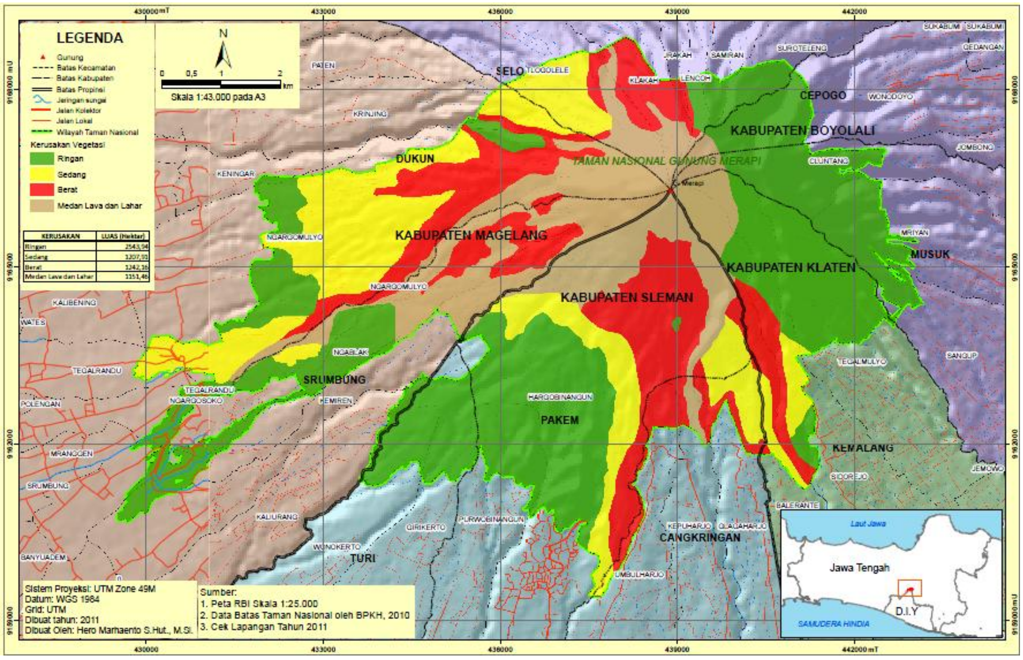

Figure 1-3. Impacted area on vegetation by the 2010 Merapi eruption
(Source : Ministry of Forestry, 2011)

Another study related with the impact of 2010 Merapi eruption was conducted by Rahayu (2011). She concluded that Code river, a main river flows to Yogyakarta, suffered sedimentation 1.5 – 2 meter and caused the capacity of the river was decreased by 52.63%.

Related with hydrological process, those conditions will impact the discharge as the output of watershed. Vegetation and sedimentation as consequence of pyroclastic flow, lava flows, and lahars had been studied. However, volcanic ashes, another volcanic hazard produced by the 2010 Merapi eruption, is mainly important to know related with hydrological process.

1.2. Problem statement

After volcano eruption, several condition change as consequence of the eruption. When volcano erupts, it affects soil layers as addition of volcanic ashes, vegetation cover change as consequences of pyroclastic flow and lava which can triggers forest fire, and river sedimentation from lahars in volcanic slope. Those changes will contribute to reduce the ability and carrying capacity of soil and river in hydrological processes.

This study focuses on the Code watershed, located in Yogyakarta Province, Indonesia. This watershed is mainly important to study since the main river of Code watershed flows to Yogyakarta city, an economic center of Yogyakarta province and highly populated. This mountainous area has been destructed by the 2010 eruption with less damage in vegetation and debris avalanche. The impacted hazards to the watershed are volcanic ashes and lahars.

During the eruption, a thick layer of ash was deposited and gives changes in soil layer. Charbonnier (2011) mentioned that the area covered by the fall is estimated around 52 km^2. That ash will change soil texture composition in top soil layer and affect infiltration in hydrological process. It is unknown how ash deposition affects the soil and infiltration in hydrological process.

Intensive rainfall in slope of Merapi triggered lahars in the stream. The amount of volcanic materials brought by the lahars flow resulted in morphological changes of the streambeds on the Merapi and its surroundings. River channels will experience sedimentation on the river and decreases bankfull dischage of the river in lower part of watershed. That change generates the lower area of watershed become flood prone area. After the 2010 eruption, part of Code river subjected to flood prone area is unknown.

There have been a number of researches consider the effect of rainfall and landuse change on discharge in Code watershed (Farida, 2009; Rahmalia, 2010; Aviani,2010). However, the study on a dynamic modeling considering the impact of Merapi eruption has not been done in the Code watershed.

1.3. Objectives

The hydrological response of the Code catchment will change due to ash deposition on the soil and the bankfull discharge is reduced due to the deposition from lahars. The present study utilizes a dynamic model to simulate the eruption impact on the discharge and further predict the Code river in lower part of Code watershed to response the predicted discharge. The main objective of this research is modeling the hydrological processes in disrupted watershed by the volcanic eruption and comparing the amount of discharge flowing to Code river, Yogyakarta with bankfull discharge of the river. The more specific objectives are:

1. To identify the changes on soil properties, soil depth and infiltration rate due to 2010 Merapi eruption.
2. To construct a hydrological model in order to accurately predict the discharge as the output of the model.
3. To assess the difference in discharge due to soil parameter change and to accurately predict the discharge based on extreme rainfall event in study area.
4. To quantify the exceedance probability of bankfull discharge due to lahars deposits.

To sum up, this research produced a model for discharge in disrupted watershed as the impact of volcanic eruption and simple possible flood prediction on Code river.

1.4. Research Questions

There are several research questions need to be addressed to achieve the research objectives, which are described in Table 1-1 below.

Table 1-1. Research objectives and research questions

No	Research objectives	Research questions
1.	To identify the changes on soil properties, soil depth and infiltration rate due to 2010 Merapi eruption.	How is soil properties change by the 2010 eruption? How is soil depth change due to 2010 Merapi eruption? How is infiltration rate change based on field measurement due to 2010 Merapi eruption?
2.	To construct the hydrological model in order to accurately predict the discharge as the output of the model.	How accurate is the model? Which parameter does have the most sensitive in the model? How to carry out calibration and validation to evaluate the model?
3.	To assess the difference in discharge due to soil parameter change and to accurately predict the discharge based on extreme rainfall event in study area.	How is the discharge change due to soil parameter change? How is the discharge if extreme rainfall event for 5, 20, 50 and 100 year return periods occurs?
4.	To quantify the excedance probability of bankfull discharge due to lahars deposits.	How is the response of Code river to the predicted discharge based on extreme rainfall event? Where part of Code river is potential to flooding?

1.5. Benefit of the research

Since Merapi erupts periodically and disrupts the watershed in its slope, this research provides a base information for stakeholders in hydrological system in Sleman and Yogyakarta city as one of efforts in flood mitigation.

1.6. Thesis structure

This thesis consists of six chapters. Each chapter explains specific subjects described as follow :

1. Chapter 1 explains about general background of this research, problem statement, aims of this study including main and specific objectives, and research question.
2. Chapter 2 comprises theoritical background of this research.
3. Chapter 3 explain about the study area of this research.
4. Chapter 4 deals with research method.
5. Chapter 5 focuses on analysis of soil parameter change due to the eruption, modeled discharge before and after the eruption, predicted discharge based on extreme rainfall event, and flooding area on bankfull discharge in some bottle neck of Code river.
6. Chapter 6 describes conclusion and recommendations.

2. LITERATURE REVIEW

2.1. Merapi eruption and lahars

Charbonnier (2011) described that on 24th October 2010, a sharp increase in seismic activity and summit deformation led to the evacuation of several villages around Merapi volcano. Merapi began to erupt on 26th October 2010. The explosion is classified as VEI 4 eruption with plume height more than 18 km and the volume was estimated more than 100×10^6 m^3. The area covered by the fall is estimated around 52 km^2 and caused around 300 causalities and 200,000 people evacuated. Schneider *et al*. (2011) stated that rapid lava dome growth around 25 m^3/s or around 2.2×10^6 m^3/d prior to the largest explosive events on November 5th 2010. Compare with previous eruption, in 2006 the peak is 0.1×10^6 m^3/d and the 100 year average 0.003×10^6 m^3/d.

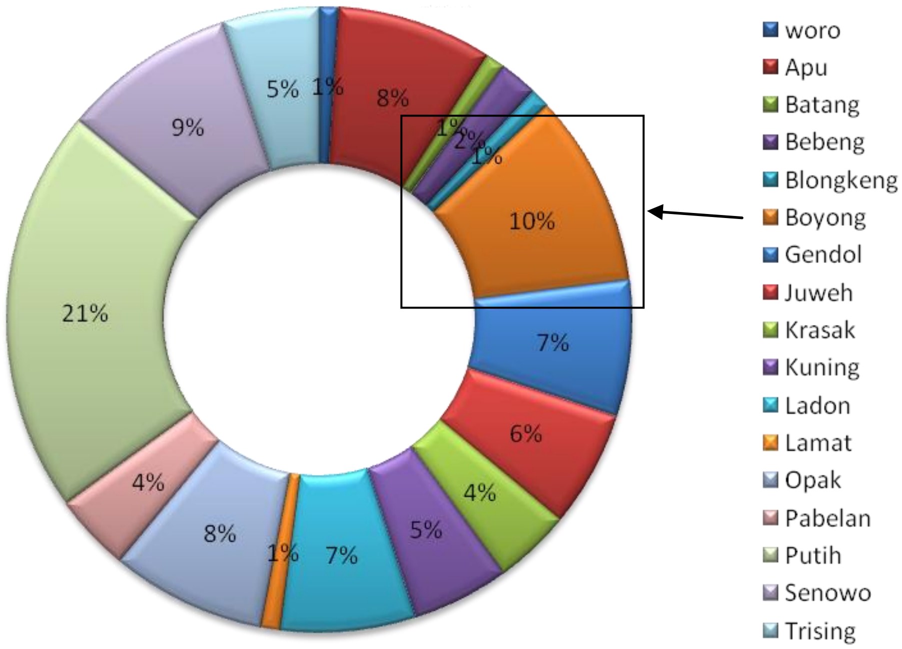

Figure 2-1. Distribution of lahars flowing to river in 2010 Merapi eruption (Source : Charbonnier, 2011)

Figure 2-1 describes the distribution of lahars along the river in slope of Merapi. Putih river is the highest river experienced lahars floods around 21% while Boyong river (main river in Code watershed) in second place with around 10 % of Merapi's lahars flowing to this river.

Historically, Merapi eruptions have been recorded since 1902 as shown in Table 2-1. From the table, we can conclude that since 1994 or last 6 eruptions, the direction tends to the South where Boyong/Code river flows and city of Yogyakarta lies on.

Table 2-1. Historical Merapi Eruption (Hartini, 2010)

No.	Year	Type of eruption	Direction	River Flowed
1.	1902 – 1904	Dome collapse	E	Woro
2.	1905 – 1906	Undifferentiated	E	Woro
3.	1909 – 1913	Dome collapse	SW	Batang
4.	1920 – 1923	Undifferentiated	W – SW	Blongkeng
5.	1930	Undifferentiated	NW, W-SW, SW	Senowo, Blongkeng, Batang
6.	1933 – 1934	Fountain collapse	NW	Senowo
7.	1942 – 1945	Dome collapse	NW, SW	Senowo, Blongkeng, Batang
8.	1953 – 1956	Dome collapse	N	Apu
9.	1957 – 1958	Dome collapse	SW	Batang
10.	1961	Dome and fountain collapse	NW, SW, SE, E, SW	Batang, Senowo, Gendol, and Woro
11.	1967 – 1968	Dome collapse	SW	Batang
12.	1969	Fountain collapse	SW, W-SW-S	Bebeng, Blongkeng, Batang, Krasak
13.	1972	Fountain collapse	SW	Batang
14.	1973	Dome collapse	W – SW	Blongkeng, Bebeng, Batang
15.	1976 – 1979	Dome collapse	SW	Batang
16.	1980 – 1983	Dome collapse	SW, SW-S	Batang, Bebeng, Putih, Krasak
17.	1984 – 1991	Dome collapse	SW	Putih/Sat
18.	1992 – 1993	Dome collapse	W	Sat/Putih
19.	1994	Dome collapse	SW, SW-S, S	Bebeng, Krasak, Bedog, Boyong
20.	1995	Dome collapse	SW, S	Krasak, Boyong
21.	1997	Dome and Fountain collapse	SW, SW-S, S	Bebeng, Krasak, Bedog, Boyong
22.	2001	Dome collapse	NW, W – SW, SW	Senowo, Lamat, Bebeng, Putih
23.	2006	Dome collapse	SW – S, S, SE	Krasak, Boyong, Gendol

Note : E: East, SE: southeast, S: south, SW: southwest, W:west, NW: northwest, N: north

2.2. Hydrologic cycle in watershed

McCuen (1998) defined the hydrologic cycle as the physical processes controlling the distribution and movement of water. He explained the cycle beginning with precipitation consists of rainfall and snowfall. Rain falling on earth may enter water body, travel over the land surface or infiltrate into the ground. Some is intercepted by vegetation, until it evaporates back to the atmosphere, and some is stored in surface depressions. Water which is stored in depressions, intercepted by vegetation, and infiltrates into the soil represent the initial losses. Water entering the upland streams travels to increasingly larger rivers and then to the seas and oceans.

Figure 2-2. Processes in the hydrological cycle at catchment scale
Q = runoff; the subscript G stands for groundwater flow; TF for throughflow;
I = interception; E = evaporation; P = precipitation (Davie, 2008)

The amount of water stored in the soil determines the amount of rain that will infiltrate during the next storm event (Mc Cuen 1998). Water stored in lakes, seas, and oceans evaporates back to the atmosphere, where it completes the cycle and is available for rainfall as illustrated in Figure 2-2 above.

Precipitation

As recognized by Davie (2008), precipitation is the release of water from the atmosphere to reach the surface of the earth. He noted that the amount of precipitation falling over a location varies both spatially and temporally (with time). The variation was influenced by static such as altitude, aspect and slope; and dynamic that is factors that do change and are by and large caused by variations in the weather.

Interception

As pointed out by De Jong and Jetten (2007), interception is a process that happens during the precipitation where the rain falls on the vegetation cover, held by vegetation canopy for some time, after which it will evaporate then it will be back into the atmosphere. One kind of method to determine vegetation cover is photographic method. Straatsma (2008) stated that current photographic methods still provide biased estimates of vegetation density because they disregard the effects of the central projection on the photograph, the bias leads to overestimation of the fractional coverage. He concluded that the amount of bias depends on the distance to the first vegetation element and its size.

Hadi (2006) mentioned that the amount of interception depends on some factors, such as the amount of rainfall, rainfall duration, rainfall distribution and vegetation characteristic. In addition, the importance of canopy interception in a catchment water balance is dependent on the size and extent of vegetation cover found within a watershed (Davie, 2008). Viessman (1989) also added that the amount of water intercepted is a function of (1) the strom character, (2) the species, age and density of prevailing plants and trees, and (3) the season of the year.

Evapotranspiration

Evaporation is the transferral of liquid water into a gaseous state and its diffusion into the atmosphere (Davie, 2008). He also explained that potential evaporation is that which occurs over the land's surface, or would occur if the water supply were unrestricted, while actual evaporation is that which actually occurs. He concluded that the evaporation above a land surface occurs in two ways – either as actual evaporation from the soil matrix or transpiration from plant. The combination of these two is often reffered to as evapotranspiration.

Infiltration

Rahmalia (2010) noted that rainfall that falls to the surface will become soil moisture, groundwater and surface runoff depends on soil texture and vegetation. Further, She explained that soil with sand particle dominated is better in absorbing and storing water than soil with other particles dominant. At a depth of 30 cm, soil with sand texture can absorb a few centimeter of water while clay texture at the same depth is only absorbing water of 100 mm or more. Suharto (2006) summarizes that the depth of root will contribute to the improvement of soil structure and balance of soil particle size distribution at deeper depths.

Prachansri (2007) noted that a number of factors affecting the infiltration rate include soil properties (including texture, structure, organic matter content, soil moisture content, pore size distribution), the amount and characteristics of precipitation (intensity, duration, etc), topography or slope gradient, management factors – e.g. cropping pattern, vegetation, land or surface cover (Aimrun *et al*., 2004; Celik, 2005; Giertz *et al*., 2005; Rivas, 2005; Stolte *et al*., 2003; Ward and Robinson, 1990).

Runoff and Discharge

Davie (2008) explained that runoff is a loose term covers the movement of water to a channelized stream, after it has reached the ground as precipitation. He added that once the water reaches a stream it moves towards the oceans in channelized form, the process referred to as streamflow or expressed as discharge, the volume of water over a defined time period. Area covering by vegetation has the ability to hold the water so the rainfall that fell on the area mostly intercepted and stored thus only a little became runoff.

2.3. Hydrological modeling

Badila (2008) stated that hydrologic models are increasingly used in water resources management and applications range from simple planning of water resources to more complex issues like assessing effects of climate change on water resources and environmental issues. According to Jetten (2011) in Spatial modeling of natural hazard process, he explained two core pitfalls of hazard modeling:

1. A hazard model is not an intelligent robot. It will not automatically predict a hazard but it can predict the spatial and temporal changes of natural processes but the user has to decide when such a process becomes hazardous.
2. A hazard model will predict nonsense if the input data are not correct and not tested against reality. The only way to ensure that the model gives good results is to understand the processes and create a good database.

As recognized by Badila (2008), the main application of a hydrologic model is to simulate river discharge in a catchment. Granell (2010) mentioned that environmental modeling such as that used for estimating river runoff often requires a long iterative process of sourcing, reformatting and introducing various types of data into the model. Further, He noted that the choice is based partially on modeling requirements but also on the data processing software available. Quan (2006) added that hydrologic models differ not only from model algorithms but also from their ability to capture certain aspects of the catchment hydrology.

Jetten (2011) mentioned some examples of the model concerned with hydrological processes are the SWAT model for large scale catchment modeling (Neitsch *et al.*, 2005), WOFOST for soil water balance and crop growth (Diepen *et al.*, 1989b), HYDRUS 1D for soil hydrology (Simunek *et al.*, 2008), EUROSEM for soil erosion (Morgan *et al.*, 1998) and LISEM for soil erosion and runoff hydrology (Hessel *et al.*, 2003), and STARWARS for landslide (Van Beek, 2002).

There are number of research have been conducted using similar method of hydrological model in Indonesia. Trimurti (2010) conducted a research on runoff assessment in Goseng catchment, central Java resulting the model is over estimates 40% than measured runoff. Hadi (2011) simulated monthly runoff in Serayu hulu and Merawu subwatershed, central Java resulting determinant factor of the model 0.22 and 1.59 respectively.

2.4. PCRaster

Visser (2005) stated that PCRaster is a Geographical Information System which consists of a set of computer tools for storing, manipulating, analyzing and retrieving geographic information. He explained that the architecture of the system permits the integration of environmental modeling functions with classical GIS functions such as database maintenance, screen display and hard copy output.

Further, Visser (2005) determined Dynamic models are built with the language provided by PCRaster. Trimurti (2010) explained that PCRaster uses involves the function of a script. This script has function to conduct the model such in nature processes using theoritically concept and algoritm operation. Visser (2005) stated that script consists of separate sections where in each section contains a certain functional part of the script. The division in sections is an essential concept of the Dynamic Modeling language. It tells the computer how to execute a program and it helps the user to structure the components of a model (Visser, 2005).

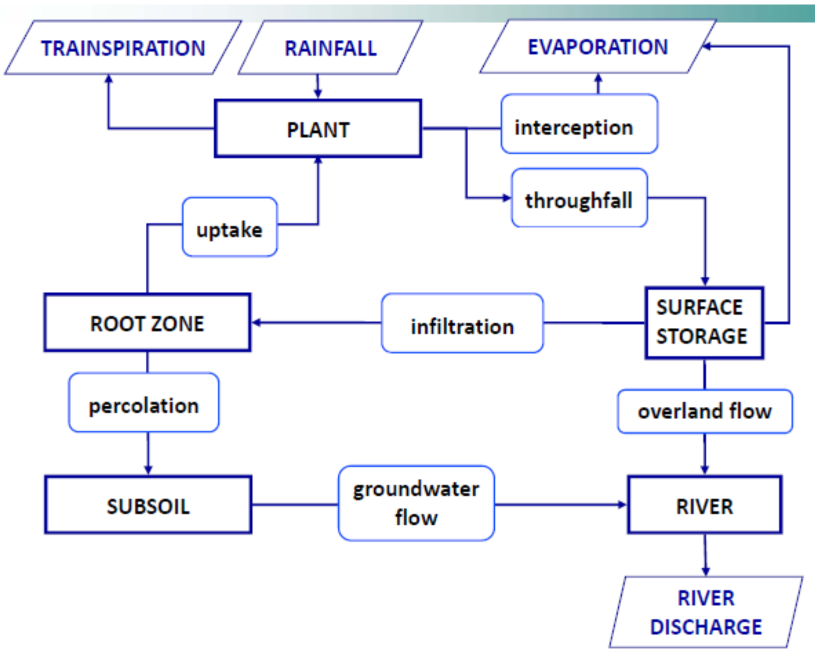

Figure 2-3. Flux of hydrological process in hydrological model (Jetten, 2011)

2.5. Sensitivity analysis, calibration, and validation

After constructing the hydrological model, it should be tested with comparing the simulated result to observed data. Jetten (2011) mentioned three tests to compete : (1) Mass Balance Check, the principle is incoming fluxes equals with outgoing fluxes and change in storage, (2) Sensitivity Analysis, the sensitivity of the model output to changes in input variables and model parameters, and (3) Calibration and Validation, check model outcomes to measured data and alter certain parameters to make the outcome fit then verify the calibrated code against an independent dataset.

Sensitivity for hydrological model can be applied in several parameter like saturated hydraulic conductivity (Nugroho, 2008; Pedzisai, 2010; Trimurti, 2010), porosity (Nugroho, 2008; Trimurti, 2010), soil depth (Quan, 2006; Nugroho, 2008; Trimurti, 2010), and canopy capacity (Quan, 2006). Trimurti (2010) noted that sensitivity analysis has two functions, (1) to find out which parameter that is most sensitive and (2) to use the result as a consideration for parameters adjustment in order to get the best parameter value that can assess the model result as close as the actual value.

Rykiel (1996) described that calibration is the estimation and adjustment of model parameters and constants to improve the agreement between model output and a data set. He also added that calibration procedures can be used to estimate parameter values that are otherwise unknown. There are some hydrologic models that provide automatic calibration while the others were not. Manual calibration based on trial and error mainly used by the researchers (Quan, 2006; Trimurti, 2010).

Mentioned by Mayer (1993), validation techniques can be grouped into four main categories, namely subjective assessment, visual techniques, deviance measures and statistical tests. When a model fails a validation test, Rykiel (1996) suggests several options to conduct: (1) The model may be re-calibrated to improve its fit to data by changing parameter values. (2) The model may be modified structurally and conceptually by revising assumptions and by changing the mathematical or logical representation of processes. (3) The application of the model may be restricted to a smaller domain where it is able to pass the validation test or where the particular test is not important. (4) Finally, failure to pass a validation test may be considered to invalidate the model.

2.6. Soil water characteristic (SWC) hydroulic properties calculator

Soil water characteristic is a computer program to estimate the hydrologic water holding and transmission characteristics of an agricultural soil profile layer. The estimating equation were developed by correlations of an extensive data set (1,722 samples) provided by the USDA/NRCS National Soil Survey Laboratory. The solutions are valid for all textures except those with clay content exceeding 60% (Saxton *et al*, 1985).

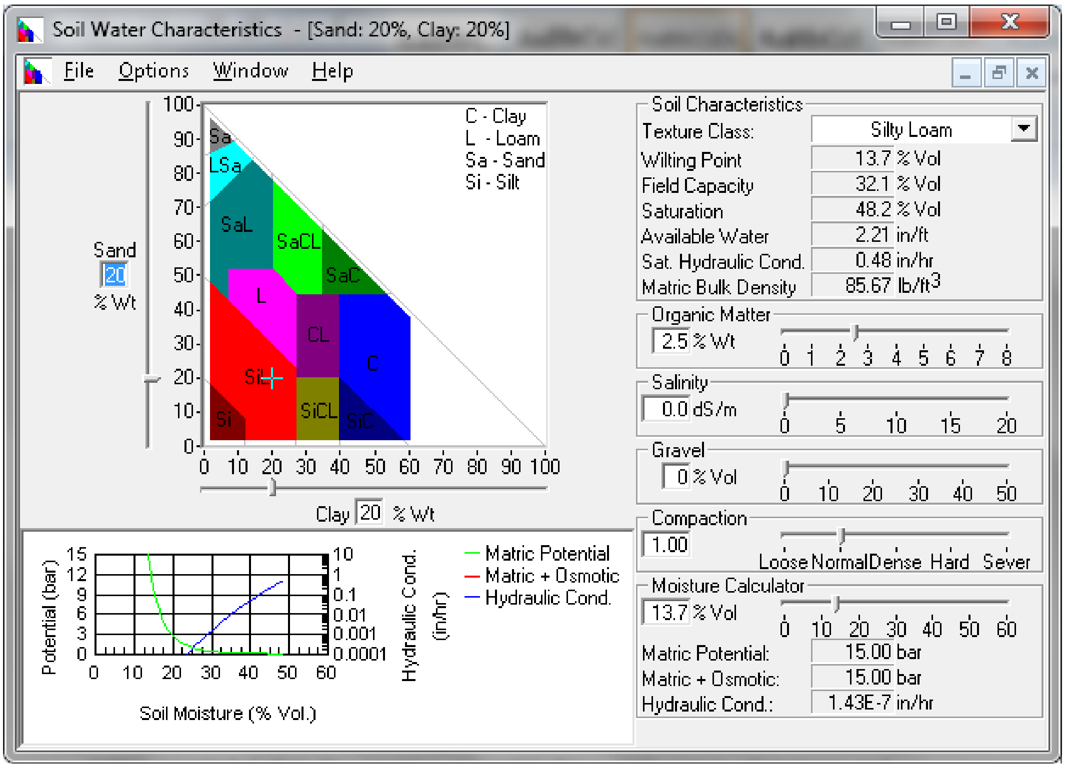

Figure 2-4. Soil water characteristic program.
Filling sand and clay fraction to determine texture class, wilting point, field capacity, saturation, available water, sat. hydraulic cond, and matric bulk density (upper right).

SWC hydroulic calculator can be used to determine Saturated hydraulic conductivity, field capacity, wilting point, saturation, etc (Figure 2-5). Saxton (1985) concluded that the equation are valid for a wide range of textures and provide reasonably accurate estimates of the unsaturated potentials and hydraulic conductivities with a minimum of readily available data.

2.7. Impact of volcanic eruption to hydrological process

The hydrologic processes in a watershed are influenced by soil characteristics, land cover, land use, topography and geology (Grayson, 2001; Diekkruger *et al*., 2006 as cited by Rahimy, 2011). Code watershed experienced less damage by the 2010 eruption where there is no significant differ in land cover, land use, topography and geology while soil characteristics were impacted by the volcanic ashes.

Ash deposition from the eruption mainly affects the soil. In hydrological process, soil will influence the infiltration and further determined the amount of groundwater flows. As cited by Prachansri (2007), the soil factors influencing the rate of infiltration are: the total amount of pores (soil porosity), the particle size distribution and the structure of pores (grain size distribution), soil structure (size distribution and structure of aggregates) and organic matter content of the soil (Juo and Franzluebbers, 2003; Wischmeier *et al*., 1971; Yamamoto and Anderson, 1973).

In addition, as cited by Rahimy (2011), soil characteristics such as depth (thickness) and saturated hydraulic conductivity (ksat) are very important in soil-water processes and strongly affect water infiltration and accordingly runoff generation (Neitsch 2002; Herbst, Diekkruger *et al*. 2006). Volcanic ashes also generate the change in soil fraction. Prachansri (2007) mentioned that sandy soils generally have higher saturated hydraulic conductivities than finer textured soils because of the larger pore space between the soil particles.

2.8. Flood

According to the American heritage dictionary, flood is the inundation of land that is normally dry through the overflowing of a body of water, especially a river. Modern geography dictionary explained that river floods have been defined as ‘events’ of such magnitude that the channels cannot accommodate the peak discharge. In other word, a flood is a flow in excess of the channel capacity, and results in inundation of low-lying flat land adjacent to the channel (Witherick *et al*, 2001)

When the surface flow fills the river with the amount of water higher than bankfull discharge, it causes the water to overflow from the levee and flooded the surrounding area. Bankfull discharge can be determined through calculation of river morphometry (Inverson *et al*, 1998).

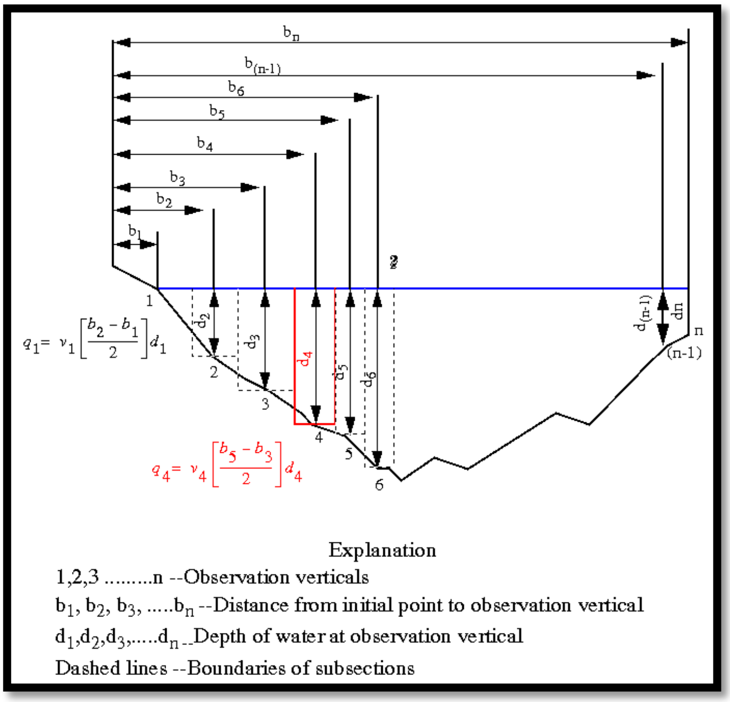

Figure 2-5. Sketch of calculation bankfull discharge (Inverson et al, 1998)

Susetyo (2008) mentioned that flood problem in urban areas can be influenced by many factors, such as drainage network within the city, rainfall, and water discharge of rivers passing through the city. There are five causes and types of urban flooding, which are, (1) Lack of drainage infrastructure, (2) Blockage of the drainage system, (3) Flooding in low-lying areas, (4) Backwater effects due to elevated downstream water levels, and (5) Inundation caused by high river water levels. (Parkinson, 2005 in Susetyo, 2008).

Another factor is the modification of river catchments by people's actions in deforestation, agriculture, land drainage, urbanization, etc., which may considerably alter the 'probability' of floods of a particular size (Witherick *et al*, 2001). He also noted that from a study of past records, an attempt is made to determine the *recurrence interval* of floods of particular dimensions i.e. the largest flood that occurred during the past 50-year period is likely to be matched by a corresponding flood during the next 50 years. In addition, recurrence event can also happen two years in a row.

3. STUDY AREA

3.1. Location, area and boundaries

Astronomically the Code watershed is located in 7° 43’ S and 110° 22’ E and administratively located in Sleman District, Special Province of Yogyakarta. It lies on 4 sub district of Sleman with total area is approximately 30 km^2 (Figure 3-1).

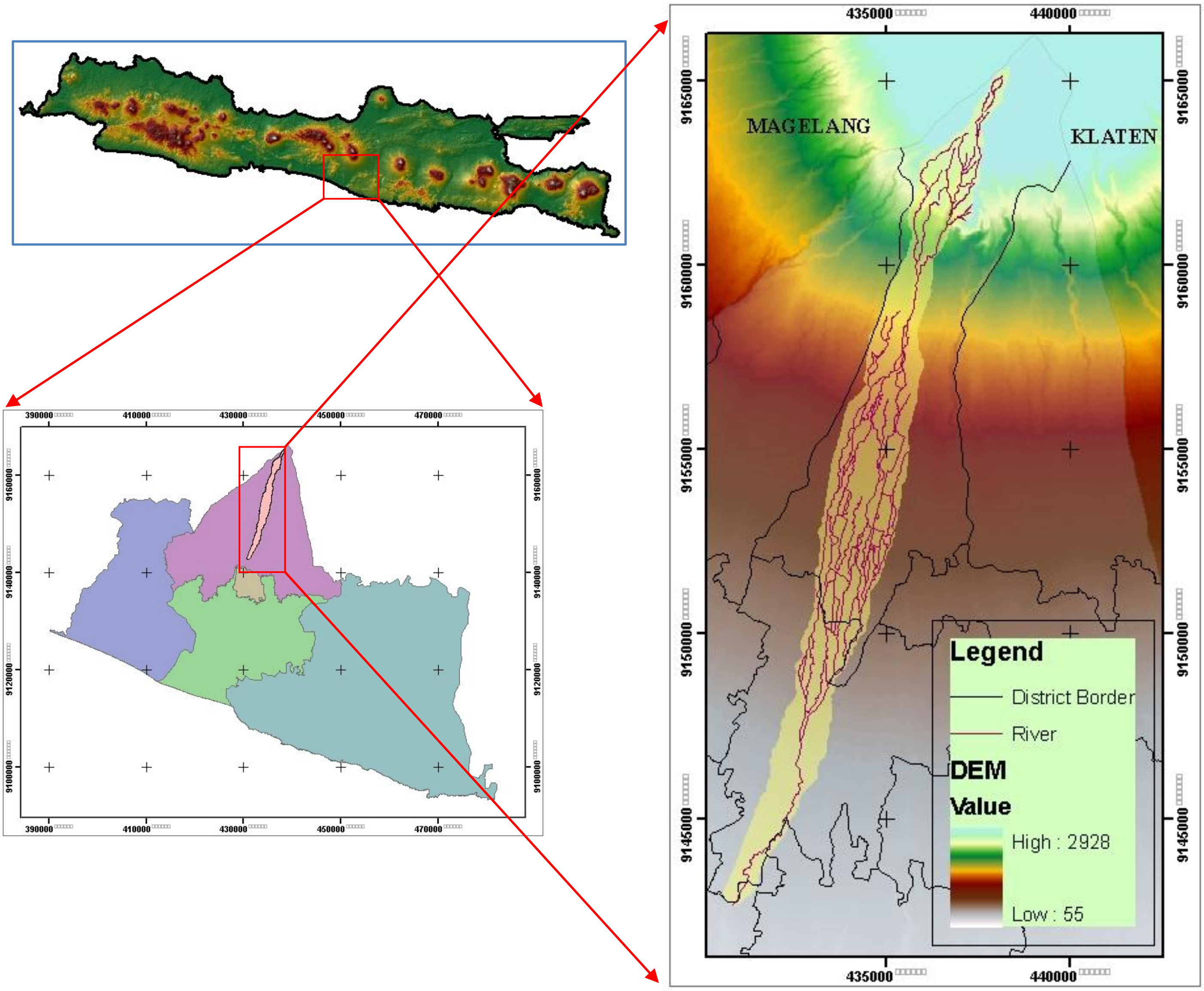

Figure 3-1. Study area of Code watershed (Source : GIS Processing)

3.2. Climate of study area

There are several rain gauges in Code watershed and surroundings (Figure. 3-2) some of them that managed by BPSDA POO (Bureau of Water Resources Management Progo Opak Oyo) are: Beran raingauges (208 m ASL), Santan raingauges (118 m ASL), Kemput (575 m ASL), Prumpung (575 m ASL), and Angin-angin (320 m ASL), while climate station managed by BMKG Yogyakarta is located in Pakem and Adisucipto airport.

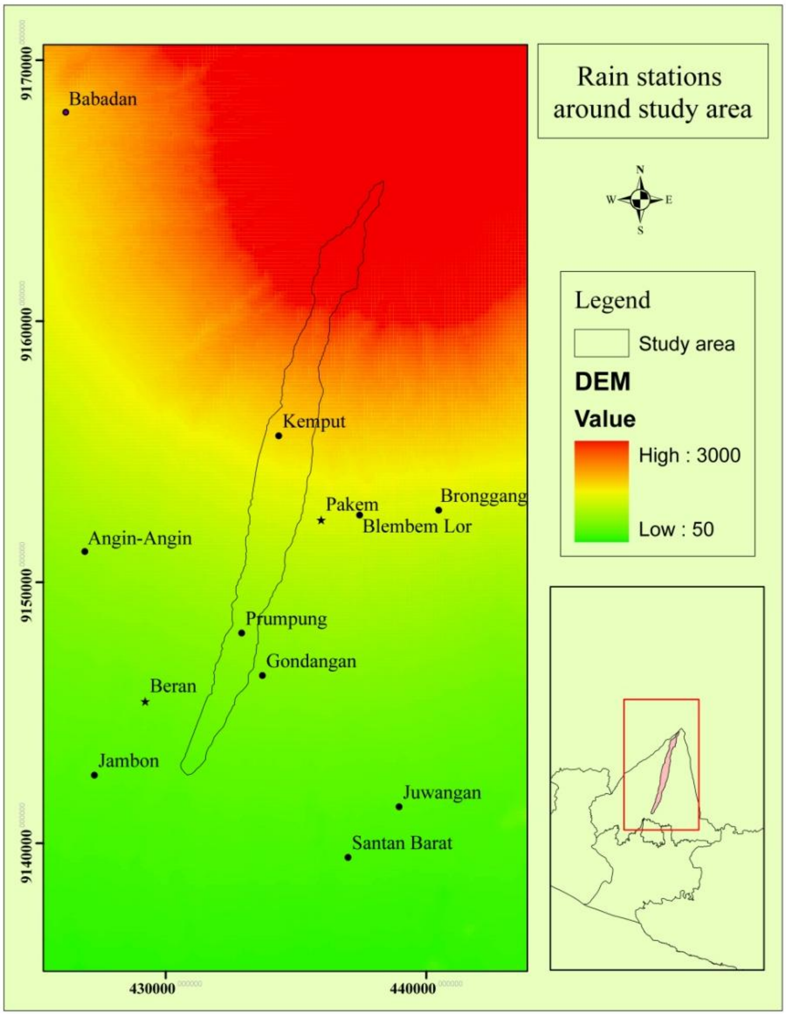

Figure 3-2. Rainstation and climate station in Code watershed and surrounding

Table 3-1. Monthly Average rainfall in Code 1986 – 2006 (Aviani, 2010)

Month	Raingauges (mm)					
	Beran	Santan	Kemput	Prumpung	Angin-angin	Pakem
January	425	507	458	372	355	385
February	415	505	459	372	301	389
March	350	405	394	319	260	288
April	226	242	264	247	162	216
May	104	91	135	106	77	103
June	83	83	82	75	54	73
July	39	44	33	35.5	25	31
August	21	22	35	22	24	27
September	16	18	27	20	16	16
October	161	126	200	142	128	132
November	285	245	354	229	180	278
December	362	376	317	348	264	290

Using Mock's equation, Aviani (2010) calculates temperature in Code watershed resulted 24.7 ^{o}C to 28.6 ^{o}C with the average temperature for periods 1986 – 2006 is 26 ^{o}C. Based on Schmidt-Fergusson classification, Rahmalia (2010) finds that Code watershed is classified as Type C and Type D. She concluded that with the average annual rainfall of 2508 mm and the average rainfall on the driest month by 22 mm reflects the study area is classified as the tropical Monson (Am), it characterized by the shorter dry season and heavy rain in the rest of the year.

3.3. Geology and geomorphology

Generally speaking, the morphological units on Merapi volcano are (i) volcanic cone, (ii) the slope which is dominated by gravitational processes; (iii) the middle slope, a material transportation slope by fluvial processes, and (iv) lower slope. In detail, the four parts of the volcano can be classified into landform units based on the similarity, rock, and processes affected its formation.

Aviani (2010) described that Code watershed was largely formed by young Merapi volcanic deposits and old Merapi volcanic deposits. The dominant formation in the study area is young Merapi volcanic deposit that extends from the slopes of Merapi to the south. Young Merapi volcanic deposits consist of tuffs, lava, breccias, andesitic and basaltic lava. Volcanic breccias are generally mold, blackish brown, tuff and rock component rather coarse sand to gravel sized. This formation is dominated by lava breccias with hardness level is andesitic, dark grey, solid, rough-textured, quite intensively fractured and filled by mineral quartz.

Besides breccias lava, deposits formation is also dominated by tuff sand. Soils in the southern part consist of sandy silt, brownish gray, soft, medium plasticity with thickness between 0.5 – 1.3 meters. In the middle part consist of sand to sandy silt, brown and rather solid to loose.

3.4. Soil conditions

Soil has a great influence in shaping the surface flow (runoff). The greater the infiltration rate the smaller the overland flow (runoff), and vice versa. Based on the Semi-detailed soil map of Yogyakarta, the study area consists of 7 soil type as follow: (1). Andic Dystropepts, (2) Andic Hapludolls, (3). Lytic Eustropepts, (4). Settlement, (5). Typic Fragiaquents, (6). Typic Hapludans, and (7). Typic Troportents.

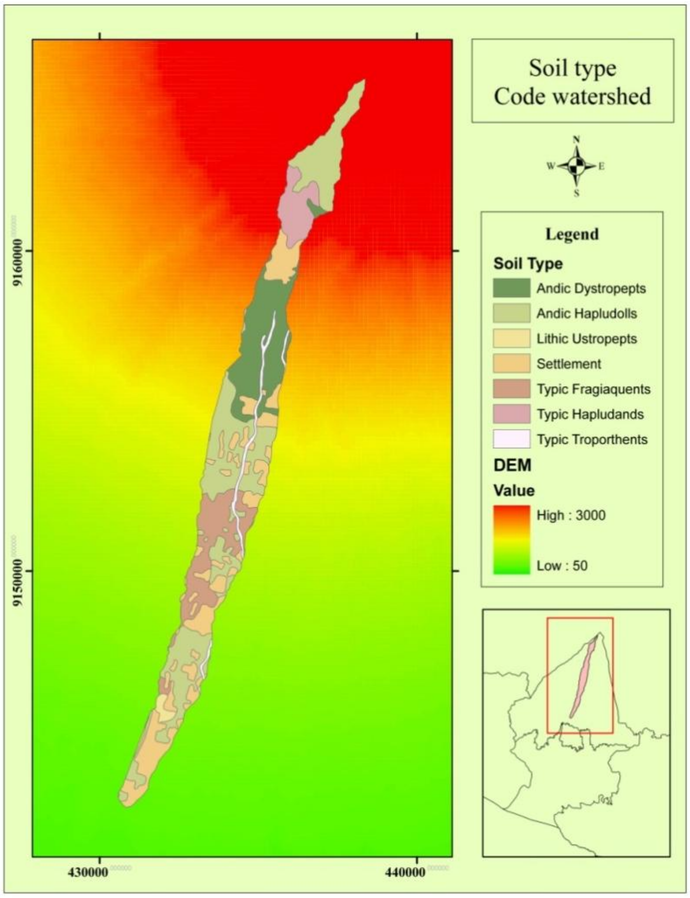

Figure 3-3. Soil type in Code watershed

3.5. Watershed morphology

Watershed morphology gives description about the watershed itself. It comprises with some parameters such as area of watershed, length of main channel, length of watershed, drainage density, and so on. Some research (Astuti, 2008; Farida, 2009; Aviani, 2010; Rahmalia, 2010) had measured watershed morphology in Code watershed as shown in table below.

Table 3-2. Morphology of Code river (Source : Astuti, 2008)

No.	Parameters	Calculation
1.	Total area	30.73 km^2
2.	Main channel length (L)	20.54 km
3.	Main channel gradient (S)	36.89 %
4.	Density drainage (D)	2.11
5.	Width factor (WF)	2.16
6.	Symmetric factor (SIM)	0.62
7.	Source factor (SF)	0.36
8.	Source frequency (SN)	0.51
9.	Number of river junction (JN)	21

4. RESEARCH METHOD

4.1. Materials, instruments and software

To set up the spatio-dynamic rainfall-runoff model for the Code watershed, a number of datasets were available, and additional data was collected in the field. To know the change of discharge as the impact of volcanic eruption, this research use dynamic hydrological model.

4.1.1. Materials

Materials used in the research are :

- Climate data obtained from Bureau of Water Resource Management Progo Opak Oyo (BPSDA POO) and Bureau of Meteorology, Climatology and Geophysics (BMKG Stasiun Geofisika) Yogyakarta.

Table 4-1. Climate data used in the research

Climate data	Duration	Temporal freq.	Source
Rainfall			
- Beran	1984 – May 2011	Daily	BPSDA POO
- Bronggang	1984 – May 2011	Daily	BPSDA POO
- Godean	1984 – 2006	Daily	BPSDA POO
- Pakem	1990 – May 2011	Daily	BMKG
- Kemput	1984 – 2010	Daily	BPSDA POO
- Prumpung	1984 – 2010	Daily	BPSDA POO
- Santan	1988 – 2010	Daily	BPSDA POO
Temperature	2010 – May 2011	Daily	BMKG
Solar radiation	2010 – May 2011	Daily	BMKG
Relative humidity	2010 – May 2011	Daily	BMKG

- Daily discharge data January 2010 – May 2011 of Pogung, Yogyakarta obtained from Bureau of Water Resource Management Progo Opak Oyo.
- Topographic map of Pakem (sheet 1408-242), Kaliurang (sheet 1408-244), Yogyakarta (sheet 1408-223), and Timoho (sheet 1408-224) scale 1:25,000.

- SPOT 5 Satellite Image on November 5th 2010 (after the eruption) and May 17th, 2008 (before the eruption).
- Digital soil map of Yogyakarta scale 1:50,000.

4.1.2. Software

The following software was used for processing the images and generating some data for input data of the model :

- PCRaster
- Nutsell 2.8
- Arc GIS 9.3
- Adobe Photoshop CS2
- Soil Water Characteristic Calculator (Pedotransfer tool)
- SPSS 17.0
- ABSCAN (Automated Baseflow Separation for Canadian Datasets)
- EasyFit 5.5 Standard
- Microsoft Office 2007 (Microsoft Word, Excell and Access)

4.1.3. Instruments

- Permeability cup and Double rings infiltrometer, to determine infiltration
- Soil bore, to take soil sample
- Global Positioning System, to determine coordinate position
- Yallon, to determine height of river section
- Gauge, to determine length of cross section
- Stopwatch, to capture time of infiltration
- Loope, to extent reading pias paper.
- Camera, to capture conditions of study area

4.2. Method

There are four main part processed in the method, (1) identifying change of hydrological parameter due to eruption, (2) constructing hydrological model, (3) predicting discharge based on extreme rainfall event and (4) determining flood prone area.

4.2.1. Change of hydrological parameter

The changes of hydrological parameter that was measured were soil properties, soil depth, and infiltration rate. Some of pre-eruption parameters were obtained from previous research in study area.

4.2.1.1. Soil properties change

Soil properties are affect infiltration in hydrological process. According to Jetten (2011) the texture and structure of the soil are the main characteristics that determine the soil hydraulic properties. These are : porosity, field capacity, wilting point, and hydraulic conductivity (ksat). These properties are highlighted to know the change due to the eruption. Soil unit analysis is based on soil type in Soil map of Yogyakarta. There are 29 soil samples (Figure 4-3) collected during field work in study area regarding landcover type and soil type, in each landcover and soil type 1 sample was taken.

Soil texture collected from the field are top soil texture that affected by ashfall during the eruption. The samples were analyzed by Laboratory of BPTP (Bureau of Agriculture Technology) Yogyakarta to determine the texture using pipette method. Obtaining soil texture, pedotransfer function was used to predict ksat, porosity, field capacity and wilting point. This research uses Soil Water Characteristics program developed by USDA-Agriculture Research Service as pedotransfer functions tool. Another parameter for soil data is Van Genuchten m parameter (Figure 4-1). It determined from literature (Jetten, 2011).

Soil properties before the eruption was obtained from Farida (2009) research conducted in 2009. She collected soil texture from each soil type in Code watershed. Using Soil water characteristic hydraulic properties calculator, this research extracted porosity, ksat, field capacity and wilting point from given soil texture.

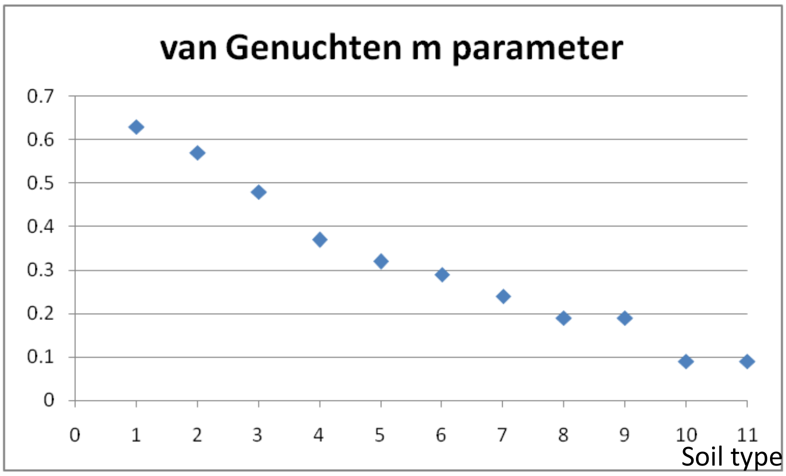

Num.	Soil Type
1	Sandy
2	Loamy Sand
3	Sandy Loam
4	Loam
5	Sandy Clay Loam
6	Silty Loam
7	Clay Loam
8	Silty Clay Loam
9	Sandy Clay
10	Silty Clay
11	Clay

Figure 4-1. Guideline values for the Van Genuchten m parameter by Hodnett and Tomasella (2002) (Source : Jetten, 2011)

4.2.1.2. Soil depth change

Soil depth was obtained from the semi-detailed digital soil map. The map has value of soil depth in each soil type with the range of 1000 – 2000 mm. Soil depth change was gained from calculation of pre eruption of soil depth from the map and post eruption of soil depth with additional of ash measurement, as the eruption produced an amount of ash that evenly spreading.

During field work, the amount of ash was determined by interviewed local people in Code watershed. The thickness's information was asked to people in every 500 meter interval from the downpart to upperpart of Code watershed. The information then be plotted in a graph to determined the linier regression and its formula. Using the regression, post-eruption soil depth was determined by adding the pre-eruption soil depth with the additional ash.

4.2.1.3. Infiltration change

Double ring infiltrometer was used to measure infiltration rate in this research. This instrument has diameter of 16.5 and 27.5 cm and height 15 cm. The sample taken follows soil sample means that at least 29 infiltration rates were taken from the study area. On the other hand, infiltration rate before the eruption was taken from Noordianto's research (2005) focusing on groundwater recharge between Boyong and Kuning river. The results of infiltration rate from field work were calculated using Horton method as shown below :

$$F_t = f_c . t + \frac{(f_o - f_c)}{K} (1 - e^{-Kt}) \tag{4.1}$$

Where :

Ft : infiltration rate at time *t* (cm/h)

*f*c : the constant or equilibrium infiltration rate (cm/h)

fo : the initial infiltration rate or maximum infiltration rate (cm/h)

K : the decay constant specific to the soil

e : 2.718

Constant *K* determined by

$$k = - \frac{1}{0.434} m \tag{4.2}$$

Where : *m* is a gradient from the curve of log $(f_o - f_c)$ and time.

Figure 4-2. up : process to obtain infiltration rate in study area,
down : Instrument to measure infiltration (left),
soil sample collected during the field work (right)

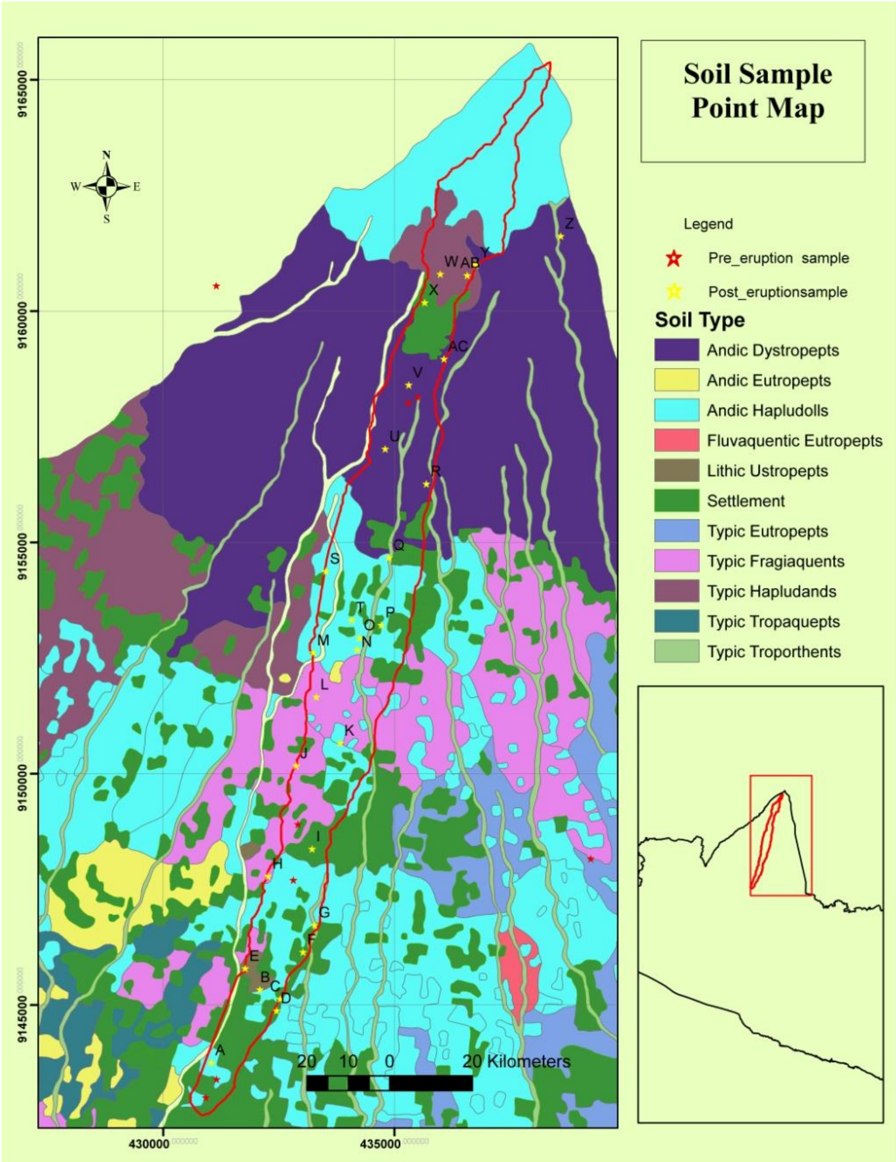

Figure 4-3. Soil Sample Taken in Before and After the 2010 Eruption

4.2.2. Constructing the hydrological model

Hydrological model is constructed to figure hydrological phenomena in the study area. The model was done using PCRaster software and Nutsell 2.8, a GIS program to facilitate the running of PCRaster. This model was employed since it is the open architecture, full control over the process description, and versatility of data input. In the model, equations describe hydrological components by using a script. The script (see Appendix 1) adopts water balance model version 1.0 constructed by Jetten (2011).

4.2.2.1. Initial input of hydrological model

The model was built in daily time steps and starts from January 1st, 2010 until May 31st, 2011. It performed hydrological process before the eruption from January – October 2010 and after the eruption is January – May 2011. The spatial resolution of the model was 10 meter. Some input components and procedure to run hydrological model are described below.

4.2.2.1.1. Landcover data

Landcover was obtained from visual interpretation using Ikonos and SPOT 5 image of 2010 after eruption. At first, the image was interpreted and delineated based on appearance on the image. All of the objects were classified based on USGS Classification Level II and resulted in landcover map with 7 types of landcover, there are built-up land, croplands and pasture, evergreen forest land, mixed rangeland, streams and canal, bare exposed rock, and transportation. Classification was done at image scale of 1:10,000 to get a better visualization.

After classification and produced pre-landcover map, binomial probability theory was applied to assess sample size (N) for ground check. The formula (Jensen, 2005) is:

$$N = \frac{Z^2(p)(q)}{E^2} \tag{4.3}$$

Where p is the expected percent accuracy of the entire map, q = 100-p, E is the allowable error, and Z =2 from the standard normal deviate of 1.96 for the 95% two-sided confidence level. With the expected map accuracies of 85% and an acceptable error of 10%, the sample size for this map would be:

$$N = \frac{2^2(85)(15)}{10^2} = 51$$

4.2.2.1.2. Rainfall data

It could be argued that hydrological model is a data hungry model. In this research, the model construct hydrological model from January 2010 to May 2011. It is based on rainfall data availability in studied area that the agency managed rainfall data can provide the dataset until May 2011.

In this research, rainfall datasets were tested using Spearman's rank-correlation method to test for absence of trend. Dahmen, 1990 recommended this method since it is simple and distribution free. It also does not require the assumption of an underlying statistical distribution. The method is based on the Spearman rank-correlation coefficient, *Rsp*, which is defined as :

$$R_{sp} = 1 - \frac{6 * \sum_{i=1}^{n}(D_i * D_i)}{n*(n*n-1)} \tag{4.4}$$

$$D_i = Kx_i - Ky_i \tag{4.5}$$

Where *n* is the total number of data, *D* is difference, and *i* is the chronological order number. Kx_i is the rank of the variable and Ky_i is transformed to its rank equivalent. The result of *Rsp* calculation above was applied to another equation to performed student t-distribution.

$$t_t = R_{sp}\left[\frac{n-2}{1-R_{sp}*R_{sp}}\right]^{0.5} \tag{4.6}$$

Those calculation then be compared with t table for a significant level of 95 percent (two-tailed) to know the dataset has trend or not.

Rainfall is a main input for water balance modeling. There are at least 7 rainfall stations in Code watershed and surrounding which have relatively good datasets. Six rainfall stations are managed by BPSDA POO (Bureau of Water Resources Management Progo Opak Oyo) while another in Pakem is managed by BMKG (Bureau of Meteorological Climatology and Geophysics) of Yogyakarta.

The rainfall station has two instruments to capture rainfall, manual and automatic instrument. Since this research conduct hydrological model after eruption in late 2010, recent data were employed to figure precipitation in studied area. Screening and testing the data for stationarity and consistency were performed to indicate consistency and homogeneity. At first, screening data from annual rainfall in each station were displayed on graph below (Graph 4-1). Secondly, Spearman's rank-correlation and student-t distribution were applied to the datasets. Result of student-t test then be compared with t-table for a significant level of 5 percent (two-tailed) to know the dataset has trend or not. The result of this data processing is shown below.

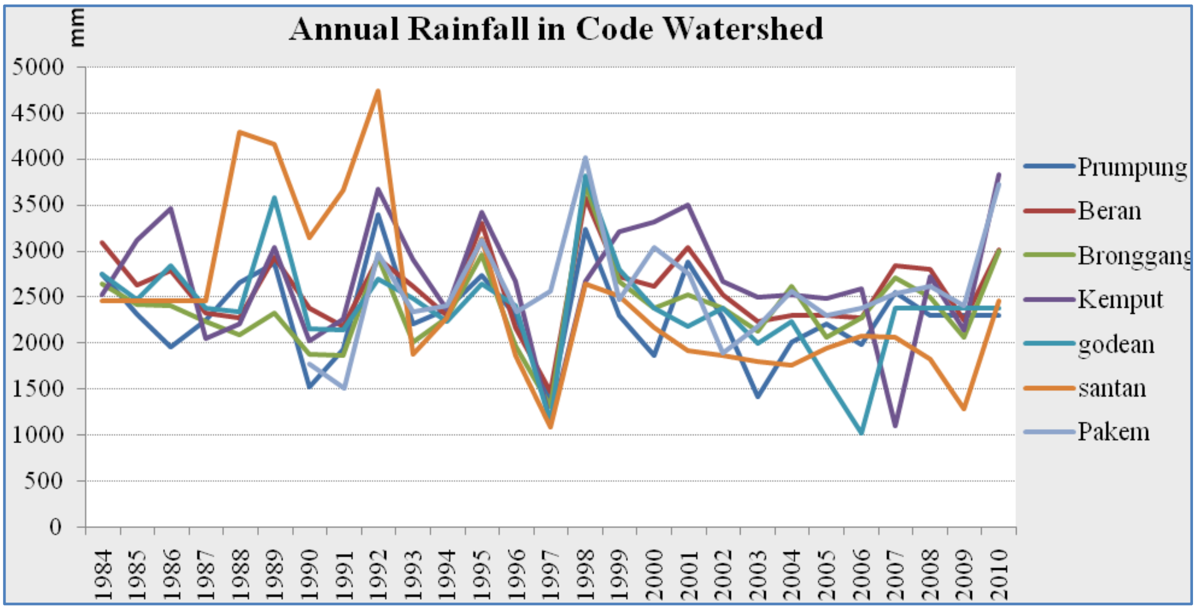

Graph 4-1. Annual rainfall in Code watershed and surrounding

Table 4-2. Calculation of Spearman's rank-correlation

Parameter	Beran	Bronggang	Godean	Kemput	Pakem	Prumpung	Santan
R_{sp}	-0.138	0.136	-0.571	-0.029	0.024	-0.218	-0.778
t_t	-0.698	0.658	-2.951	-0.136	0.107	-1.026	-5.539
t-table 95 % ($\pm$2.06)	in range	in range	out range	in range	in range	in range	out range

From the table 4-3 above, there are Godean and Santan that have trend of dataset while the others have not trend. Double Mass Curve Analysis was employed to know data consistency. All of dataset from rainfall station were applied in the analysis except Godean and Santan. The results of the analysis were figured as slope of curve in each rainfall dataset (Graph 4-2).

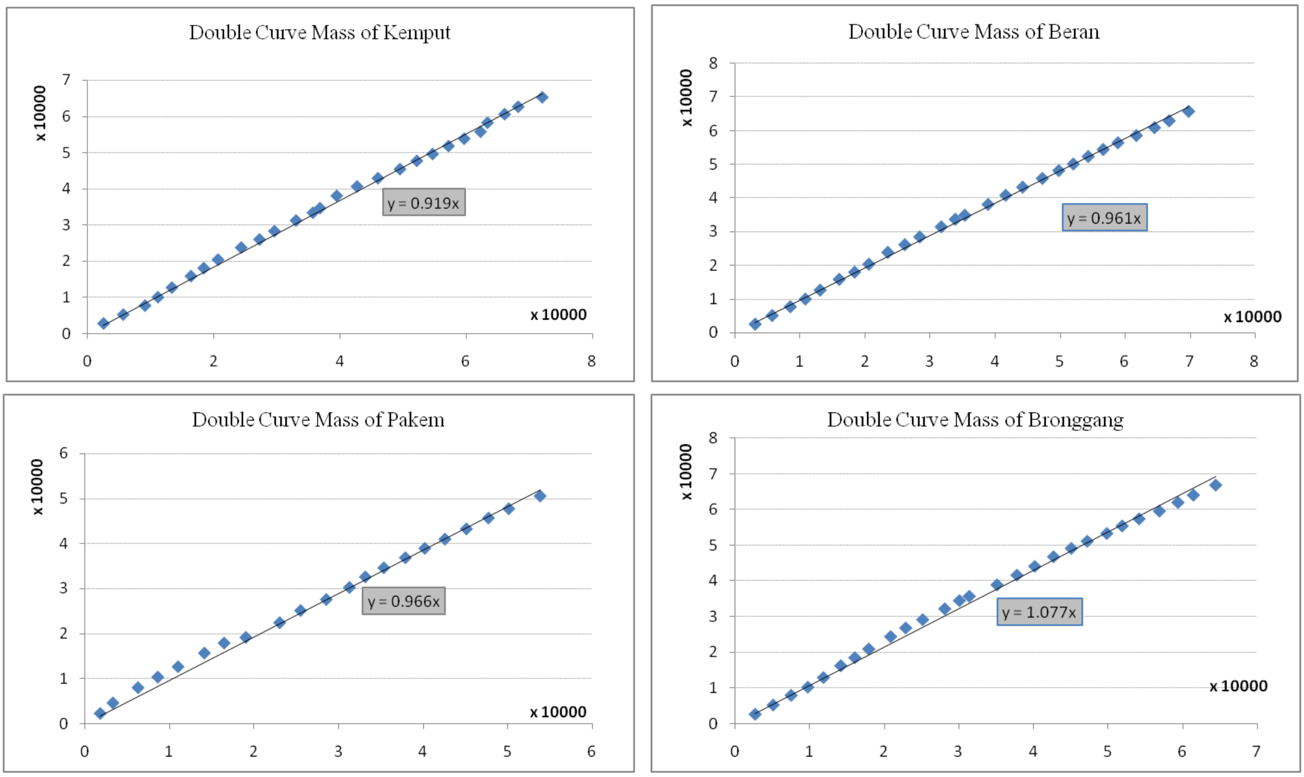

Graph 4-2. Result of double mass curve analysis

From the graph 4-2 above, slope of some rainstations in study area were classified as consistent data with value around 0.9 – 1.1. It could be concluded that the data were performed well. All of dataset from rainstations above can be used as the input of precipitation in the model.

Knowing consistency of the data, unfortunately 2011 dataset from Kemput and Prumpung were in bad quality (Figure 4-4). The model also required rainfall stations were located within study area. In this case, 2 stations were moved to study area virtually. This research used 2 (two) dataset from Pakem and Beran (see Appendix 2). Isnugraha (1975) in Hadi (2011) stated that World Meteorological Organization (WMO) recommended the minimal rainfall gauge density on the research area, one station in 600 - 900 km^2 for flat area, and one station in 100 – 250 km^2 for mountainous area. Since the study area lies on mountainous area with 30 km^2, two rainfall stations are good enough to represent the precipitation.

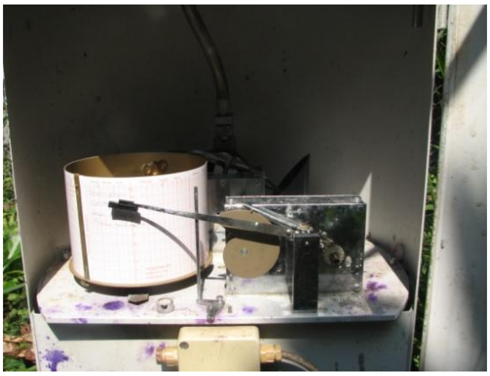

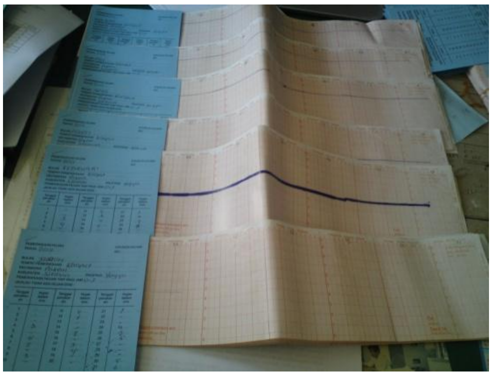

Figure 4-4. Left : Instrument of rainstation,
Right : rainfall datasets of January – May 2011 in Kemput rainstation (it shows that there is no record of rainfall at that period).

After deciding rainstations, rainfall datasets were interpolated using inverse distance interpolation with power of 2. The interpolation was processed in PCRaster using command :

"P = inversedistance (study area, rainfall data, 2, 0, 0)"

4.2.2.1.3. Vegetation cover data

Vegetation cover was determined through field measurement. This research used two methods to obtain vegetation cover. First, sampling plot was conducted with area of 2 x 2 meter for seedling or crops and 10 x 10 meter for trees or rangeland and forest. Second method is photographic method by taking picture of the canopy. Through Adobe Photoshop software, the image was modified into black and white to determine the canopy and calculated using grid method to define percentages of vegetation cover. The processes are: open the image on Adobe photoshop software thus highlighted the image with grid line using View menu show Grids. The image then was edited by Color Range in Select menu. To facilitate grid calculation, it uses grayscale preview and pointed to leaf so the leaf will performed lighter than others and the percentage of vegetation cover can be determined. Finally, both methods (sampling plot and photographic method) were averaged to determine vegetation cover of vegetated landcover.

Figure 4-5. Process on vegetation cover calculation using Adobe Photoshop 2.0 (left), and sampling plot in mixed rangeland (right)

Number of sample taken in each landcover type is three samples for each vegetated landcover type except for the croplands and pasture landcover. In croplands, three dominant kinds of vegetation in study area were carried out to represent croplands. There are corns, peanut and paddy representing croplands.

4.2.2.1.4. Interception

Jetten (2011) explained that vegetation intercepts rainfall directly in the canopy and the amount of rain reaching the soil surface is decrease as the process of interception. Davie (2001) also stated that some of this intercepted water may be evapored; referred to as interception loss. The amount of interception loss from an area is climate dependent.

To know the amount of interception can be calculated using Storage maximum equation, such as Von Hoyningen-Huene equation. Kuriakose (1996); de Jong and Jetten (2007); Hadi (2011), using that equation as shown below :

$$Smax = 0.935 + 0.498*LAI - 0.00575*LAI^2 \qquad (4.7)$$

Where LAI can be obtained from equation as mentioned in Jetten (2011) as

$$LAI = \frac{ln\,(1 - cover)}{-0.4} \tag{4.8}$$

According to profile of Yogyakarta province, there are 45,424 ha, 74,563 ha, 62,539 ha, and 63,275 ha of paddy field, corn, peanut, and cassava respectively in Yogyakarta. Since croplands were planted by the farmer with various agricultural commodities, this research decided corn, peanut and paddy as representative of crops in study area.

Interview with the farmer resulting grow periods of those crops. Farmer plants crops (corn, peanut, cassava, tobacco and chili) in April and August while in December they plants paddy. July and November, croplands were empty of vegetation as they harvest the land while in Paddy field, there always shrubs grow in the area.

Table 4-3. Calculation of cover, LAI and smax on selected landcover

Month	**Cover (%)**				**LAI**				**Smax (mm)**			
	Forest	**Crops**	**Garden**	**Paddy**	**Forest**	**Crops**	**Gardei**	**Paddy**	**Forest**	**Crops**	**Garde**	**Paddy**
Jan	89.19	52.08	84.54	52.08	5.56	1.84	4.67	1.84	1.59	1.83	3.13	1.83
Feb	89.19	60.41	84.54	60.41	5.56	2.32	4.67	2.32	1.59	2.06	3.13	2.06
March	89.19	19.79	84.54	19.79	5.56	0.55	4.67	0.55	1.59	1.21	3.13	1.21
April	89.19	9.20	84.54	7.81	5.56	0.24	4.67	0.20	1.59	1.05	3.13	1.04
May	89.19	37.75	84.54	52.08	5.56	1.19	4.67	1.84	1.59	1.52	3.13	1.83
June	89.19	64.14	84.54	60.41	5.56	2.56	4.67	2.32	1.59	2.17	3.13	2.06
July	89.19	0.00	84.54	19.79	5.56	0.00	4.67	0.55	1.59	0.94	3.13	1.21
Aug	89.19	9.20	84.54	7.81	5.56	0.24	4.67	0.20	1.59	1.05	3.13	1.04
Sept	89.19	37.75	84.54	52.08	5.56	1.19	4.67	1.84	1.59	1.52	3.13	1.83
Oct	89.19	64.14	84.54	60.41	5.56	2.56	4.67	2.32	1.59	2.17	3.13	2.06
Nov	89.19	0.00	84.54	19.79	5.56	0.00	4.67	0.55	1.59	0.94	3.13	1.21
Dec	89.19	7.81	84.54	7.81	5.56	0.20	4.67	0.20	1.59	1.04	3.13	1.04

Script applied in PCRaster to calculate vegetation cover was determined by the command created by Hadi (2011), as follow :

"Cover = if (day ge daymonth1, covermonth1 + (day-daymonth1)/(daymonth2-daymonth1+0.0001)*(covermonth2-covermonth1),cover)"

"Coverm = min(Cover, 0.95)"

After obtaining vegetation cover, interception determined by following script in PCRaster :

"LAI = ln(1-Coverm)/-0.4;"

"Smax = max(0, 0.935+0.498*LAI-0.00575* sqr(LAI))"

"Interception = min(Smax,(rainfall-potential evapotranspiration))"

4.2.2.1.5. Evapotranspiration data

Raes (2009) stated that the reference evapotranspiration (*ETo*) is a climatic parameter and can be computed from weather data. The method to determine reference evapotranspiration (*ETo*) is obtained from FAO Penman-Monteith method which use daily temperature, solar radiation, humidity, and wind speed (see Appendix 3). Equation of FAO Penman-Monteith method (FAO, 1998) are :

$$ET_o = \frac{0.408\,\Delta\,(R_n - G) + \gamma\,\frac{900}{T + 273}\,U_2(e_s - e_a)}{\Delta + \gamma\,(1 + 0.34\,U_2)} \tag{4.9}$$

Where :

ET_o : reference evapotranspiration (mm/day)
R_n : Net radiation at the crop surface ($MJ/m^2.day$)
G : Soil heat flux density ($MJ/m^2.day$)
T : Mean daily air temperature at 2 meter height (^oC)
U_2 : Wind speed at 2 meter height (m/s)
e_s : Saturation vapour pressure (KPa)
e_a : Actual vapour pressure (KPa)
e_a - e_a: Saturation vapour pressure deficit (KPa)
Δ : Slope vapour pressure curve (KPa/ ^oC)
γ : Psychometric contant (KPa/ ^oC)

Some parameters were calculated using formula below :

$$\gamma = 0.665\ x\ 10^{-3}\ P \tag{4.10}$$

$$P = 101.3\left(\frac{293 - 0.0065\,Z}{293}\right)^{5.26} \tag{4.11}$$

$$e_s = \frac{e^o(T_{max}) + e^o(T_{min})}{2} \tag{4.12}$$

$$e_a = e^o(T_{min}) \frac{(RH_{max})}{100} \tag{4.13}$$

$$e^o(T) = 0.6108. exp\left[\frac{17.27T}{T + 237.3}\right] \tag{4.14}$$

$$\Delta = \frac{4098 \left[0.6108. exp\left[\frac{17.27T}{T + 237.3}\right]\right]}{(T + 237.3)^2} \tag{4.15}$$

$$G = C_s \frac{T_i - T_{i-1}}{\Delta t} \Delta z \tag{4.16}$$

Where :
P : Atmospheric pressure (kPa)
Z : Elevation above sea level (m)
$e^o(T)$: Saturation vapour pressure (kPa)
RH : Relative humidity (%)
Cs : Soil heat capacity ($MJ/m^3.C$)
Δt : Length of time interval (day)
Δz : Effective soil depth (m)
G : for day period, as the magnitude of the day soil heat flux beneath the grass reference surface is relatively small, it may be ignore and thus G ≈ 0 (FAO, 1998).

4.2.2.1.6. Actual evapotranspiration

The actual evapotranspiration is the sum of the actual transpiration (Ta) and actual soil surface evaporation (Ea). It is calculated using equation below (Hadi, 2011) :

$$Ta = ETo * fc * K_c \tag{4.17}$$

$$Ea = ETo * (1 - K_c) \tag{4.18}$$

$$Eta = Ta + Ea \tag{4.19}$$

Where :

Eta : Actual evapotranspiration (mm)
ETo : Refference evapotranspiration (mm)
fc : Fractional vegetation cover
Kc : Crop factor

4.2.2.1.7. Infiltration and percolation

In the model, infiltration is a fraction of saturated hydraulic conductivity. It was determined through precipitation and infiltration capacity related with saturated hydraulic conductivity. In addition, percolation was calculated based on van genuchten equation and applied in PCRaster by command below :

Perc = Ksat*sqrt(theta_e)*sqr(1-(1-(theta_e**(1/m_param)))**m_param)
Ksat : Saturated hydraulic conductivity
Theta_e : (theta-theta_r)/(theta_s-theta_r)
m_param : van genuchten m parameter

4.2.2.1.8. Runoff

Runoff is assumed as overland flow or surface runoff. Runoff obtained from calculation of infiltration capacity, local drainage direction and effective rainfall in PCRaster script. In the model, runoff was determined by using command:

runoff = accuthresholdflux(LDD, Precipitation-Interception, Infiltration capacity);

4.2.2.1.9. Discharge data

Modeled discharge obtained from the equation calculating total baseflow and peakflow flowing to the outlet in the watershed. The model performs daily discharge in meter cubic. Discharge was carried out from the model with the script below:

Qsim.tss = timeoutput(outlet, Qpeakm3+Qbasem3);

On the other hand, measured discharge (see Appendix 4) was obtained from Pogung station managed by BPSDA POO, Yogyakarta as validation in the model result. The data was in pias paper and performed in height of water level (meter). The data then be converted into discharge (m^3/s) using formula of rating curve in Pogung as follow:

$$Q = 8.22\ (H - 0.05)^{2.05} \tag{4.20}$$

Where Q is discharge (mm/s) and *H* is water level height (meter). The formula was determined since 2007 and checked annually. After the 2010 eruption, the formula has not been updated. Discharge output from the model was compared to bankfull discharge as flood prediction. Graph of daily discharge measured by the instrument are presented below (Graph 4-3).

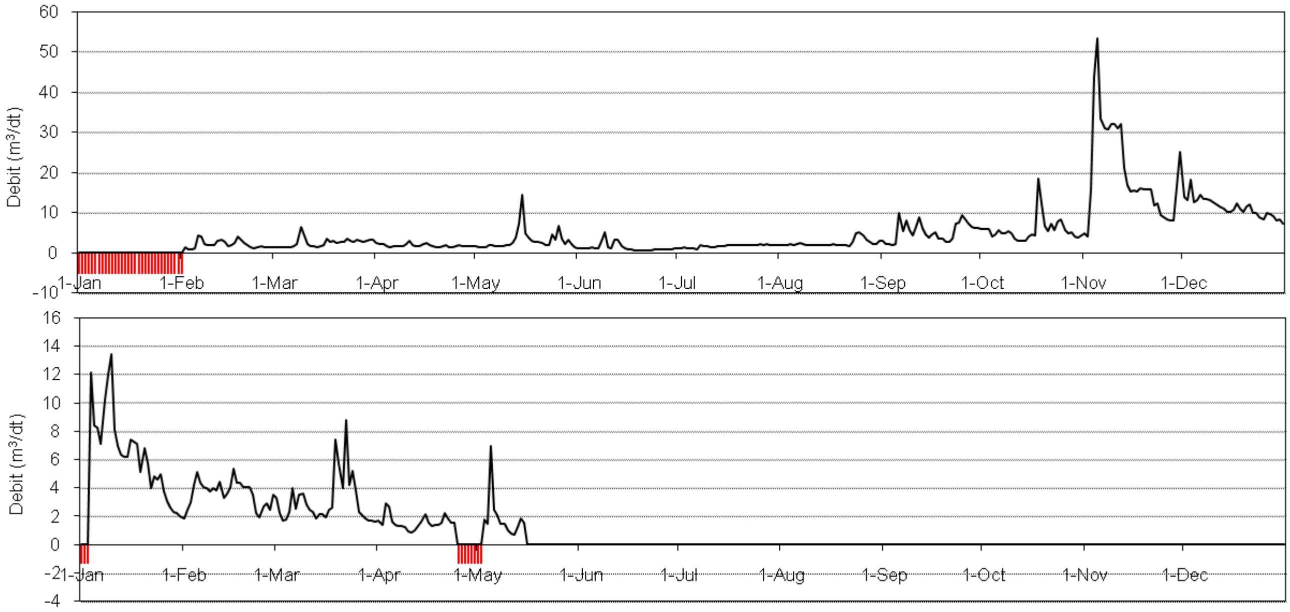

Graph 4-3. Daily discharge in Pogung station (Outlet of Code watershed)

Measured discharge can be divide into baseflow and peakflow (surface runoff) using baseflow separation techniques. There are number of software available to separate baseflow, such as ABSCAN (Automated Baseflow Separation for Canadian datasets), BFI (a computer program for determining index to baseflow), HYSEP (hydrograph separation program of USGS), Low Flows 2000 (tool for estimating low flow in the United Kingdom), etc.

Being freeware, this research took ABSCAN software to separate baseflow of measured discharge in Pogung. Based on Parker (2006), ABSCAN is suitable for use with any distributed runoff models, and can easily be adapted for use in non-Canadian datasets. He also explained that the software offers several filtering algoritms (Lyne and Hollick, Chapman, and Eckhardt). The algoritms can be found in User's Guide of ABSCAN (Parker, 2006). Calculated by the software, baseflow and runoff of Pogung represents on the Graphs below.

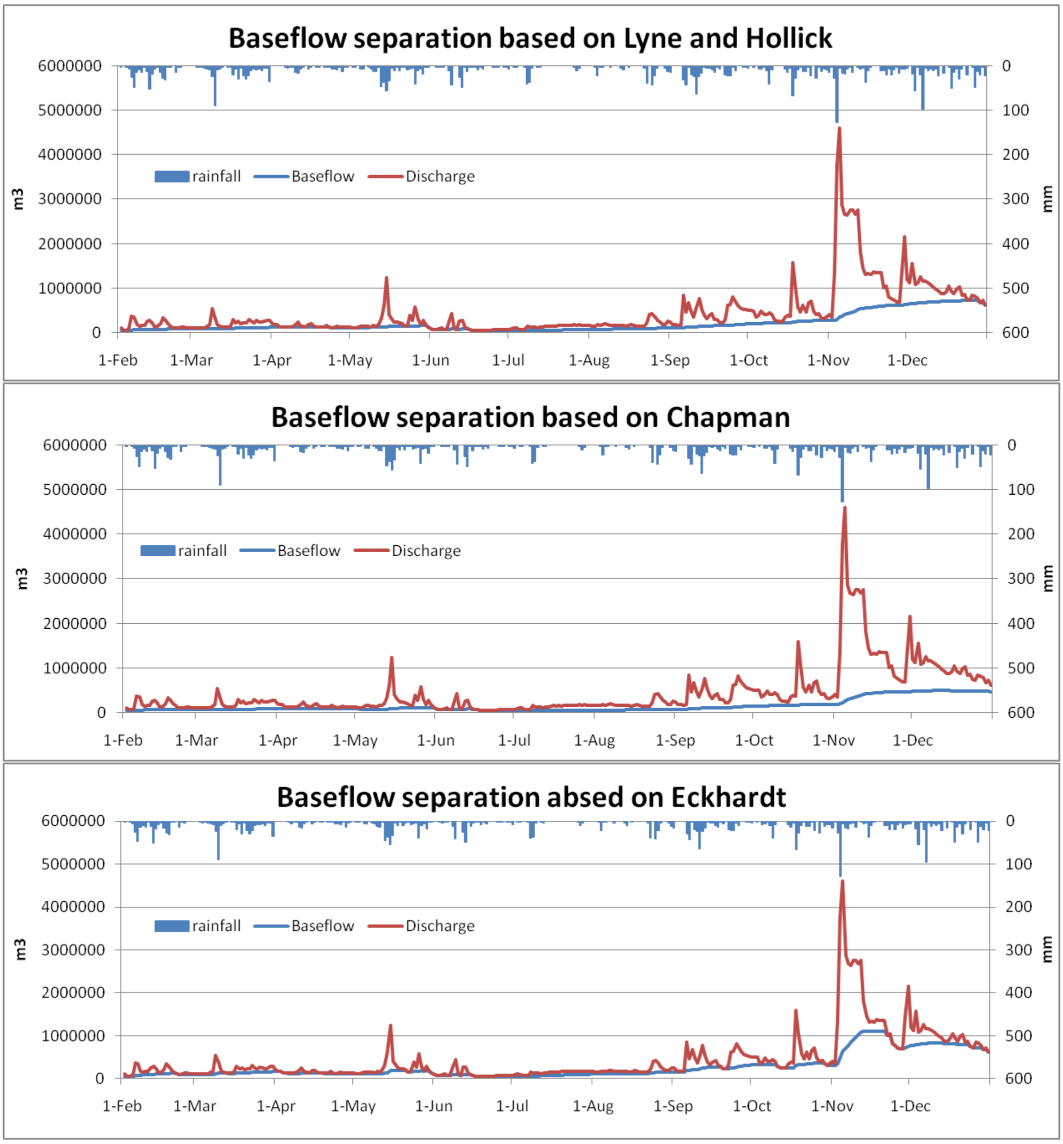

Graph 4-4. Baseflow separation using ABSCAN software

4.2.2.2. Mass balance check

Mass balance check is obtained by calculating all parameters in the hydrological processes. The principle is the incoming fluxs should be equals with the outgoing and storage.

4.2.2.3. Initial run

Initial run presented daily discharge produced by the model. The modeled discharge was compared to measured discharge obtained from the instrument in Pogung station. Comparing both discharge, Visual technique using graphic and plot was involved in the analysis. Statistical tests also were employed to know the correlation and deviation among them.

The method to compare those data is Pearson Product Moment Correlation method (McCuen, 1998). The equation to obtain the correlation is:

$$r = \frac{\sum x_i y_i - \left(\frac{\sum x_i \sum y_i}{n}\right)}{\sqrt{\sum x_i{}^2 - \left(\frac{(\sum x_i)^2}{n}\right)} \cdot \sqrt{\sum y_i{}^2 - \left(\frac{(\sum y_i)^2}{n}\right)}} \tag{4.21}$$

Where r is correlation coefficient; x_i is value of variable x; and y_i is value of variable y. This correlation indicates the strength and the direction of the relationship between variables.

Deviance measures are applicable when observed and simulated data can be paired according to time, location, treatment, etc (Mayer *et al*, 1993). He noted that an alternative to using absolute differences is to use second moments and using its square root, derive the root mean square error RMSE as :

$$RMSE = \sqrt{\frac{[\sum(y_i - ý_i)^2]}{n}} \tag{4.22}$$

$$NRMSE = \frac{RMSE}{x_{max} - x_{min}} \tag{4.23}$$

$$CV\ (RMSE) = \frac{RMSE}{\bar{x}} \tag{4.24}$$

Where y_i represent observed values, $ý_i$ simulated values, *n* the number pairs, *x* the value, and $\bar{x}$ average values.

4.2.2.4. Sensitivity analysis

Saturated hydraulic conductivity (Ksat), porosity, soil depth and maximum storage are the components of hydrology that were involved for sensitivity analysis. Those values were increased and decreased by 5%, 25% and 50% to know the response in the discharge result. The model had 24 simulations to run. The result plotted in a graph to determine the most sensitive parameters in the model.

4.2.2.5. Calibration

Considering the rank of sensitive parameter in the model, calibration was done by trial and error through decreasing or increasing parameter's values. Statistical analyses were considered to determine the calibrated model. The analyses are MAE, MA%E, RMSE, and Pearson correlation. Using rank, combination through trial and error which presents a better correlation and less deviation will be chosen as a calibrated model. The equation to determine MAE and MA%E (Mayer, 1993) are:

$$MAE = \frac{\sum |y_i - \acute{y}_i|}{n} \tag{4.25}$$

$$MA\%E = \frac{100\left[\sum\left(\frac{|y_i - \acute{y}_i|}{|y_i|}\right)\right]}{n} \tag{4.26}$$

4.2.2.6. Validation

Deviance measures and statistical test (Meyer, 1993) were employed in validation processes. RMSE, MAE, and MA%E were applied for deviance measures while student t-test and linier regression performed statistical test of modeled discharge. Student t-test was done using SPSS 17.0 software to determine relationship between measured and modeled discharge.

Beside comparing modeled after calibration and measured discharge, validation also was determined by comparing modeled discharge with independent data. Cited from Rykel (1996), The notion of validation by comparison to an independent set of data has subsequently been mentioned by many authors (e.g., Odum, 1983; Shugart, 1984; Jorgensen, 1986; Power, 1993). The independent data that was chosen is measured discharge data from Kaloran station. Kaloran station located in Kaloran, Bantul (sta no.1 in Figure 5-10) that records discharge in southern part of Code river (lower part of watershed).

4.2.3. Predicted discharge change due to soil and extreme rainfall event

Resulted of calibrated and validated model, predicted discharge due to soil change and extreme rainfall event were defined. The predicted discharge shows the impact of the eruption to the discharge.

4.2.3.1. Predicted discharge change due to soil change

Based on the first objective, there are several changes due to the eruption. This section simulated the discharge through the model to predict the discharge when those changes happen. Mean error and student t-test were also employed to describe the changes between initial model with simulated model based on those changes. Number of day with discharge more than 1 million m^3/day was highlighted to compare between initial model with simulated model. The discharge that more than 1 million m^3/day is assumed as discharge that potential to cause flooding.

4.2.3.2. Predicted discharge due to extreme rainfall event

In this section, rainfall data as an input in hydrological model were calculated using frequency analysis of Gumbell distribution. This distribution was selected based on distribution fitting test on extreme rainfall data 1984-2010 in Code watershed (see Appendix 5). Equations to define extreme event by Gumbell are:

Standard Deviation

$$Sx = \sqrt{\frac{(\sum x)^2 - \ \sum x^2/_n}{n-1}} \qquad (4.27)$$

Gumbell Distribution equation

$$\sigma = \frac{\sqrt{6} \quad Sx}{\pi} \qquad (4.28)$$

$$\mu = \times - 0.5772\sigma \qquad (4.29)$$

$$X = \sigma * \ - \ln[-\ln(Pl)] + \mu \qquad (4.30)$$

Where :

Sx : Standard deviation

x : maximum rainfall in a year

n : number of data

× : Mean / average of maximum rainfall

Pl : Left Probability on given return period

X : Predicted Rainfall on given return period

Using those equation, applied on rainfall data series from 1984 – 2010, Gumbel distribution determined rainfall value on some return periods. The data which is calculated is only extreme rainfall data means that in each year, maximum rainfall in a day is taken. About four return periods of 5 years, 20 years, 50 years, and 100 years have been made. Those rainfall data involved as an input on hydrological model and give predicted discharge.

To have an event based model, the extreme rainfall event should be placed correctly in the model that performs a year simulation. Since rainfall is local phenomena, history data of extreme rainfall event in study area had been overviewed to determine predicted time of extreme rainfall (Table 4-5).

Table 4-4. Extreme rainfall event in study area (mm)

Year	Date	Extreme rainfall	Rainfall of a day	
			Before	After
1984	4-Feb	120	30	10
1985	13-Feb	106	1	1
1986	24-Nov	104	4	17
1987	2-Feb	125	0	8
1988	10-Nov	90	14	5
1989	3-Mar	116	21	13
1990	7-Jan	77	1	0
1991	11-Apr	75	34	0
1992	15-Nov	110	0	30
1993	25-Mar	95	52	2
1994	25-Mar	76	73	14
1995	21-Jun	93	27	0
1996		no data		
1997	13-Feb	56	39	21
1998		no data		
1999	6-Mar	70	3	43
2000	22-Nov	200	11	15
2001	23-Mar	125	0	27
2002	25-Dec	165	2	20
2003	4-May	92	0	0
2004	17-Jan	125	75	0
2005	23-Feb	161	8	8
2006	10-Apr	145	0	5
2007		no data		
2008	11-Mar	188	10	22
2009	17-Nov	83	16	25
2010	9-Mar	102	27	25

Based on Table 4-5, extreme rainfall event occurs in January (2 events), February (5 events), March (7 events), April (2 events), May (1 event), June (1 event), November (5 event), and December (1 event). Considering that case, predicted extreme rainfall event from Gumbel calculation was put in randomly day of those month in the yearly model. To simulate, 2010 rainfall data was replaced with the extreme rainfall event on certain days (8 days in 8 months) resulting 8 predicted discharge. Averaged result of the discharge from those simulations was taken as predicted discharge of particular extreme rainfall event.

4.2.4. Flood prediction

The last objective is to predict flooding along Code river. One dimensional flood prediction by comparison bankfull discharge with predicted discharge resulted from the model. Bankfull discharge of Code river was taken from Widiyanto (2007) and Rahayu (2011) figuring pre and post eruption condition (see Appendix 6).

4.2.4.1. Response of Code river to predicted discharge

Since the model produced daily discharge, hydrograph of flood event was built to predict peak discharge, time base, and time to peak. Natural unit hydrograph was applied in this procedure. To determine Natural Unit Hydrograph, some flood events were collected in period of after the eruption.

There were 4 flood event derived from Pias paper of Automatic Water Level (AWLR) in Pogung, the outlet of Code watershed. Those flood events were selected as they give the peak of water level more than 2 meter. The events occur at January 3rd, January 9th, March 19th, and March 22nd 2011 with the peak of water level 2.96m, 2.46m, 2.88m, and 2.05m respectively. Natural Unit Hydrograph was derived from those events using principle of superposition (see Appendix 7).

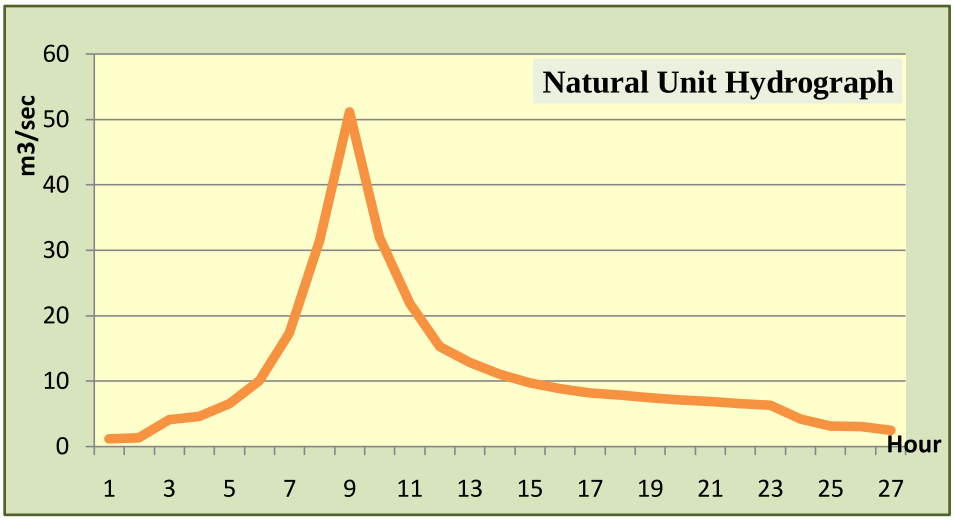

Graph 4-5. Natural unit hydrograph after the eruption

Considering the natural unit hydrograph, daily discharge resulting from the model was converted into unit hydrograph. Through the hydrograph, peak discharge in m^3/s can be derived and the result were compared with the bankfull discharge.

4.2.4.2. Determining flood prone section

Flood prone section of Code river was determined through the comparison and figured in a map. Comparison was carried out between predicted discharge and bankfull discharge. The bankfull discharge was measured by Widiyanto (2007) and Rahayu (2011) using manning's method. The result is flood prone area considering extreme rainfall event in 5, 20, 50, and 100 year return period in Code river, especially in Yogyakarta city.

5. RESULT AND DISCUSSION

5.1. Change of soil properties, soil depth and infiltration due to 2010 eruption

Knowing the impact of 2010 Merapi eruption in Code watershed is based on several evidences founded in the area. Being less destructive by the eruption, soil in Code experienced more change due to additional ash produced by the fall. Below are some explanations of the change related with the additional ash to soil that impacted hydrological process in the watershed.

5.1.1. Soil properties change

Using Soil Water Characteristic Hydraulic Properties Calculator, soil texture from 29 samples extracted some soil parameters. There are saturated hydraulic conductivity, field capacity, wilting point, and saturation. The values than grouped based on soil type produced by the soil map scale 1:50.000.

Table 5-1. Soil Properties calculated by soil water characteristics program

No	Soil Type	Sand	Silt	Clay	Porosity	Ksat	FC	WP
1.	Andic Dysropepts	73.50	22.75	3.75	43.23	96.52	11.15	3.20
2.	Andic Hapludolls	73.00	21.33	5.67	42.98	80.01	12.17	4.25
3.	Lithic Ustropepts	80.00	14.50	5.00	42.35	96.77	9.85	3.50
4.	Typic Fragiaquents	68.67	28.00	3.33	43.53	97.28	12.40	3.27
5.	Typic Hapludands	66.50	30.50	3.00	46.45	93.98	15.40	5.35
6.	Typic Tropothents	75.50	21.00	3.50	42.20	99.57	9.95	2.55

* all values are in % except for Ksat in mm/h

The result shows that topsoil in study area dominated by sand fraction with more than 65%, while clay is the lowest with only 3-5%. The other parameters such as field capacity, wilting point, and Ksat were not significantly differ among soil types. To know the change of those parameters, soil properties before the eruption must be known. Farida (2009) had measured soil properties in Code watershed before the 2010 eruption as shown in table 5-2.

Table 5-2. Soil Properties in Code watershed before the eruption (Farida, 2009)

No	Soil Type	Sand	Silt	Clay	Porosity	Ksat	FC	WP
1.	Andic Dysropepts	72.82	13.94	13.24	40.73	43.43	17.70	9.80
2.	Andic Hapludolls	58.00	29.40	12.60	48.63	35.05	20.50	9.20
3.	Lithic Ustropepts	63.23	15.37	21.40	29.94	17.78	24.00	14.30
4.	Typic Fragiaquents	66.96	21.49	11.55	47.55	5.08	18.50	9.20
5.	Typic Hapludands	63.88	14.66	21.46	48.42	18.03	23.80	14.30
6.	Typic Tropothents	56.45	24.00	19.55	44.32	18.29	24.80	13.70

* all values are in % except for Ksat in mm/h

From two tables above, porosity, field capacity, and wilting point were generally decreased. In general, the sand fraction increased while the clay fraction decreased. It could be argued that spreading ashfall by the eruption is the main factor for this change.

Student t-test was applied to know the influence of eruption to those parameters. Porosity, ksat, field capacity and wilting point of pre and post eruption have been involved in the test (see Appendix 10). According to the result, porosity has Sig.(2-tailed) 0.95 or higher than 0.025 (significance level alpha = 0.05). It means that there is no difference of porosity in pre and post eruption. In contrary, ksat, field capacity and wilting point have Sig.(2-tailed) < 0.025 means that there is difference between those value in pre and post eruption. To sum, 2010 Merapi eruption gives impact on ksat, field capacity and wilting point but does not impact on porosity.

Table 5-3. Paired samples test on soil properties derived from pedotransfer functions

		Paired Differences					t	df	Sig. (2-tailed)
		Mean	Std. Deviation	Std. Error Mean	95% Confidence Interval of the Difference				
					Lower	Upper			
Pair 1	Pre_Pore - Post_Pore	-0.19	6.58	2.69	-7.10	6.71	-0.07	5	.950
Pair 2	Pre_Ksat - Post_Ksat	-71.07	18.12	7.40	-90.10	-52.06	-9.61	5	.000
Pair 3	Pre_FC - Post_FC	9.73	3.81	1.56	5.73	13.73	6.25	5	.002
Pair 4	Pre_WP - Post_WP	8.06	2.61	1.07	5.32	10.81	7.53	5	.001

Another way to determine the change of soil properties is through comparing soil properties in affected and non-affected area by the pyroclastic flow. From soil sample map, sample Z was taken in affected area by the pyroclastic area in Kinahrejo. The result from SWC calculator of this sample compared with sample Y which taken from same soil type, Andic Dystropepts. The result is shown in table below.

Table 5-4. Comparison of soil properties in Affected and Non-Affected Area

Code	Landcover	Sand	Silt	Clay	Porosity	Ksat	FC	WP
Y	Evergreen Forest	77	22	1	42.3	22.6	20.9	13.8
Z	Built-up Area	78	19	3	46.6	112	11.5	4.0

Generally, both soil textures represent relatively same composition of sand, silt, and clay. It could be argued that both area experienced equal ash by the eruption which affects soil properties so there is no significantly differ in both result. Differentiate among them are the value of porosity and ksat that significantly higher in affected area (Z). Meanwhile, field capacity and wilting point in affected area (Z) is lower than that in non-affected area (Y).

5.1.2. Soil depth change

With the interval of 500 meter of 23 km length in Code watershed means that 46 information on ash thickness should be taken. Unfortunatelly, in some places there were unknown information of the thickness due to forgetfullnes, no built-up unit/no people to asked, and a difficult terrain. That cases make the 500 meter interval that have been planned did not work properly.

During field work, 41 information of ash thickness were obtained from local people. The information be plotted and made into linear regression (Figure 5-1). The trendline was concluded as ash thickness considering the distance from the top of Merapi.

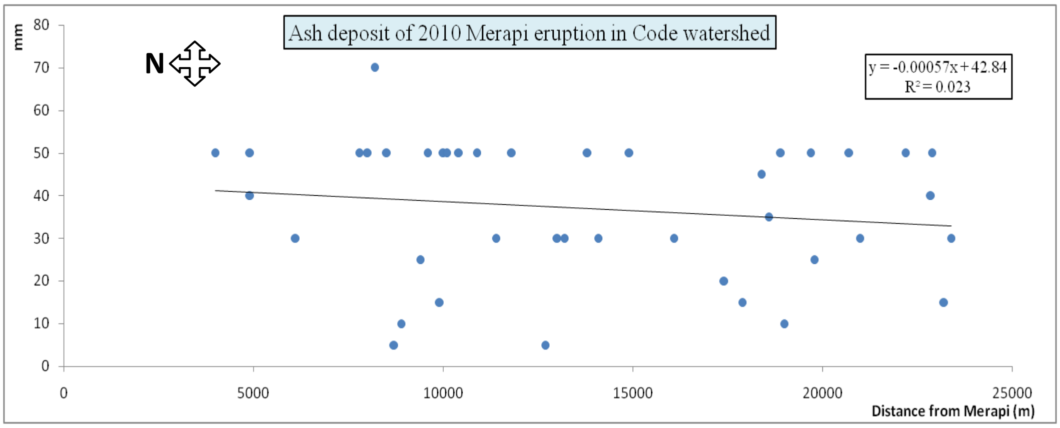

Figure 5-1. Information of ash thickness from local people

According to the ash thickness, post-eruption soil depth was determined by overlying pre-eruption soil depth map with ash thickness map from field work (Figure 5-2). Limitation occurs correlated with the assumption of linier spread of the ash following latitude without considering wind direction. Another thing to consider is the ash have been cleaned by people in built-up unit or swept away by the erosion. It might be resulted in a decreasing of the ash thickness. To sum up, it can be concluded that the change of soil depth due to 2010 Merapi eruption in Code watershed is 32 – 41 mm.

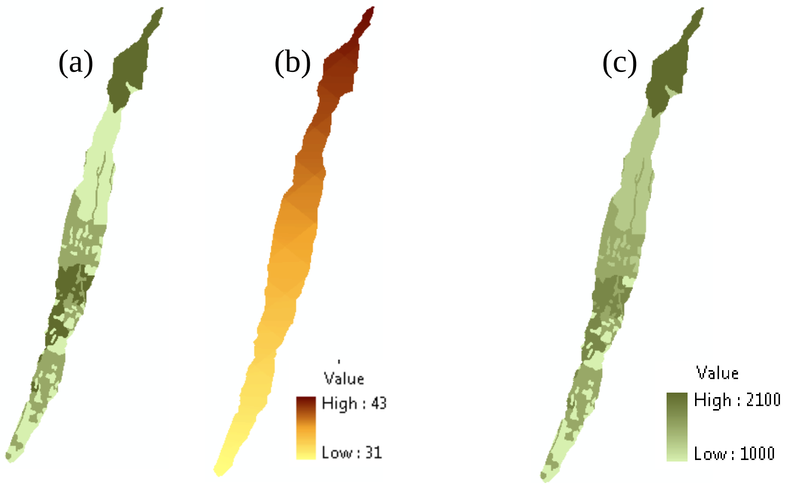

Figure 5-2. Overlay process of post eruption soil depth (value in mm)
(a) soil depth before eruption, (b) ash thickness, (c) soil depth after eruption

5.1.3. Infiltration change

Using Horton method, Table 5-5 shows infiltration rate based on soil type in Code watershed from 29 samples (see Appendix 8). Those values were averaged from several sample based on soil type. The lowest rate of 0.362 cm/min occurs in Typic Hapludands while the highest of 0.764 cm/min in Andic Dystropepts.

Table 5-5. Infiltration Rate in Code watershed
(Source : Laboratory analysis and field measurement)

No	Soil Type	Organic matter	Carbon content	Infiltration Rate (cm/min)	Texture
1.	Andic Dysropepts	2.27	1.32	0.764	Sandy Loam
2.	Andic Hapludolls	2.19	1.27	0.637	Sandy Loam
3.	Lithic Ustropepts	1.77	1.03	0.543	Loamy sand
4.	Typic Fragiaquents	1.66	1.54	0.440	Sandy Loam
5.	Typic Hapludands	4.55	2.64	0.362	Sandy Loam
6.	Typic Tropothents	1.55	0.90	0.652	Loamy sand

To compare the infiltration rate before and after the eruption, a research conducted by Noordianto (2005) was delivered to this study. He measured infiltration rate in four locations between Boyong and Kuning river (see Appendix 9). Based on his research, averaged infiltration rate near Code watershed gained 1.38 and 0.79 cm/min in Tanen and Banteng respectively.

According to Sosrodarsono *et al* (1993), measuring infiltration rate using double/single ring infiltrometer has the same problem : (1) the effect of splash rainfall are not taken into account, (2) effects of air pressure in the soil does not occur, and (3) structure of the soil around the instrument had been disturbed when the instrument is installed. Regarding those problems, as cited by Asdak (2007) from Dunne and Leopold (1978), infiltration rate that was obtained using that method generally 2 – 10 times higher than what happened in the field. Infiltration also related with the time when the measurement was taken.

Considering to the result and condition, it could be argued that the eruption makes the infiltration rates in Code watershed decreased. Being added by the ash, sand fraction in study area was increased. Prachansri (2007) noted that soil containing large amount of the sand and silt tend to form crusts and become compacted, which significantly reduces the infiltration rate.

5.2. Constructing the hydrological model

Hydrological model in this research was developed in PCRaster and Nutshell program. The model used the script constructed by Jetten (2011) with adjusted input for initial condition, i.e. initialize soil moisture is 1.5 times of field capacity (see Appendix-1 of initialize variables section). Hydrological model divided into 2 models, model pre eruption during 2010 and model post eruption during January 2011 – May 2011.

5.2.1. Initial input of hydrological model

To construct hydrological model, there are steps to follow. Build initial map, determine landcover, rainfall data, soil properties data, evapotranspiration data, and vegetation cover data are the steps. Below are the initial inputs to construct hydrological model.

5.2.1.1. Landcover data

The result of ground check on landcover interpretation (Table 5-6) gives 90.2 % that is correct. It means that in general it is enough to be used, but interpretation on croplands had many miss. It is related with seasonal behavior. Most of the farmers cultivate their land as paddy field and other agricultural plants following season. In the wet season, they plant paddy while in the dry season when the water is not enough for paddy they grow crops such as corn, peanut, chili, cassava, tobacco, etc. In fact, in some part where the water is relatively abundant, farmers plant paddy all year round.

Table 5-6. Result of ground check in landcover

Landcover	Area (m^2)	N	Correct	Wrong	Percentage	Result
Bare exposed rock	3,047,656	5	4	1	80 %	
Build-up land	4,417,043	7	7	0	100 %	
Croplands and pasture	12,920,717	21	17	4	81%	
Evergreen forest land	2,057,991	3	2	1	67%	**90.2 %**
Mixed rangeland	7,000,804	12	12	0	100%	
Streams and canal	983,011	2	2	0	100%	
Transportation	15,487	1	1	0	100%	

Since paddy field has different characteristic with other crops field, it is always inundated, paddy field should be extracted from croplands and pasture. The new landcover map has been created with the addition of paddy field (Figure 5-3).

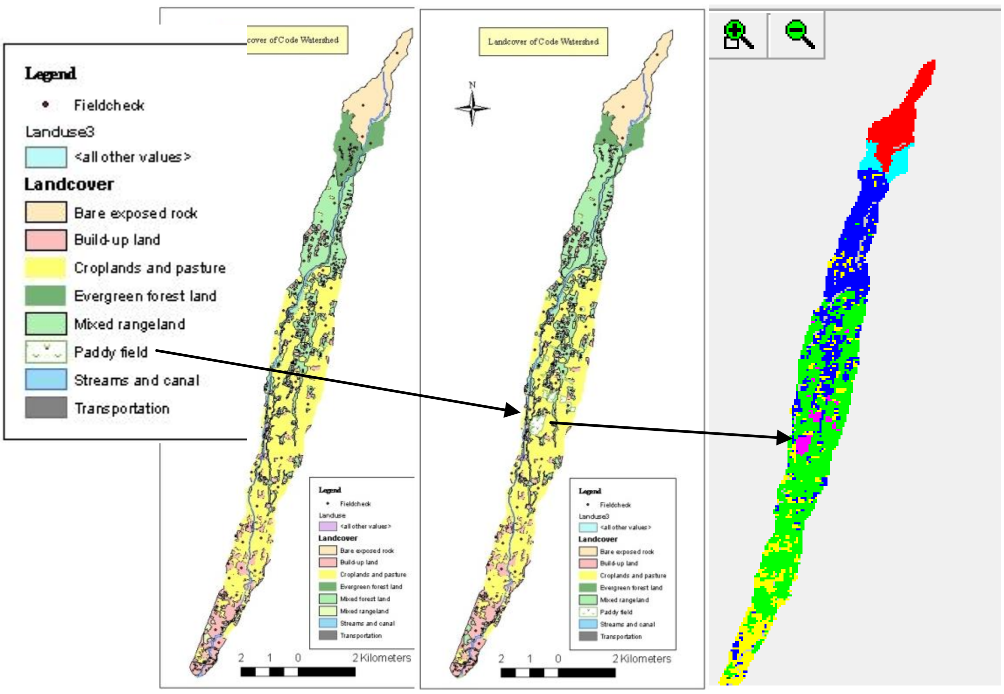

Figure 5-3. Landcover in Code watershed; before (left) and after (center) groundcheck, landcover map in the model (right)

5.2.1.2. Rainfall data

Data processing on rainfall data resulted datasets from Pakem and Beran to involve in the model. Graph below shows the data of those two rainfall stations and result of inverse distance interpolation with power of 2 resulted from the model.

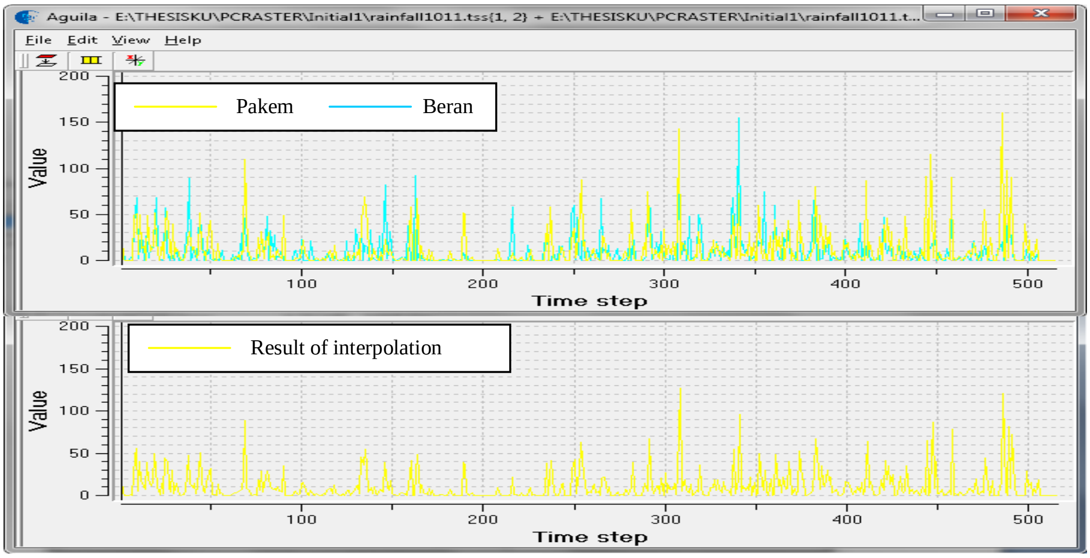

Graph 5-1. Rainfall data of 2010 – May 2011 in study area

5.2.1.3. Vegetation cover data

Vegetation cover was determined through indirect method using photograph and field measurement. Actually, the value of vegetation cover especially for crop was in monthly period considering the planting and harvesting period in a year. Considering that crops grow faster in just three month, equation from Hadi (2011) applied in the model. This method assumed that vegetation cover and further maximum storage of crops will differ in daily period representing the growth (Figure 5-4).

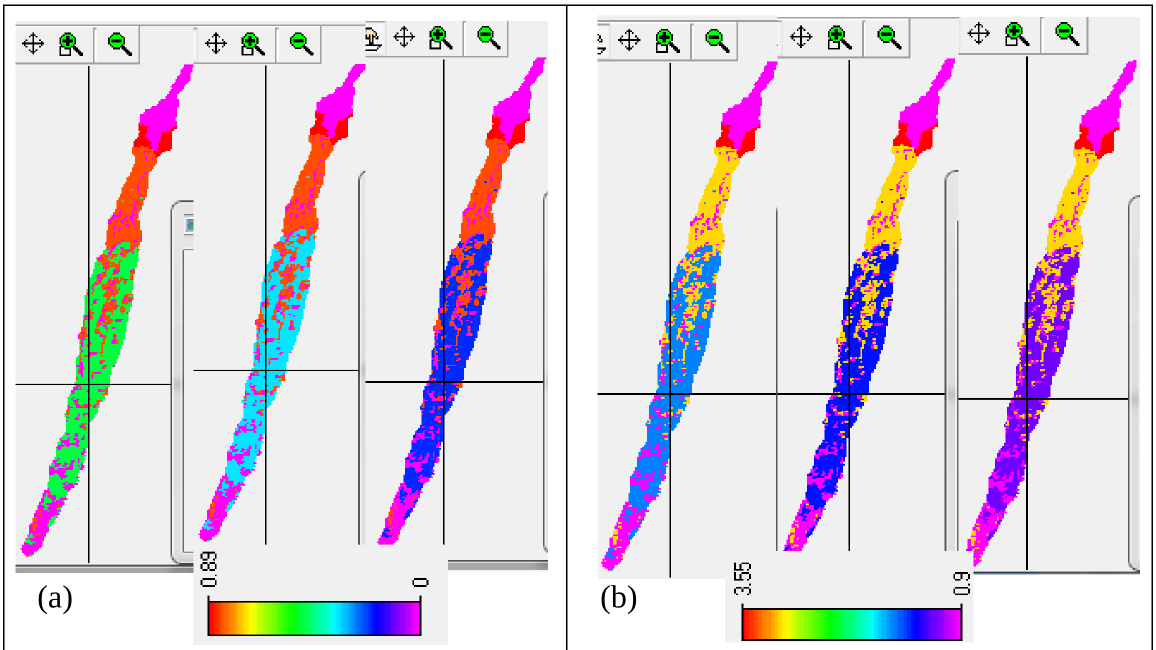

Figure 5-4. Left to right (a) : vegetation cover in the model of day 40th, 50th and 60th.
Left to right (b) : maximum storage in the model of day 40th, 50th, and 60th.

5.2.1.4. Evapotranspiration data

Result of reference evapotranspiration (ETo) calculation using FAO Penman-Monteith method was transformed into time series data as an input in the model. Below is the graph of timeseries data of reference evapotranspiration compared with actual evapotranspiration.

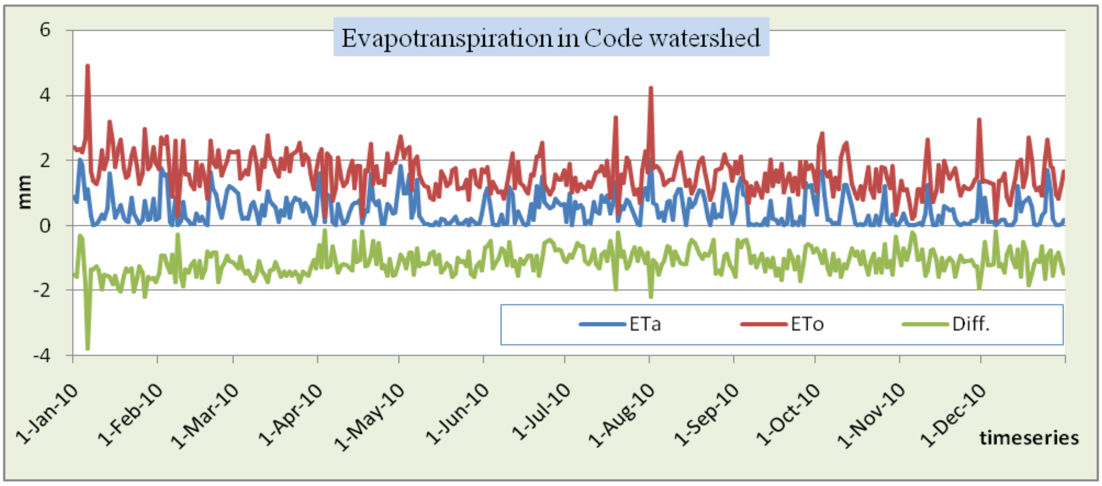

Graph 5-2. ETo and ETa of 2010 in Code watershed

5.2.2. Mass balance check

The principle of mass balance check is incoming fluxes equals with outgoing fluxes and change in storage (Figure 2-3). Based on the figure, incoming flux cames from rainfall while the outcoming are tranpiration, evaporation, and river discharge. A complete water balance from the model is shown in figure below.

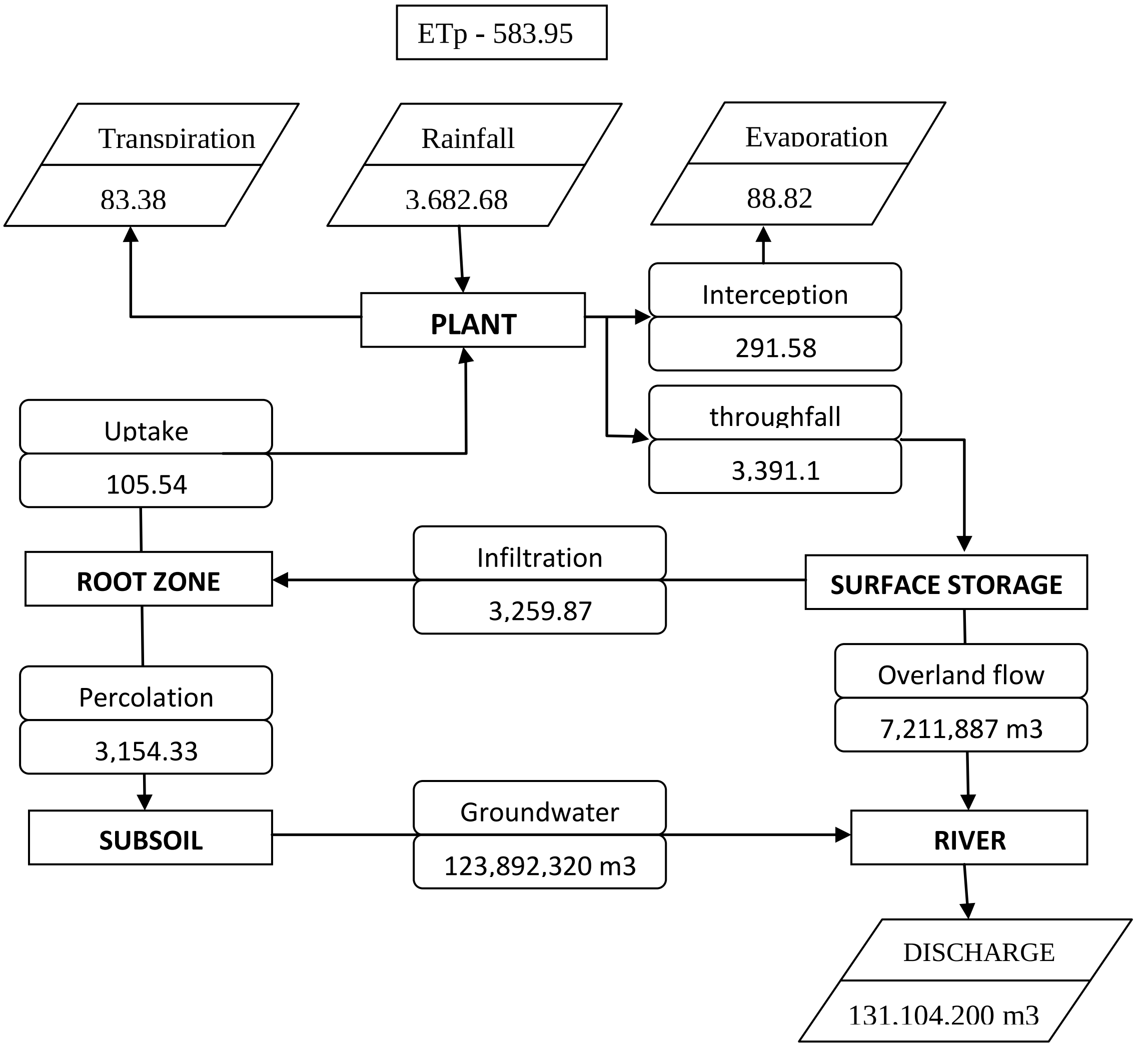

* all values are in mm/cell except for groundwater, overlandflow, and discharge
The study area consists of 303,902 cell, with 1 cell area = 100 m^2.

Figure 5-5. The mass balance check based on the model

Table 5-7 below shows the different amount of those fluxs obtained from the model. Groundwater result in the model is 123,892,320 m^3 while on percolation in the model is 95,850,690 m^3. It means that about 28,041,629 m^3 was added by the subsoil become groundwater. The deviance also occurs in overland flow where about 3,230,770 m^3 was added into overland flow.

Table 5-7. Deviance of mass balance check in the model

	Percolation	Surface storage (Throughfall - Interception)	Ground water	Overland flow	Unit
Amount	3,154	131	4,076	237	mm/cell
convert to m (/ 1000)	3.15	0.13	4.08	0.24	m/cell
times nr. Cell (x 303902)	958,507	39,811	1,238,923	72,119	m/area
times cellarea (x 100)	95,850,690	3,981,116	123,892,300	7,211,887	m^3

According to Graph 4-4, measured discharge was separated using ABSCAN program results yearly baseflow and peakflow as shown on Table 5-8 below. It can be concluded that the model failed to separate baseflow and peakflow. Baseflow in the model tends to higher while peakflow lower than amount in the measured. This deviance on mass balance check might be caused by an error in groundwater part in the model. This section is mainly affected by the soil depth.

Table 5-8. Baseflow and peakflow difference of model and measured discharge

Datasets of 2010	Baseflow (m^3)	Peakflow (m^3)	Discharge (m^3)
Hydrological model	123,892,300	7,211,887	131,104,187
Lyne and Hollick	68,820,887	79,828,839	148,649,727
Chapman	50,955,649	97,694,077	148,649,727
Eckhardt	90,408,068	58,241,658	148,649,727

5.2.3. Initial run

There are two outputs of the model, the first is modeled discharge before the eruption and another is modeled discharge after the eruption. Modeled discharge before the eruption has time period of 2010 with eruption occurs during late October until early December 2010. The result of the modeled discharge is shown on graph 5-3 below.

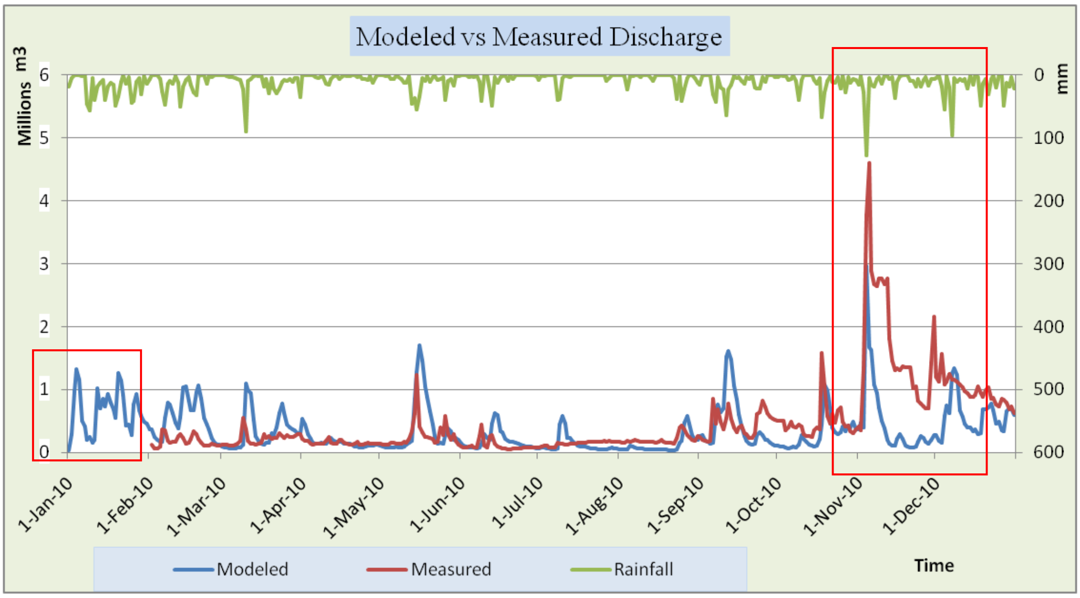

Graph 5-3. Daily Modeled and Measured Discharge of Code watershed

Based on the graph 5-3 above, modeled discharge noted that the highest discharge occurs in 4th November 2010 gains 2,956,920 m^3/day. On the other hand, the highest discharge in measured discharge occurs in 5th November 2010 reach 4,608,867 m^3/day. In addition, rainfall data recorded the depth of 127.24 mm in 4th November 2010. This is the cause of increasing the modeled discharge gained its peak in this year.

Based on visual observation through the graph, generally the model performs well enough in presenting the peak discharge. That case as shown in February – October 2010 while in January 2010 the value of measured discharge is missing. During the eruption (26th October 2010 – December 2010), measured discharge was noted higher than modeled discharge. To have a better visualization, monthly discharge as shown below.

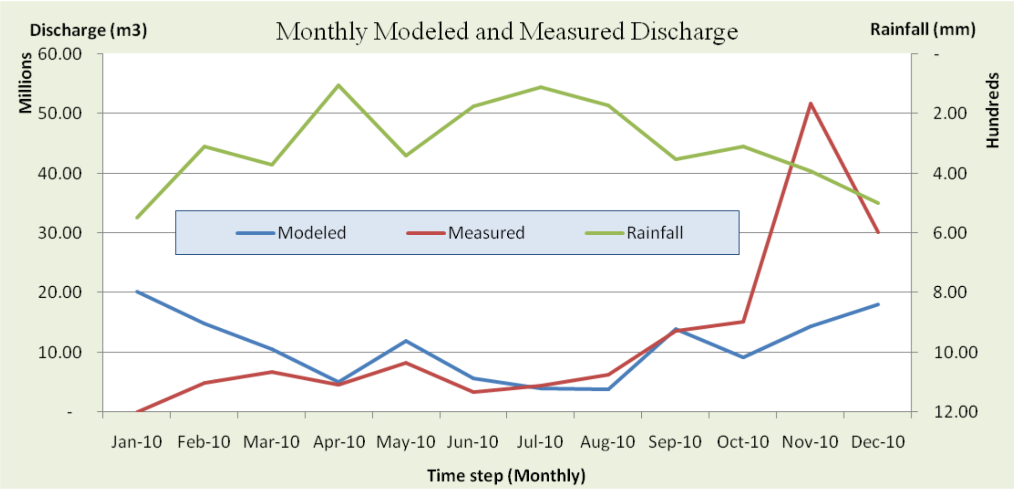

Graph 5-4. Monthly modeled and measured discharge of Code watershed

According to the Graph 5-4, during the eruption in late October until early December 2010 measured discharge has extremely higher of the amount of water than modeled discharge. During that period, 32,327,396 m^3 of discharge occurs based on the model while measured discharge at the same period noted 81,802,633 m^3. This condition might be happened as the eruption gives lahars to the river, and the instrument recorded water level with additional lahars in the river. This sedimentation on the river section that measured might be caused the discharge data was extremely high than before. In general, modeled discharge was closer to measured discharge if excluding January which has no data and November-December 2010 which eruption occurs.

After the eruption, the model has a larger discrepancy (error) compared to the measured discharge as shown below.

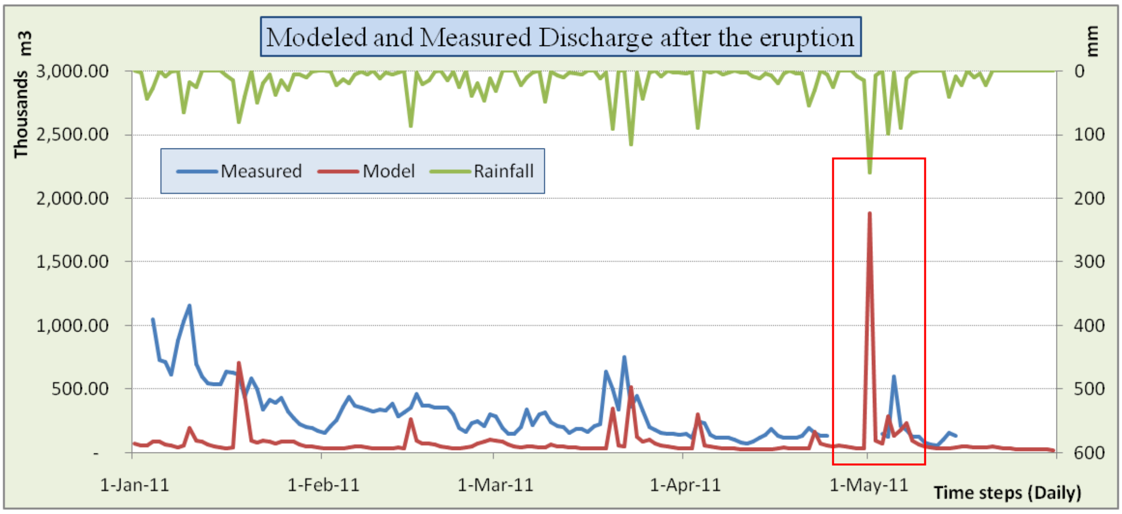

Graph 5-5. Modeled and measured discharge of post eruption

Post eruption model noted that the highest discharge of 1,882,840 m^3 occurs in May 1st, 2011. At that time, Pakem rainfall station recorded rainfall depth of 160 mm in a day. Unfortunately the instrument was not recorded the discharge in May 1st, 2011. In addition, as reported by local newspaper (www.tribunnews.com, www.krjogja.com), Purwokinanti, Sayidan, Terban, Sorogenen. Danurejan, Jetis, Gowongan, and Cokrodiningratan in Yogyakarta city and Sorogenen in Bantul regency, are down part of Code river, experienced flood by the event. This event also causes AWLR instrument to measure discharge in Kaloran, Bantul broken.

Figure 5-6. AWLR instrument in Kaloran, Bantul (downpart of Code watershed)

In addition, measured discharge records the highest discharge until May 2011 is 1,159,266 in January 10th, 2011. Comparison was also carried by plotting those discharges into scattered graph (Graph 5-6).

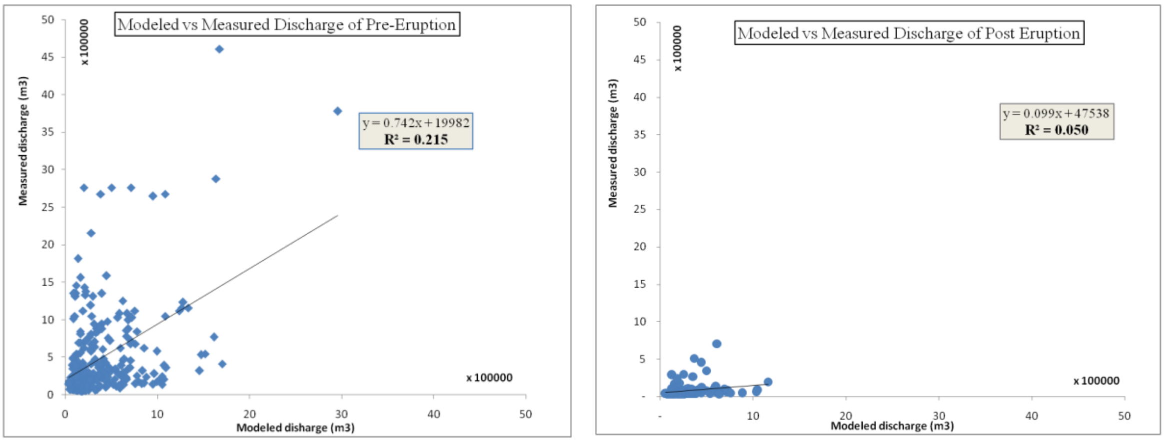

Graph 5-6. Correlation of modeled and measured discharge on pre and post eruption

According to table 5-8, NRMSE gives 18 % for modeled discharge indicate pre eruption model has less residual variance than post eruption model that gives 46 %. Coefficient of variation of the RMSE is defined as the RMSE to the mean of the observed values. Coefficients of variation are 1.60 and 3.99 for modeled before and after the eruption respectively. The Pearson's correlation coefficient noted 0.46 and 0.22 for before and after the eruption respectively. The correlation determines the closeness of measured and modeled discharge.

Table 5-9. Deviation of modeled discharge to measured discharge

Parameter	Modeled Pre Eruption		Modeled Post Eruption	
Mean	359.189.60	m^3	83,566.34	m^3
X min	32.350.40	m^3	21,400.50	m^3
X max	2.956.920.00	m^3	1,882,840.00	m^3
RMSE (Root Mean Square Error)	530,488.55	m^3	310,677.81	m^3
Normalized RMSE (NRMSE)	18	%	46	%
Coefficient of variation RMSE	1.60		3.99	
Pearson's Correlation	0.46		0.22	

Source : Calculation of Model result on Microsoft Excel 2007

It could be argued that this lower correlation was caused by some deficiencies in the model. First, precipitation in the model resulted from rain stations which located outside of the study area. The station itself does not represent the whole area since there is no rain station in upper part of study area, so it just represents lower and middle part of study area. Cited from Barry (1992) as recognized by Salter (1918) from analysis of British data, the effect of altitude on the vertical distribution of precipitation in mountain areas is highly variable in different geographical locations. To gain adequate understanding of these variations, He recommends to consider the basic condensation processes and the ways in which mountains can affect the cloud and precipitation regimes.

Second, soil properties such as saturated hydraulic conductivity, field capacity and wilting point were generated from the soil properties calculator produced by the United States. Deficiencies may occur since the soil in study area is typically mountainous type and probably not appropriates with soil reference in pedotranfer calculation.

Third, landcover classification was done based on visual interpretation through SPOT 5 satellite image. Generally, vegetation cover was determined through NDVI calculation from satellite image. Limited in image visualization, some unit were generalized and grouped into a type of landcover, in example built-up unit in some case were coincided with plants or crops but generalized as built-up area. This deficiency causes vegetation cover become lower than actual value and further affected maximum storage in the model. Forth, soil depth data was generated from digital soil map data. The depth analysis follows soil unit type with general value between 100 until 200 cm.

5.2.4. Sensitivity analysis

There are four hydrological component tested with sensitivity analysis. Saturated hydroulic conductivity (Ksat), soil porosity, maximum storage, and soil depth are the components. This analysis was employed to find out which component is the most sensitive to the discharge. The analysis was performed in the model by increasing and decreasing the components value in 5%, 25%, and 50%. The result of the analysis is presented below.

Table 5-10. Sensitivity analysis on the hydrologic model

Parameter simulation		-50%	-25%	-5%	Initial	5%	25%	50%
Ksat	Min	20,161.7	26,421.5	31,196.4	32,350.4	33,587.1	37,909.1	38,327.3
	Max	3,187,730	3,090,750	2,995,040	2,956,920	2,928,730	2,802,220	2,709,090
	Average	377656.17	363,157	358,939.2	359,189.6	358,090.31	346,212.56	344,801.06
	Total Year	137,844,503	132,552,304	131,012,813	131,104,205	130,702,964	126,367,584	125,852,386
	Different	6,740,297	1,448,098.3	-91,392.7		-401,240.9	-4,736,621	-5,251,820
	Percentage	105%	101%	100%		100%	96%	96%
Pore	Min			36,453.6	32,350.4	24,712.7	7,895.55	2,673.82
	Max			3,028,060	2,956,920	2,884,060	2,498,320	2,135,120
	Average			356,497.35	359,189.6	359,548.79	346,054.72	335,880.39
	Total Year			130,121,533	131,104,205	131,235,307	126,309,974	122,596,344
	Different			-982,672		131,102	-4,794,232	-8,507,862
	Percentage	0%	0%	99%		100%	96%	94%
Smax	Min	32,440.4	32,401.8	32,363.7	32,350.4	32,344.5	32,317.9	32,293.4
	Max	299,9160	2,984,680	2,964,990	2,956,920	2,949,710	2,932,430	2,901,070
	Average	368,561.85	364,406.68	360,336.33	359,189.6	358,063.25	353,989.74	347,931.27
	Total Year	134,525,076	133,008,438	131,522,759	131,104,205	130,693,086	129,206,255	126,994,915
	Different	3,420,871	1,904,232.9	418,554		-411,119.4	-1,897,950	-4,109,290
	Percentage	103%	101%	100%		100%	99%	97%
Soil depth	Min	10,030.9	23,598.4	32,013.2	32,350.4	32,772.6	34,256.7	36,121.2
	Max	3,148,100	3,154,390	3,021,700	2,956,920	2,814,180	2,672,540	2,924,910
	Average	88,226.581	220,837.54	349,905.68	359,189.6	368,969.58	496,696.48	573,080.58
	Total Year	32,202,702	80,605,702	127,715,573	131,104,205	134,673,897	181,294,215	209,174,411
	Different	-98,901,503	-50,498,504	-3,388,632		3,569,692.1	50,190,009	78,070,206
	Percentage	25%	61%	97%		103%	138%	160%

* Unit: min, max, and average are m^3/day; total year and different are m^3/year

From table 5-9, it can be concluded that soil depth is the most sensitive among four components tested. Besides, soil depth gives different response to the discharge compare to the others. Ksat, soil porosity and maximum storage decrease the discharge when those values increased while soil depth gives positive response to the discharge (Graph 5-7). Increasing the storage in canopy makes more water intercepted and gives opportunity for the sun energy to evaporate the water back to the atmosphere. This small cycle contributed to the decrease of discharge in the end.

Soil depth according to Seyhan (1977) is the zone where precipitation first enters and the water moves vertically either by means of evapotranspiration to the atmosphere or by means of downward percolation from the unsaturated soil water zone to the saturated zone toward the groundwater table.

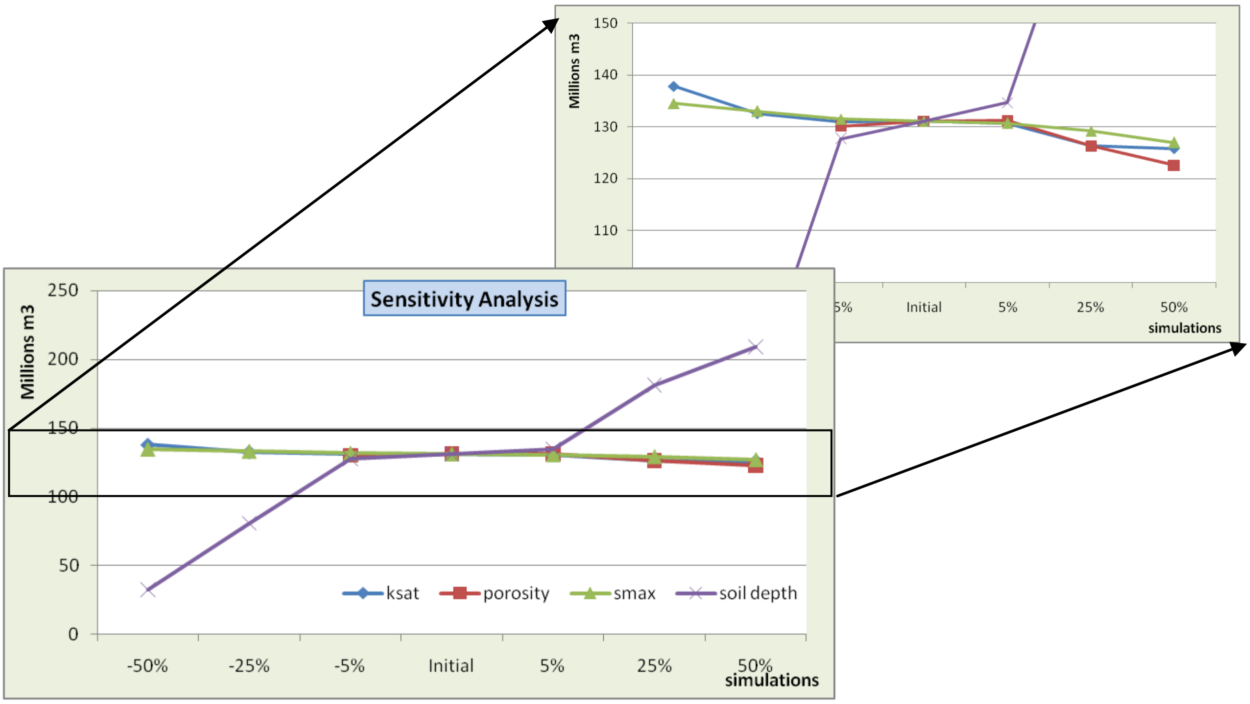

Graph 5-7. Response of modeled discharge by manipulating its components

In the model, soil depth correlated with baseflow and peakflow but give different result in the discharge. The process involved unsaturated depth, storage, infiltration capacity, ground water depth, and groundwater loss. Two processes of soil depth correlating the discharge is shows on Figure 5-7 below.

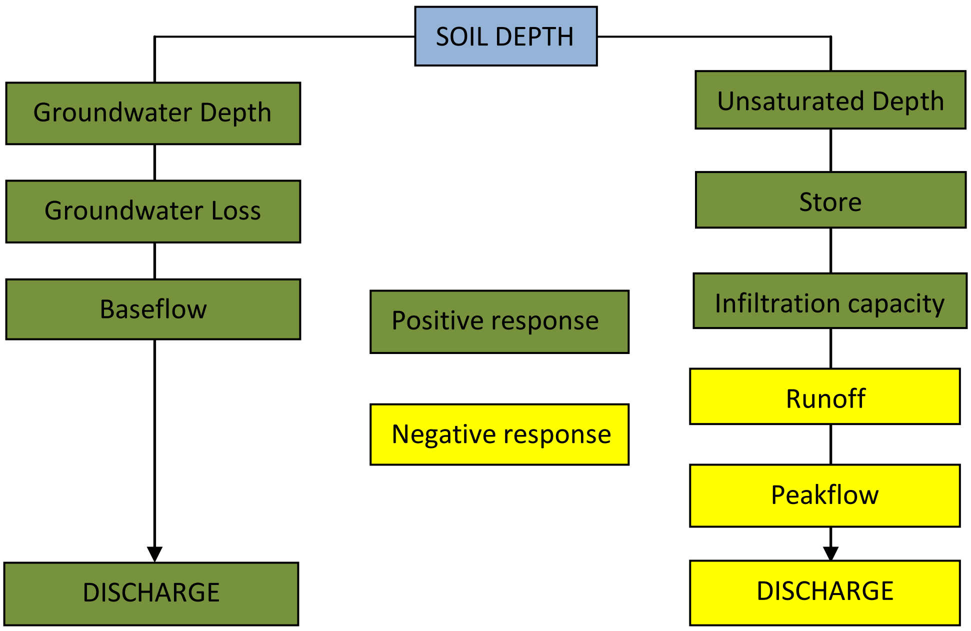

Figure 5-7. Flux of Soil Depth influencing discharge in the model

Based on the model, soil depth influences the discharge in two ways. First, soil depth will influence groundwater and further caused baseflow increase. In contrary, high infiltration capacity makes less water become runoff. This case contributes to the less of discharge from peakflow. The Graph 5-8 below shows how the discharge in Code river is came from. Mostly the amount of discharge is taken from the baseflow. That is why the soil depth becomes the most sensitive in the model.

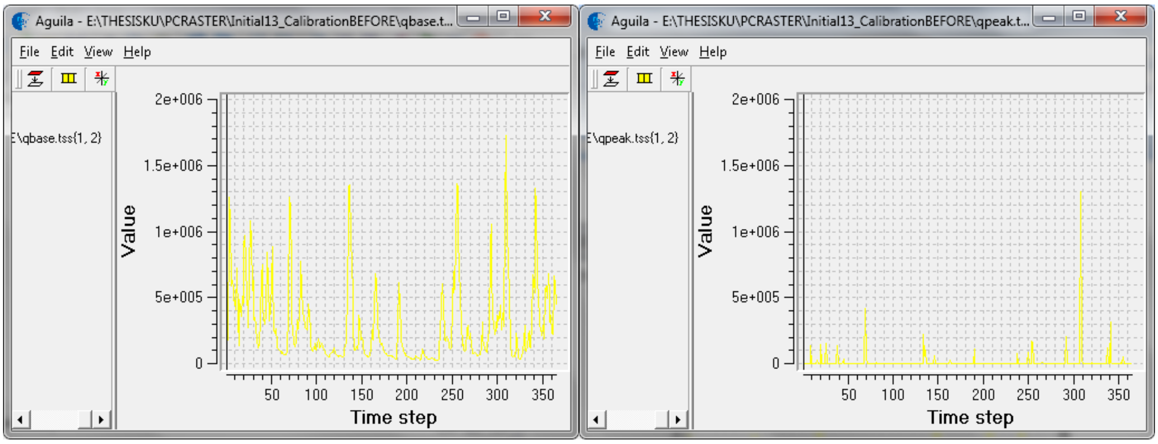

Graph 5-8. Baseflow (left) and peakflow (right) of the model

5.2.5. Calibration

Result of sensitivity analysis was considered in calibration process. The most sensitive parameter was simulated with less change than the others. After run several simulation using iteration process, the best composition of the model resulting discharge as measured discharge is presented in Table 5-11 below.

Table 5-11 Calibration process on pre-eruption model

Simulation	Mean	MAE	MA%E	RMSE	Correl	R^2	Σ Rank
initial	359,189.60	309,974.50	83.36	530,488.55	0.46	0.22	11
a_cal = 1	289,836.87	287,683.54	66.24	546,532.50	0.44	0.19	15
a_cal = 0,11	249,403.59	359,762.74	83.87	639,329.51	0.30	0.09	20
margin = 100	259,082.15	315,244.20	66.32	595,196.37	0.36	0.13	20
margin = 300	258,545.04	315,785.22	66.32	595,126.97	0.36	0.13	20
a+5, b+5, c+5, d+5	290,903.08	284,451.66	66.29	544,810.53	0.44	0.19	11
a+5,b+10,c+10,d+10	260,269.97	313,778.06	63.99	595,262.95	0.35	0.13	18
a+5,b-50,d-50	280,591.15	312,342.42	68.07	588,904.12	0.36	0.13	20
a+15,b-50,d-50	276,260.47	305,985.74	63.39	586,814.82	0.37	0.14	17
a+25,b-50,d-50	358,817.57	294,175.16	71.08	560,946.84	0.41	0.17	20
a+50,b-50,d-50	368,412.98	287,610.46	69.64	548,304.63	0.43	0.19	18
a+50, b-60, c-10, d-60	386,029.59	295,170.70	77.08	548,679.58	0.43	0.19	20

Note : a : soil depth, b : ksat, c : soil porosity, d : maximum storage,
± indicate increased/decreased value by percent. (a+5 means the value of soil depth increased by 5%)
Mean, MAE, RMSE was in m^3; MA%E in %.

Rank of MAE, MA%E, RMSE, Correlation, and R^2 to determine the best model :
Rank 1 Rank 2 Rank 3 Rank 4

Simulation to obtain the best fit of the model results that initial model with a_cal = 0.41 and margin = 200, is the best composition compared to the other. a_cal is calibration factor in the model to measure infiltration capacity (see in infiltration section on the script in Appendix-1) and margin is a value to represent unsaturated zone (see in adjust water balance component on the script of Appendix-1). Although the simulation gives 2 lower rank for initial and simulation with increased all value with 5%, the initial was chosen considering mean of the model that is closer to the mean of measured discharge of 446,395.63 m^3.

Calibration process on post-eruption model was done by a same process. The adjustment to get a good enough model represent the real discharge was pointed on seventh simulation. The proportion of soil depth was decreased by 15 %, while porosity, ksat, and storage maximum were increased by 5%. This composition gives correlation of 0.30 with R^2 is 0.09.

Table 5-12 Calibration process on post-eruption model

Simulation	Mean	MAE	MA%E	RMSE	Correl	R^2	Σ Rank
initial	77.863.11	235,300.90	72.58	310,677.81	0.22	0.05	20
b+5, c+5, d+5	367,089.69	212,289.42	86.00	309,985.03	0.26	0.07	20
a+1, b-5, c-5,d-5	369,835.60	213,495.48	85.85	321,837.11	0.26	0.07	20
a+5, b-5, c-5,d-5	377,016.06	217,116.25	88.36	317,904.95	0.27	0.07	20
a-5, b+10, c+10, d+10	358,212.94	207,763.00	83.35	308,699.22	0.25	0.06	20
a-10, b+5, c+5, d+5	343,848.81	203,997.46	77.85	306,605.74	0.28	0.08	20
a-10, b+25, c+50, d+50	349,686.77	196,717.62	81.91	278,752.13	0.23	0.06	18
a-15, b+5, c+5, d+5	323,433.09	196,261.60	71.44	288,403.51	0.30	0.09	12
a-15, b+15, c+15, d+15	323,145.30	193,757.17	71.00	283,634.31	0.29	0.08	13
a-15, b+25, c+25, d+25	324,170.27	192,760.14	71.91	279,113.08	0.28	0.08	13
a-15, b+25, c+50, d+50	330,370.31	189,468.96	73.60	270,188.97	0.27	0.07	14

note : table explanation as Table 5-10

Those two calibrations on pre and post eruption model did not give a well enough result. Correlation on both model were below 0.5 and percentage of error (MA%E) still high. The author assumed that this condition happens as the model can not figured out additional lahars in the discharge. The operator who managed measured discharge data once told to the author that the data after the eruption is extremely high and unusual. The instrument that recorded water level in Pogung has missing value in 2011. It recorded that 27 of 151 or 18 % daily discharge during January – May 2011 were unrecorded. The highest discharge noted by the model obtained from rainfall depth 160 mm was no record in the instrument.

Graph 5-9 below shows measured and modeled discharge after calibration process. According to pre eruption model, modeled discharge is generally over predicted when figuring peak discharge and become under-forecasting during October 2010. Post eruption model, except in the early period, the modeled discharge is overestimates to measured discharge.

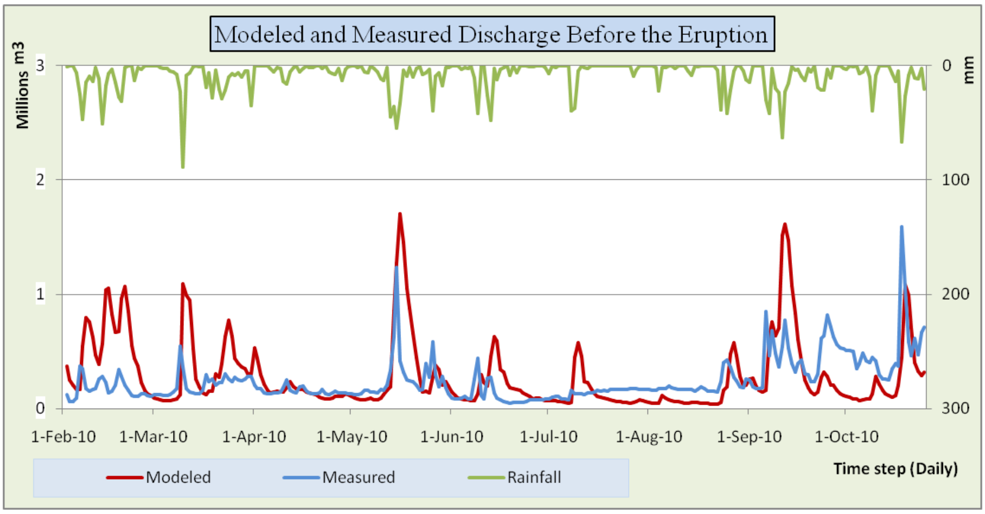

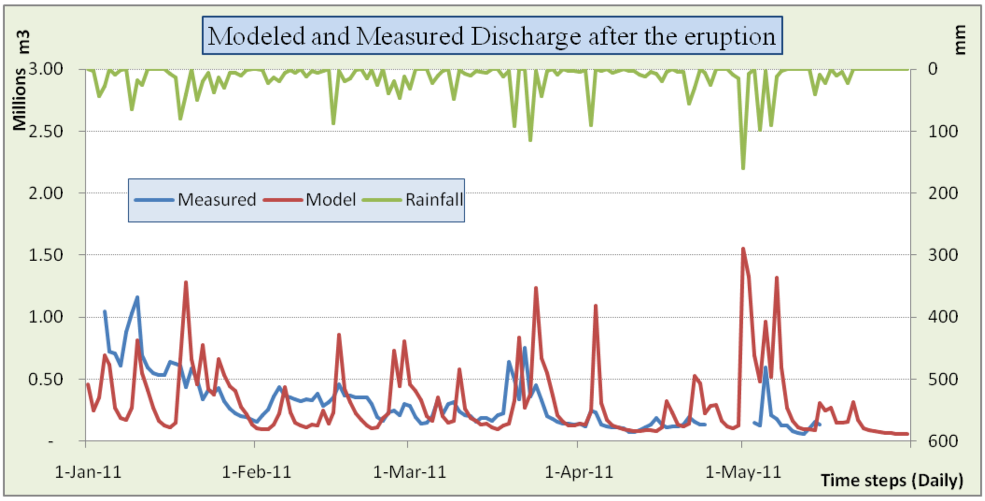

Graph 5-9. Modeled and measured discharge after calibration process.

5.2.6. Validation

Validation process came from deviance measures, paired t-test, and linier regression (Table 5-13). Those processes were applied on calibrated model (Table 5-11 and 5-12) of pre and post eruption.

Table 5-13. Statistical test in validation process

Data set	Deviance measures			Paired	Linier regression	
	RMSE	MAE	MA%E	t-test *)	Slope	R^2
Pre_eruption	530,488.55	309,974.50	83.36	-3.07	0.65	0.22
Post_eruption	288,403.51	196,261.60	71.44	0.61	1.02	0.09

* t-table is 1.97 for pre-eruption and 1.96 for post-eruption

Student t-test shows that pre-eruption model has different value between model and measured discharge. While in post-eruption model, there is no significant differ between model and measured discharge (see Appendix 11). To gain a better value, comparison between model and measured discharge in pre-eruption model was performed uses data of January – October 2010. It means that in pre-eruption model, discharge during the eruption was neglected. Student t-test shows that during that period modeled and measured discharge has no significant differ (see Appendix 11).

Process on independent data, pre-eruption modeled discharge was compare with measured discharge from Kaloran station (southern part of the Code watershed in Code river). The result of validation is shown on Table 5-14 below. According to statistical test, correlation between modeled discharge to Kaloran dataset is 0.5 with determinant factor is 0.24. Student t-test shows that sig. (2-tailed) is below significant level alpha of 0.05 means that there is a difference between modeled discharge and Kaloran dataset.

Table 5-14. Statistical test in validation process compare to Kaloran dataset

Data set	**Deviance measures**			**Correlation**	**Linier regression**	
	RMSE	**MAE**	**MA%E**		**Slope**	**R^2**
Kaloran	354,510	204,198	121.12	0.5	0.16	0.24

Statistical test using student t-test on modeled discharge and Kaloran dataset

Pair of Kaloran - Modeled	Mean	Std. Deviation	Std. Error Mean	95% Confidence Interval of the Difference		t	df	Sig. (2-tailed)
				Lower	Upper			
	-147,858	291,864	16,042	-179,416	-116,300	-9.2	330	.000

To conclude, modeled discharge in pre and post eruption did not reflect a good result with high RMSE and MA%E. In addition, when compare with rainfall data, measured discharge was correlated with rainfall data resulting 0.52 and 0.16 for pre eruption and post eruption respectively. This low correlation might be one reason why the deviance between modeled and measured discharge is high. Another reason was caused by miss of mass balance check. It concluded that the model did not perform well to represent the water balance.

5.3. Predicted discharge to soil change and extreme rainfall event

According to previous discussion, there are several changes in Code watershed as consequences of Merapi eruption. In this sub-chapter, those changes (ksat, soil depth, and soil properties) were involved in the model to know.

5.3.1. Predicted discharge due to soil change

According to the result on the first objectives, there were several changes on the soil related with the eruption. The changes are ksat, soil properties and soil depth as discussed on sub-Chapter 5.1. To know the impact of those changes on the discharge, those changed parameters were involved in the model. Model to run is the pre-eruption model since it has a year rainfall value so it can figure a complete season with dry and wet season (Graph 5-10).

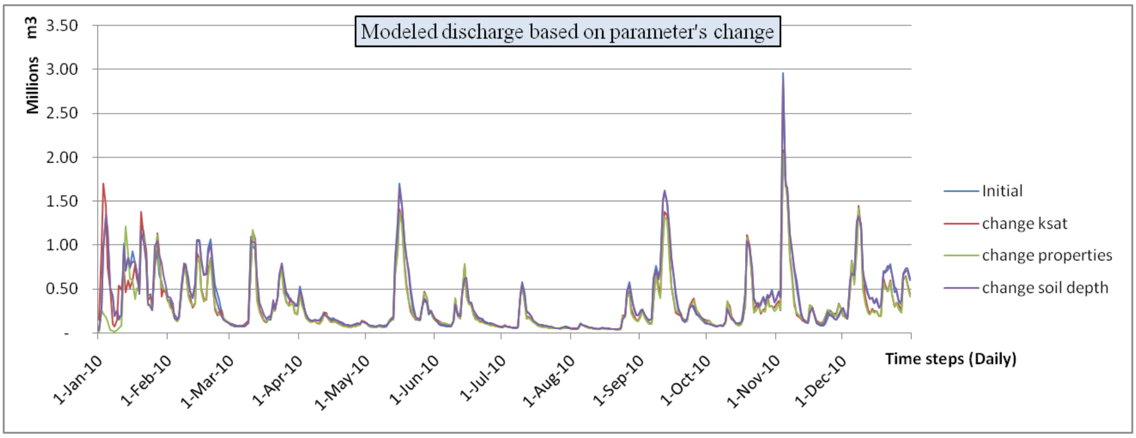

Graph 5-10. Daily discharge based on simulation on parameter's change

Based on student t-test (Table 5-15), the changes on ksat and soil properties result difference between mean discharge of initial model and mean discharge of the change model. In addition, soil depth change simulation was not differed. Correlation between initial discharge to the others discharge reaches more than 0.9 or has relatively similar among them.

Table 5-15. Paired samples test – differences

Pair	Correl	Std. Deviation	Std. Error Mean	95 % Conf. interval Lower	95 % Conf. interval Upper	t	df	Sig. (2-tailed)
Initial - ksat_change	.941	126,892	6,641.8	27,656.2	53,778.5	6.1	364	.000
Initial - properties_change	.925	145,933	7,638.5	47,546	77,588.1	8.2	364	.000
Initial - soildepth_change	.994	38,990.1	2,040.8	-7923.9	102.6	-1.9	364	.056

To sum up, the model noted that consequences of soil depth change related with additional ash deposition of 32-41 mm is the most significant to discharge change as it makes 27 days in a year with discharge more than 1 million m^3. In contrary, soil properties change that related with the change of ksat, porosity, field capacity and wilting point caused the discharge decreased.

Table 5-16. Discharge change as consequence on impact of Merapi eruption

Parameters	Initial model	Change		
		Ksat	Soil properties	Soil depth
Minimum discharge (m^3)	32,350	42,753	19,332	32,561
Maximum discharge (m^3)	2,956,920	2,082,690	2,045,960	2,907,280
Average daily discharge (m^3)	359,189	318,472	296,622	363,100
Total discharge in a year (m^3)	131,104,205	116,242,365	108,267,224	132,531,601
Number of days with discharge more than 1 million m^3	25	19	17	27

5.3.2. Predicted discharge due to extreme rainfall event

Using distribution fitting test, 30 kinds of distribution were analyzed to find the best distribution for rainfall data in Code watershed (see Appendix 5). The test resulted Gumbell maximum distribution was the first rank based on Kolmogorov smirnov and Chi squared. Rainfall data of 1984-2010 calculated by gumbell distribution resulting predicted extreme rainfall in 5, 20, 50, and 100 year (Table 5-17).

Table 5-17. Calculation of extreme rainfall on 4 return periods

Scenario	Pr	Pl / F	Σ	μ	x (Rainfall)
P(5 year)	0.2	0.8	30.79	88.27	134.45 mm
P(20 year)	0.05	0.95	30.79	88.27	179.72 mm
P(50 year)	0.02	0.98	30.79	88.27	208.41 mm
P(100 year)	0.01	0.99	30.79	88.27	229.90 mm

Those four return periods of extreme rainfall events were applied in the model. Since the extreme rainfall event can not be predicted, simulation to gain discharge was done by randomly put the extreme value in the month that has extreme rainfall history. During one year period, there were 8 extreme rainfall event simulated and averaged as the discharge figuring the event.

Table 5-18. Predicted discharge based on extreme rainfall event

Month	5 year	20 year	50 year	100 year
January	1,429,800	2,395,090	3,246,540	3,851,390
February	1,118,790	1,760,700	2,492,300	2,998,020
March	1,539,170	2,466,940	3,250,800	3,803,580
April	1,117,420	1,863,200	2,553,220	3,016,430
May	1,535,600	2,426,790	3,219,120	3,797,270
June	1,303,560	1,275,590	2,196,410	2,679,750
November	1,660,070	2,572,170	3,356,280	3,928,560
December	1,672,630	2,615,290	3,439,450	4,051,110
Average	1,422,130	2,171,967	2,969,264	3,515,760

* all values are in m^3/day

Predicted discharge resulted above (Table 5-18) were obtained from extreme rainfall event in a day. The fact, the duration of the extreme rainfall might be less than a day. That caused the instantaneous discharge might be higher than the averaged value that were modeled.

5.4. Flood prediction

To define flooding area in Code river, bankfull discharge in Code river (downpart of Code watershed) were involved in this research. Through comparison the bankfull discharge and predicted discharge by the model, flood can be predicted resulting one dimensional flood. Predicted discharge resulted from the model are 1,422,130 m^3/day, 2,171,967 m^3/day, 2,969,264 m^3/day, and 3,515,760 m^3/day for extreme rainfall event of 5, 20, 50, and 100 year return period respectively.

5.4.1. Response of Code river to predicted discharge

According to extreme rainfall event, there are several daily discharge produced by simulations on the model. To predict flood, discharge in m^3/s is needed. Those daily discharge produced by the model were segmented by natural unit hydrograph (Graph 4-5). Assuming by percentage per hour, those daily discharge were applied in the unit hydrograph below.

Table 5-19. Hourly discharge based on predicted discharge in extreme rainfall event

Hour	Natural Hydrograph	Percentage	Return Period			
			5 Year	20 Year	50 Year	100 Year
1	1.1394	0.39%	5,522.92	8,434.95	11,531.30	13,653.65
2	1.3006	0.44%	6,304.17	9,628.12	13,162.47	15,585.03
3	4.0743	1.39%	19,748.40	30,161.00	41,232.68	48,821.58
4	4.5559	1.55%	22,083.06	33,726.64	46,107.21	54,593.28
5	6.5543	2.23%	31,769.31	48,520.09	66,331.13	78,539.42
6	10.0131	3.41%	48,534.38	74,124.76	101,334.91	119,985.67
7	17.3280	5.91%	83,990.31	128,275.30	175,363.34	207,639.09
8	31.5116	10.74%	152,739.83	233,273.91	318,905.44	377,600.22
9	51.1829	17.44%	248,088.12	378,895.84	517,983.10	613,318.27
10	31.9675	10.90%	154,949.25	236,648.27	323,518.48	383,062.30
11	21.9056	7.47%	106,178.47	162,162.45	221,689.98	262,492.18
12	15.2274	5.19%	73,808.65	112,725.23	154,105.06	182,468.20
13	12.7835	4.36%	61,963.01	94,633.81	129,372.53	153,183.64
14	11.0389	3.76%	53,506.66	81,718.75	111,716.54	132,278.05
15	9.6882	3.30%	46,959.42	71,719.40	98,046.56	116,092.11
16	8.8388	3.01%	42,842.47	65,431.72	89,450.77	105,914.25
17	8.1609	2.78%	39,556.77	60,413.59	82,590.55	97,791.41
18	7.8489	2.68%	38,044.20	58,103.50	79,432.46	94,052.06
19	7.4025	2.52%	35,880.55	54,799.03	74,914.98	88,703.13
20	7.1280	2.43%	34,549.96	52,766.88	72,136.85	85,413.69
21	6.8292	2.33%	33,101.83	50,555.20	69,113.29	81,833.65
22	6.5333	2.23%	31,667.43	48,364.50	66,118.42	78,287.56
23	6.2620	2.13%	30,352.37	46,356.06	63,372.70	75,036.50
24	4.1238	1.41%	19,988.31	30,527.42	41,733.59	49,414.69
TOTAL		100%	1,422,129.85	2,171,966.44	2,969,264.36	3,515,759.63

* all values are in m^3/hour

The highest discharge occurs in hour ninth. To determine the discharge in m^3/s, all values (daily discharge) were divided with 3,600 resulting 68.9 m^3/s, 105.3 m^3/s, 143.9 m^3/s, and 170.4 m^3/s for 5, 20, 50, and 100 year return period respectively. This result was compared to bankfull discharge in Code river to predict flooding area. Response of Code river to predicted discharge was gained from comparison between predicted discharge and bankfull discharge below.

Table 5-20. Response of Code river to predicted discharge
(Source of Bankfull Discharge : Widiyanto, 2007 and Rahayu, 2011)

No. Sta	Pre-eruption					Post-eruption				
	Bankfull Discharge	5 year 68.91	20 year 105.25	50 year 143.88	100 year 170.37	Bankfull Discharge	5 year 68.91	20 year 105.25	50 year 143.88	100 year 170.37
50	542.14	473.23	436.89	398.26	371.77	275.49	206.58	170.24	131.61	105.12
49	391.76	322.85	286.51	247.88	221.39	274.2	205.29	168.95	130.32	103.83
48	598.04	529.13	492.79	454.16	427.67	337.78	268.87	232.53	193.90	167.41
47	651.28	582.37	546.03	507.40	480.91	382.97	314.06	277.72	239.09	212.60
46	813.22	744.31	707.97	669.34	642.85	681.86	612.95	576.61	537.98	511.49
45	621.93	553.02	516.68	478.05	451.56	277.66	208.75	172.41	133.78	107.29
44	21.59	-47.32	-83.66	-122.29	-148.78	4.19	-64.72	-101.06	-139.69	-166.18
43	47.97	-20.94	-57.28	-95.91	-122.40	14.84	-54.07	-90.41	-129.04	-155.53
42	55.38	-13.53	-49.87	-88.50	-114.99	7.69	-61.22	-97.56	-136.19	-162.68
41	107.81	38.90	2.56	-36.07	-62.56	58.91	-10.00	-46.34	-84.97	-111.46
40	270.92	202.01	165.67	127.04	100.55	111.73	42.82	6.48	-32.15	-58.64
39	441.98	373.07	336.73	298.10	271.61	139.38	70.47	34.13	-4.50	-30.99
38	148.87	79.96	43.62	4.99	-21.50	94.77	25.86	-10.48	-49.11	-75.60
37	149.15	80.24	43.90	5.27	-21.22	14.91	-54.00	-90.34	-128.97	-155.46
36	177.61	108.70	72.36	33.73	7.24	38.49	-30.42	-66.76	-105.39	-131.88
35	127.01	58.10	21.76	-16.87	-43.36	47.92	-20.99	-57.33	-95.96	-122.45
34	415.92	347.01	310.67	272.04	245.55	86.05	17.14	-19.20	-57.83	-84.32
33	201.18	132.27	95.93	57.30	30.81	45.87	-23.04	-59.38	-98.01	-124.50
32	181.16	112.25	75.91	37.28	10.79	48.77	-20.14	-56.48	-95.11	-121.60
31	209.37	140.46	104.12	65.49	39.00	76.5	7.59	-28.75	-67.38	-93.87
30	280.94	212.03	175.69	137.06	110.57	120.95	52.04	15.70	-22.93	-49.42
29	241.88	172.97	136.63	98.00	71.51	128.26	59.35	23.01	-15.62	-42.11
28	99.14	30.23	-6.11	-44.74	-71.23	53.61	-15.30	-51.64	-90.27	-116.76
27	313.1	244.19	207.85	169.22	142.73	112	43.09	6.75	-31.88	-58.37
26	534.1	465.19	428.85	390.22	363.73	304.6	235.69	199.35	160.72	134.23
25	168.71	99.80	63.46	24.83	-1.66	83.33	14.42	-21.92	-60.55	-87.04
24	182.38	113.47	77.13	38.50	12.01	34.09	-34.82	-71.16	-109.79	-136.28
23	517.11	448.20	411.86	373.23	346.74	246.27	177.36	141.02	102.39	75.90
22	642.71	573.80	537.46	498.83	472.34	207.32	138.41	102.07	63.44	36.95
21	203.67	134.76	98.42	59.79	33.30	195.89	126.98	90.64	52.01	25.52
20	145.41	76.50	40.16	1.53	-24.96	57.57	-11.34	-47.68	-86.31	-112.80
19	151.11	82.20	45.86	7.23	-19.26	48.91	-20.00	-56.34	-94.97	-121.46
18	229.31	160.40	124.06	85.43	58.94	165.59	96.68	60.34	21.71	-4.78
17	417.14	348.23	311.89	273.26	246.77	388.99	320.08	283.74	245.11	218.62
16	59.18	-9.73	-46.07	-84.70	-111.19	33.73	-35.18	-71.52	-110.15	-136.64
15	77.69	8.78	-27.56	-66.19	-92.68	70.24	1.33	-35.01	-73.64	-100.13
14	175.76	106.85	70.51	31.88	5.39	87.43	18.52	-17.82	-56.45	-82.94
13	227.1	158.19	121.85	83.22	56.73	94.71	25.80	-10.54	-49.17	-75.66
12	175.92	107.01	70.67	32.04	5.55	117.24	48.33	11.99	-26.64	-53.13
11	293.67	224.76	188.42	149.79	123.30	238.75	169.84	133.50	94.87	68.38
10	165.3	96.39	60.05	21.42	-5.07	77.38	8.47	-27.87	-66.50	-92.99
9	95.87	26.96	-9.38	-48.01	-74.50	79.22	10.31	-26.03	-64.66	-91.15
8	95.03	26.12	-10.22	-48.85	-75.34	46.82	-22.09	-58.43	-97.06	-123.55
7	440.72	371.81	335.47	296.84	270.35	187.9	118.99	82.65	44.02	17.53
6	16.55	-52.36	-88.70	-127.33	-153.82	2.51	-66.40	-102.74	-141.37	-167.86
5	240.1	171.19	134.85	96.22	69.73	87.61	18.70	-17.64	-56.27	-82.76
4	111.36	42.45	6.11	-32.52	-59.01	38.48	-30.43	-66.77	-105.40	-131.89
3	60.1	-8.81	-45.15	-83.78	-110.27	14.5	-54.41	-90.75	-129.38	-155.87
2	212.06	143.15	106.81	68.18	41.69	163.58	94.67	58.33	19.70	-6.79
1	118.01	49.10	12.76	-25.87	-52.36	61.31	-56.38	-43.94	-82.57	-109.06

Indicates the section prone to flood

5.4.2. Determining flood prone section

Based on the Table 5-20 above, there are number of section prone to flood by the extreme rainfall event as shown on figure 5-8, 5-9, and 5-10 below.

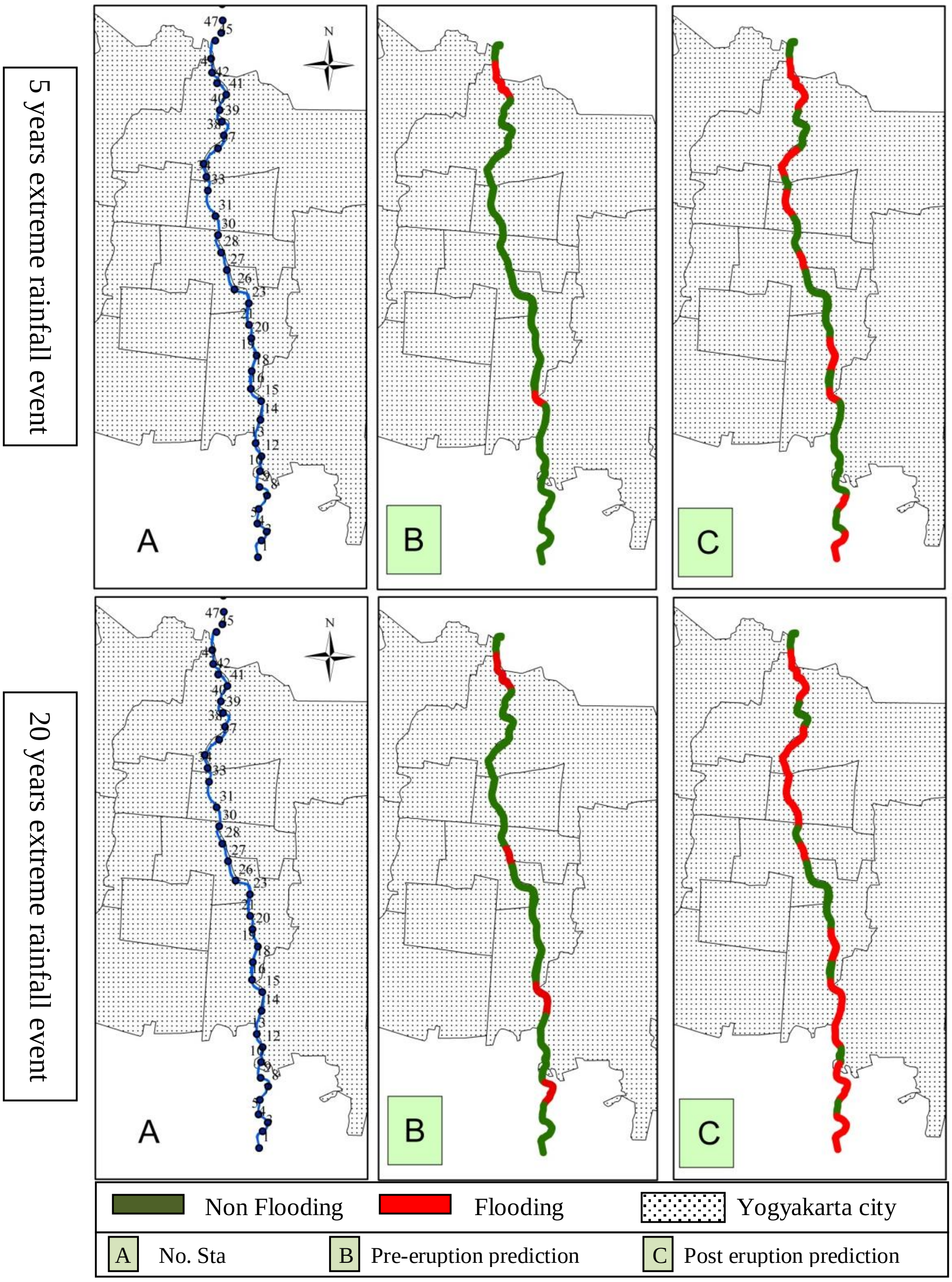

Figure 5-8. Flood prediction based on 5 and 20 year return period of extreme rainfall

From the Figures 5-8 above, 2010 eruption gives significant impact to predicted flood. In 5 year return period event, six sections of Code river will exced the water in pre-eruption simulation and the number increased to 38 % or 19 of 50 section will exced the water when the rainfall occurs in post-eruption simulation. Based on 20 year return period event, pre-eruption simulation gives 20 of 50 sections in Code river are prone to flood. In addition, post-eruption simulation produced 29 sections were prone to flood.

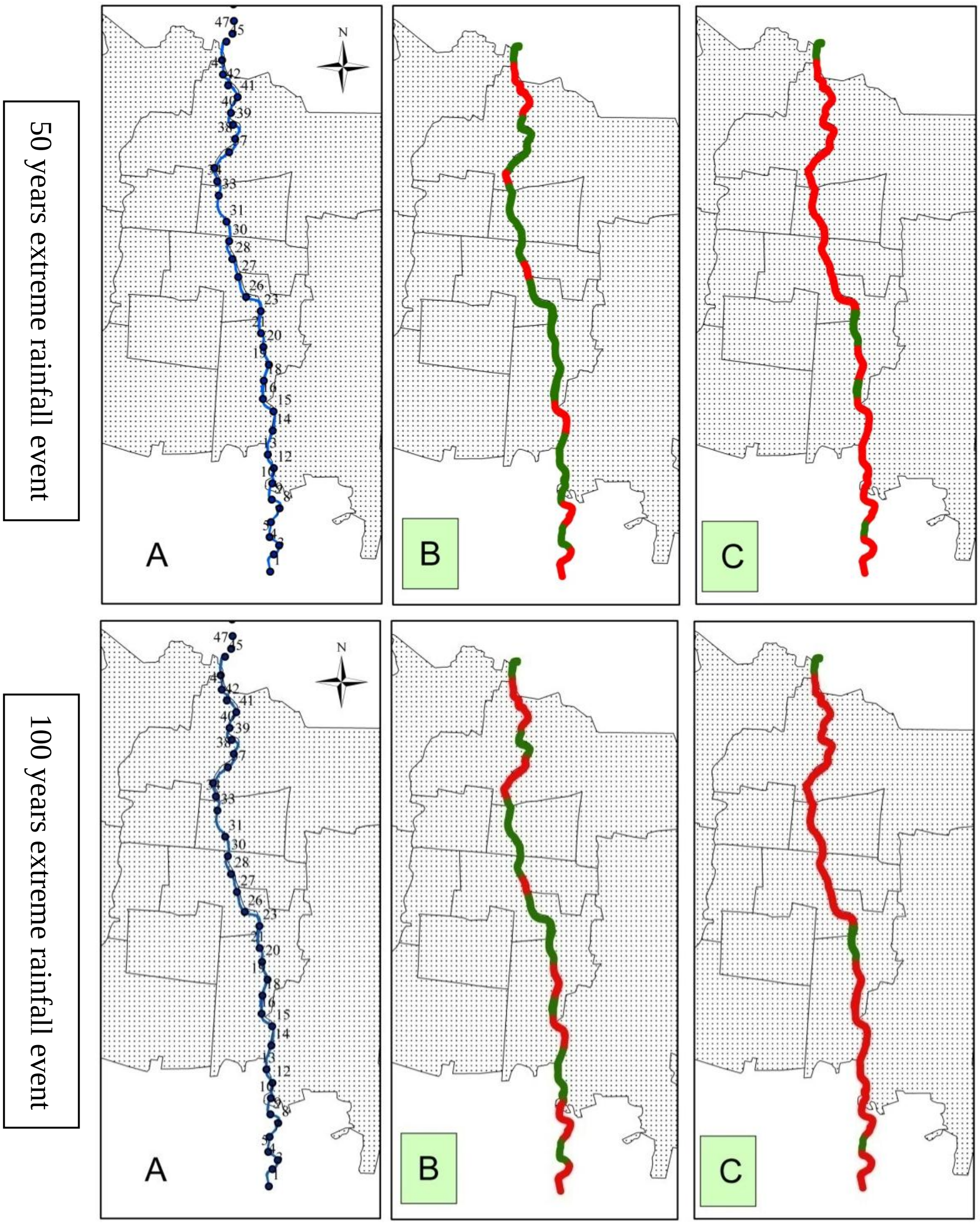

Figure 5-9. Flood prediction based on 50 and 100 year return period

Around 14 sections are proned to flood in 50 year return period event when simulated using pre-eruption condition. The number of section prone to flood increased when simulated on post-eruption condition. It noted that 35 section or 70 % of Code river will exceed the water when 50 year return period of extreme rainfall occurs.

Rainfall event of 100 year return period made 20 sections in Code river prone to flood in pre-eruption simulation. On the other hand, 37 sections are grouped into flood prone area when post-eruption simulation was processed. It means that the eruption makes 17 sections in Code river were classified into flood prone area when 100 year return period of extreme rainfall occurs. Table below summarize the change of section that prone to flood by the eruption.

Table 5-21. Number of section prone to flood in pre and post eruption

	Pre-eruption				Post-eruption			
	5 year	20 year	50 year	100 year	5 year	20 year	50 year	100 year
Number of section prone to flood	6	10	14	20	19	29	35	37
Percentage (compared to 50)	12%	20%	28%	40%	38%	58%	70%	74%

Related with administration boundaries, Jetis, Gondokusuman, Gedong tengah and Mergangsan are subdistricts that prone to flood (Figure 5-10). Actually, exceeding the water will caused the discharge in the next section will decrease and it might be there is no flood anymore when more water exceed in upper section of the river.

To sum up, compared with the other changes as previous discussion, bankfull discharge changes as consequence of the eruption has the most impact to the discharge. The change was caused by sedimentation in the river.

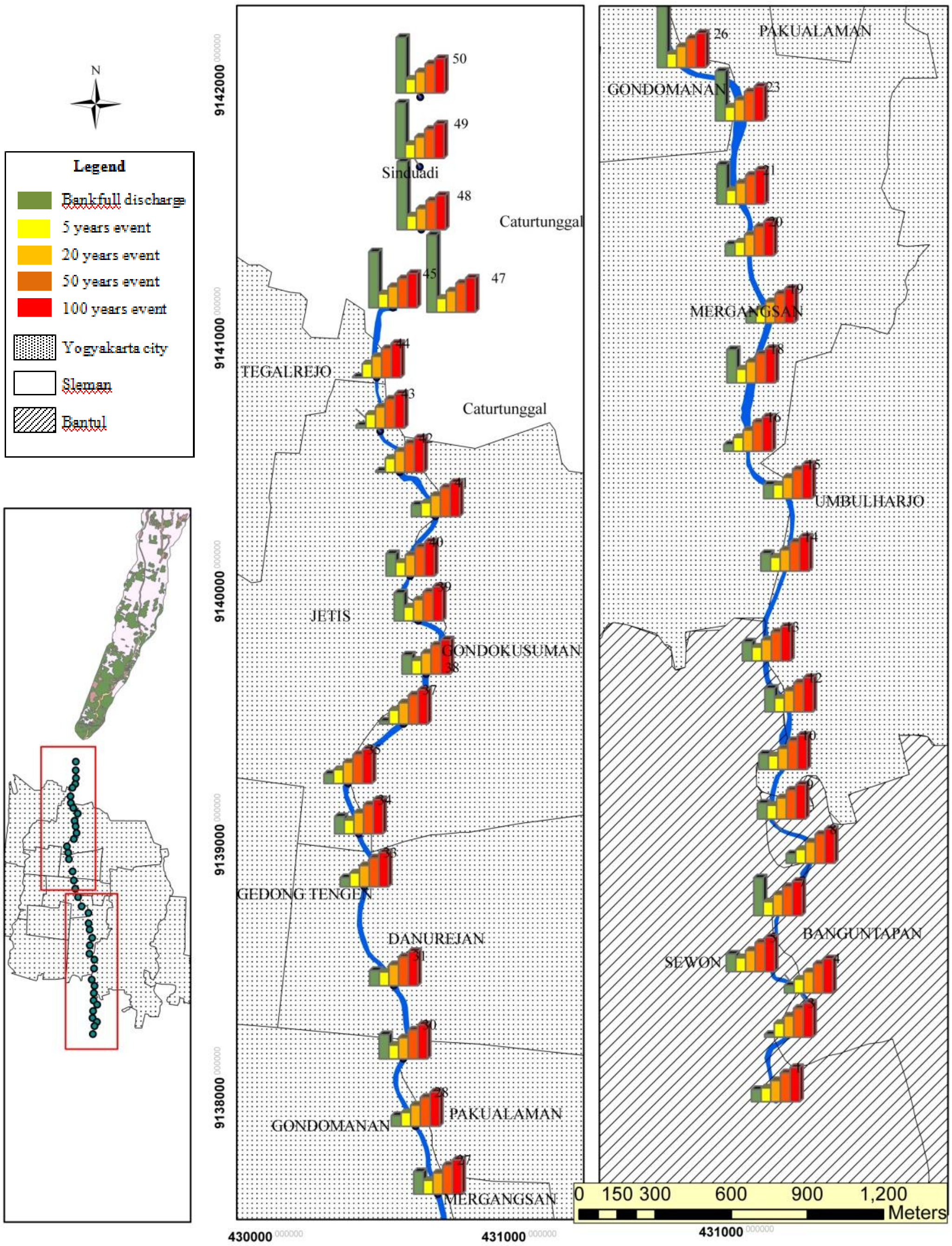

Figure 5-10. Flood prone section in Code river

6. CONCLUSIONS AND RECOMMENDATIONS

6.1. Conclusions

The result as described and discussed in previous chapter supports the following conclusions answering research objectives and questions.

6.1.1. Change of soil properties, soil depth and infiltration due to eruption

Due to the 2010 Merapi eruption, Code watershed experienced less impact by only ash deposition and lahars affected the area. Due to that condition, changes in hydrological process were related with soil and infiltration. Soil depth has significant impact correlated with the discharge due to the last eruption. Research questions in this objective are:

1. Soil properties change

   The eruption changes soil texture composition, the amount of sand fraction increased while clay fraction decreased. It could be argued that spreading ashfall by the eruption is the main factor for this change. In general soil properties such as porosity, field capacity, and wilting point were generally decreased while ksat was decreased.

2. Soil depth change

   Through interviewed to local people, the change of soil depth due to 2010 Merapi eruption in Code watershed is 32 – 42 mm. The change is caused by ash deposition during the eruption.

3. Infiltration rate change

   Infiltration rate before the eruption based on Noordianto (2005) is 1.38 and 0.79 cm/min in Tanen and Banteng respectively. After the eruption, infiltration rate in Code gained 0.362 – 0.764 cm/min. According to those result, It could be argued that the eruption makes the infiltration rates in Code watershed decreased.

6.1.2. The hydrological model

Hydrological model used in this research adopted the water balance model version 1.0 constructed by Jetten, 2011. It uses PCRaster and Nutshell 2.8 to perform the model. The output of the model is daily discharge.

1. The most sensitive parameter, calibration and validation

   Soil depth is the most sensitive parameter to the discharge resulted in the model. It performs positive response while the other parameters tested, Ksat, porosity and maximum storage gives negative response to the discharge when the value was increased.

   Initial model of pre eruption gives the highest rank of calibration process and calibration in post eruption model was done by decreasing soil depth 15 % while porosity, ksat, and storage maximum are increased by 5%. Validation was done by comparing the modeled discharge with rainfall data resulting the model are correlated with the rainfall.

2. Accuracy of the model

   Through mass balance check, deviance measures, statistical analysis, calibration and validation, accuracy of the model was defined. It could be concluded that the model has low accuracy compared to the measured data. The main problem occurs in mass balance check where there is unbalance of input and output from the model. Pearson correlation between modeled and measured discharge gives 0.46 for the pre eruption model and 0.22 for the post eruption model. Deviance measures through RMSE shows 530,488 m^3 and 310,677 m^3 for pre and post eruption model respectively. In addition, the amount of discharge in the model is lower than the amount in measured discharge for the pre eruption model. Meanwhile, the post eruption model performs higher than the measured discharge.

6.1.3. Predicted discharge to soil change and extreme rainfall event

There are two simulation based model applied in the research, simulation on soil change and simulation on extreme rainfall event. Those simulations resulting predicted discharge due to impact of eruption in Code watershed and extreme rainfall event.

1. Predicted discharge due to soil change

   The change on soil depth as consequence of ash deposit has no significant impact to the discharge but it caused number of high discharge (more than 1 million m^3/day) increased. In contrary, change on ksat and soil properties has significant impact to the discharge resulting the amount decreased.
2. Predicted discharge if extreme rainfall event occurs

   Based on the extreme rainfall event, the discharge gained 1,422,130 m^3/day when the 5 year return period of extreme rainfall event occurs. Scenarios on 20, 50 and 100 year return periods gives the amount of discharge in a day reaching 2,171,967 m^3/day, 2,969,264 m^3/day, and 3,515,760 m^3/day respectively.

6.1.4. Quantifying the Code river response due to predicted discharge

Flood prediction was done through comparison the predicted discharge from the model with bankfull discharge of Code river. Previous researches conducted by Wijayanto (2007) and Rahayu (2011), 50 sections had been measured to obtained the bankfull discharge before and after the 2010 Merapi eruption.

1. The response of Code river to the predicted discharge

   About 19 of 50 sections were prone to flood when 5 year extreme rainfall event occurs. In addition, the sections that prone to flood become 29, 35 and 37 of 50 sections when the extreme rainfall event of 20, 50 and 100 year return period occurs respectively.

2. Flood prone section

   Sub disctrics that prone to flood are Jetis, Gondokusuman, Gedong tengah and Mergangsan.

6.2. Recommendations

1. As the model did not work really well, some input data for the model should describe a better presentation of the actual condition. In this case, rainfall station in upper part of the watershed is needed to obtain a better result in the model. Also for soil depth that is the most sensitive, it should be better if it was obtained from a field measurement.
2. Vegetation cover should performs better if obtained from a satellite image representing vegetation characteristic such as SPOT 5, Aster, MODIS, etc.
3. Rating curve of Code river should be update as the river experienced sedimentation due to the last eruption.
4. Prone to flood, Code river should be maintain to obtain a better capacity of bankfull discharge in some section.

Reference

Asdak, C., 2007, *Hidrologi dan Pengelolaan Daerah Aliran Sungai* (*Hydrology and Watershed Management) Fourth Edition*, Gadjah Mada University Press, Yogyakarta.

Astuti, R.T., 2008, *Landcover and Landuse Evaluation 1994-2005 in Code Watershed from Hydrological Aspect*, Thesis of Gadjah Mada University, Yogyakarta.

Aviani, E.N., 2010, *Analisis Efek Perubahan Penggunaan Lahan terhadap Debit Puncak di DAS Code menggunakan Model Rasional Modifikasi* (*Analysis of The Effect of Landuse Change Towards Peak Discharge Code Sub Catchment Using Modified Rational Model)*, Thesis, University of Gadjah Mada, Yogyakarta.

Badila, R. A., 2008, *Flood Modelling in Pasig-Marikina River Basin*, MSc Thesis, International Institute for Geo-information Science and Earth Observation, Enschede.

Bappeda, 2011, *Buku Profil Daerah Istimewa Yogyakarta (Profile of Yogyakarta Province)*, Bappeda, Yogyakarta.

Barry, R.G., 1992, *Mountain Weather and Climate Second Edition*, Routledge, Chapman and Hall Inc, London.

Basayigit L., 2010, *Prediction of Soil Loss in Lake Watershed Using GIS : A Case Study of Edigir Lake Turkey*, Natural & Environmental Sciences NES 1-1 (2010) 1 - 11

Boundon, G., Camus, G., Gourgaud, A., Lajoie, J., 1992, *The 1984 nuee-ardente deposits of Merapi volcano, Central Java, Indonesia: stratigraphy, textural characteristics, and transport mechanism*, Buletin of Volcanology (1993) 55:327-342

Charbonnier, S., 2009, *The Dynamics and Hazards of Small-Volume Pyroclastic Flows : a Case Study of The 2006 Eruption of Merapi Volcano, Java, Indonesia*, Phd Thesis, Keele University, United Kingdom.

Charbonnier, S., 2011, *Material in Short Course on Volcanic Hazards Day 2 : Volcanic Hazards at Merapi*, Yogyakarta.

Davie, T., 2008, *Fundamentals of Hydrology Second Edition*, Taylor and Francis E-Library, London.

De Jong, K., 1997, *PCRaster homepage; info, software and manuals*. (Available online from http://www. pcraster.geo.uu.nl/ /)

De Jong, S. M. and Jetten, V. G., 2007, *Estimating spatial patterns of rainfall interception from remotely sensed vegetation indices and spectral mixture analysis,* International Journal of Geographical Information Science, 21:5, 529-545.

Deursen, W.V., 2004, *Quick start tutorial : Importing ArcView Ascii Grid Maps in PCRaster*, Carthago Consultancy, the Netherlands.

Deegan, F.M., Troll, V.R., Freda, C., Misiti, V., Chadwick, J.P., 2011, *Fast and Furious : Crustal CO_2 Release at Merapi Volcano, Indonesia*, Geology Today Vol. 27 No.2 March-April 2011, Blackwell Publishing Ltd.

Dove, M.R., 2008, *Perception of Volcanic Eruption as Agent of Change on Merapi Volcano, Central Java,* Journal of Volcanology and Geothermal Research 172 (2008) 329–337.

FAO, 1998, *Crop Evapotranspiration – Guidelines for computing crop water requirements*, downloaded from www.fao.org/doccrep/X0490E/X0490E00.htm on October 10th 2011.

Farida, A., 2009, *Prediksi Banjir Menggunakan Model ANSWERS Kasus di DAS Code Yogyakarta (Flood Prediction using ANSWERS, case study in Code watershed),* MSc Thesis, University of Gadjah Mada, Yogyakarta

Gertisser, R., Charbonnier, S.J., Troll, V.R., Keller, J., Preece, K., Chadwick, J.P., Barclay, J., and Herd, R.A., 2011, *Merapi (Java, Indonesia) : Anatomy of a Killer Volcano*, Geology Today Vol.27 No.2 Blackwell Publishing Ltd.

Granell, C., Diaz, L., Gould, M., 2010, *Service-oriented Applications for Environmental Models: Reusable Geospatial Services,* Journal of Environmental Modeling and Softwares 25 (2010) 182-198.

Hadi, A. N., 2011, *Analyzing Runoff Dynamics Through Parameterizing a Hydrological Model in a Watershed A Case Study in Upper Part of Serayu Watershed, Central Java Province, Indonesia*, MSc Thesis UGM-ITC, Yogyakarta

Hartini, K.S., 2010, *Morphologic Analysis of Merapi Edifice in Studying Merapi – Type Eruption, to Improve Volcanic Hazard Map*, MSc Thesis, ITC, International Institute of Geoscience and earth Observation, Enschede, The Netherlands.

Inverson, R. M., Schilling, S.P., Vallance, W., 1998. *Objective Delineation of Lahar Inundation Zones*, Geol. Soc. Am. Bull, 110, 972–984.

Jetten, V., Straatsma, M., Alkema, D.,(2011), *Spatial Modelling of Natural Hazard Processes*, ITC, International Institute of Geoscience and Earth Observation, Enschede, The Netherlands.

Karssenberg DJ., 1996, *PCRaster Manual.* 367 pp.

Kuriakose, S. L., 1996, *Effect of Vegetation on Debris Flow Initiation, Conceptualisation and Parameterisation of a Dynamic Model for Debris Flow Initiation in Tikovil River Basin, Kerala, India, using PCRaster*, MSc Thesis, ITC, the Netherlands.

Mayer, D. G., and Butler, D. G., 1993, Statistical validation, Ecology Modelling, 68; 21-32.

McCuen, R. H., 1998, *Hydrologic Analysis and Design Second Edition*, Pearson Education, New Jersey, United States.

Ministry of Forestry Indonesia, 2011, *Survey Kondisi Tumbuhan dan Satwa Liar Taman Nasional Gunung Merapi Paska Erupsi Tahun 2010 (Survey on Vegetation and Wildlife in Mount Merapi National Park After the 2010 Eruption)*, Balai Taman Nasional Gunung Merapi, Yogyakarta.

Nugroho, C., 2008, *Hydrological – Slope Stability Modeling for Landslide Hazard Assessment by Means of GIS and Remote Sensing Data*, MSc Thesis UGM-ITC, Yogyakarta.

Noordianto, M. H., 2005, *Karakteristik Imbuhan Air Tanah Bebas di Sebagian Sisi Selatan Gunungapi Merapi Antara Kali Boyong dan Kali Kuning Daerah Istimewa Yogyakarta (Characteristic of Groundwater Recharge in Southern Part of Merapi Vulcano Between Boyong River and Kuning River, Yogyakarta Special Province)*, Thesis, University of Gadjah Mada, Yogyakarta.

Parker, G., 2006, *Automated Baseflow Separation for Canadian Datasets (ABSCAN): User's Guide*, Thinkew Analytics, Ottawa.

Pedzisai, E., 2010, *Rainfall-Runoff Modelling for Flash Floods in Cuong Thinh Catchment; Yen Bai Province:Vietnam*, MSc Thesis, International Institute for Geo-information Science and Earth Observation, Enschede.

Prachansri, S., 2007, *Analysis of Soil and Land cover Parameters for Flood Hazard Assessment; A Case Study of the Nam Chun Watershed, Phetchabun, Thailand*, MSc Thesis, International Institute for Geo-information Science and Earth Observation, Enschede.

Quan, N. H., 2006, *Rainfall-runoff Modeling in the Ungauged Can Le Catchment, Saigon River Basin,* MSc Thesis, International Institute for Geo-information Science and Earth Observation, Enschede.

Raes, D., 2009, *The ETo Calculator Reference Manual Version 3.1*, Food and Agriculture Organizations of the United Nations Land and Water Division, Rome, Italy.

Rahayu, T.S., 2011, *Studi Banjir Sungai Code di Wilayah Perkotaan setelah Erupsi Merapi 2010* (*Study of Code River Flood in Urban Area After Merapi Eruption 2010)*, MSc Thesis, University of Gadjah Mada, Yogyakarta.

Rahimy, P., 2011, *Effect of Soil Depth and Saturated Hydraulic Conductivity Spatial Variation on Runoff Simulation by the Limburg Soil Erosion Model (LISEM), a Case Study in Faucon Cacthment, France,* MSc Thesis, International Institute for Geo-information Science and Earth Observation, Enschede.

Rahmalia, T., 2010, *Perbandingan Metode Thronthwaite-Mather dan Metode Mock untuk Prediksi Ketersediaan Air di DAS Code (Comparison of Thronthwaite-Mather Method and Mock Method for Water Availability Prediction at Code Watershed)*, Thesis, University of Gadjah Mada, Yogyakarta.

Rykiel, E. J., 1996, *Testing ecological models : the meaning of validation*, Ecological Modelling 90 (1996) 229-244.

Sastrodarsono, S., Takeda, K., 1993, *Hidrologi untuk Pengairan (Hydrology for Irrigation)*, Pradnya Paramita, Jakarta.

Schreier, H., 2005, *Challenges in Mountain Watershed Management*, Springer Global Change and Mountain Regions : 617-625.

Seyhan, E., 1977, *Fundamentals of hydrology*, Geografisch Instituut der Rijksuniversiteit te Utrecht, Nederland.

Straatsma, M.W., Warmink, J.J. and Middelkoop, H., 2008, *Two novel methods for field measurements of hydrodynamic density of floodplain vegetation using terrestrial laser scanning and digital parallel photography*, International Journal of Remote Sensing, 29:5, 1595-1617.

Suharto, E., 2006, *Kapasitas Simpanan Airtanah pada Sistem Tata Guna Lahan Tahura Raja Lelo Bengkulu (Capacity of Groundwater Storage in Landuse System of Tahura Raja Lelo Bengkulu)*, Journal of Ilmu-ilmu Pertanian Indonesia Vol 8 No.1, 2006 : 44-49.

Susetyo, C., 2008, *Urban Flood Management in Surabaya City : Anticipating Changes in the Brantas River System*, ITC MSc Thesis, the Netherlands.

Thornwaite, C. W., and Mather J. R., (1955), *The Water Balance*, Centerton, New Jersey, United States.

Trimurti, W., (2010), *Runoff Assessment of Small Catchment Using Spatial Semi-Physical Hydrological Model A Case Study of Goseng Catchment, Karanganyar Regency, Central Java Province, Indonesia*, MSc Thesis, University of Gadjah Mada, Yogyakarta.

Viessman, W., Lewis, G. L., Knapp, J. W., (1989), *Introduction to Hydrology Third Edition*, Harper & Row Publishers, New York.

Visser, S.M., 2005, *WEPS in PCRaster*, Phd Thesis

Widiyanto, C., 2007, *Kajian Hidrologi dan Hidraulika Sungai Code Kota Yogyakarta (Study of Hydrology and Hydraulic Code River of Yogyakarta)*, MSc Thesis, University of Gadjah Mada, Yogyakarta.

Wijayanti, P., 2010, *Karakteristik Air Tanah Berdasarkan Penggunaan Lahan di antara Sungai Boyong dan Sungai Kuning Yogyakarta (Groundwater Characteristic Based on Landuse Between Boyong River and Kuning River Yogyakarta)*, Thesis, University of Gadjah Mada, Yogyakarta.

Witherick, M., Ross, S., Small, J., 2001, *A Modern Dictionary of Geography Fourth Edition*, Oxford University Press, New York.

http://www.tribunnews.com/2011/05/01/banjir-luapan-kali-code-sampai-bantul accessed on 14th January 2012.

http://www.volcanodiscovery.com accessed on Desember 1st 2011.

APPENDIXS

Appendix 1. PCRaster script of Dynamic Hydrological Model

```
# Determining the Impact of Volcanic Eruption
#
# DYNAMIC HYDROLOGICAL MODEL
# No Version
# Description: 2010 Merapi Eruption to Code watershed
# timestep: day
# input : daily rainfall and daily ETp
#  dem, soil map + soil data, land cover images
# First time step is January 1st 2010, until May 31st 2011
# Agus Yasin, UGM-ITC      -- script adopted from Jetten (2011)
```

```
#! --matrixtable --radians --lddout
# global options, do not touch!

binding
### Input ###
  DEM = dem.map;                # digital elevation model
  mask = mask.map;
  LDD = ldd.map;
  outlet = outlet.map;

  soilunit1 = presoilcode.map;    # soil properties of pre eruption
                          # 1= Andic Dystropepts
                          # 2= Andic Hapludolls
                          # 3= Lithic Ustropepts
                          # 4= Pemukiman
                          # 5= Typic Fragiaquents
                          # 6= Typic Hapludands
                          # 7= Typic Troporthents

 soilunit2 = postsoilcode.map;    # soil properties of post eruption
                          # 1= Andic Dystropepts
                          # 2= Andic Hapludolls
                          # 3= Lithic Ustropepts
                          # 4= Pemukiman
                          # 5= Typic Fragiaquents
                          # 6= Typic Hapludands
                          # 7= Typic Troporthents

  soildata1 = soils1.tbl;        # Soil data of pre eruption
                          # 1= Ksat
                          # 2= pore
                          # 3= field capacity,
                          # 4= wilting point
                          # 5= van genuchten n

  soildata2 = soils2.tbl;         # Soil data of post eruption
                          # 1= Ksat
                          # 2= pore
```

```
                              # 3= field capacity,
                              # 4= wilting point
                              # 5= van genuchten n
  rainfall_tss = rainfall1011.tss; # rainfall data in mm/day
  ETP_tss = etp1011.tss;          # Potential evapotranspiration [mm/day]
                                  # based on Penman-Monteith method
  intens_tss = intensity1011.tss;
  stations = rainstations.map;     # map with two rainfall stations
                              # 1= Beran
                              # 2= Pakem
  soildepth = soildepth.map;       # soil depth in mm
  rivfrac = riverwidth.map;        # river width map of Code
  landunit = landcover.map;        # land cover types
                              # 1= Bare exposed rock
                              # 2= Build-up land
                              # 3= Croplands and pasture
                              # 4= Evergreen forest land
                              # 5= Mixed rangeland
                              # 6= Paddy field
                              # 7= Streams and canal
                              # 8= Transportation

### Output ###
#maps
  theta_s = pore.map;              # porosity (fraction)
  theta_fc = fieldcap.map;         # field capacity (fraction)
  theta_wp = wilting.map;          # wilting point (fraction)
  SoilMoisture = moist;            # daily soil moisture maps (mm)
  interception = intc;             # daily interception (mm)
  unsatdepth = unsdep;             # depth unsaturated zone (mm)

#graphs
  p_tss = pavg.tss;                    # average daily rainfall (mm)
  pcum_tss = pcumavg.tss;              # average cumulative rainfall (mm)
  ETpavg_tss = etpavg.tss;             # average daily ETp (mm)
  ETpcum_tss = ETpcumavg.tss;          # average cumulative ETp (mm)
  intccum_tss = intcum.tss;            # average cumulative interception (mm)
  ETfact_tss = ETfactor.tss;           # average daily ratio ETa/ETp
  eta_tss = ETaavg.tss;                # average daily ETa (mm)
  etacum_tss = ETacumavg.tss;          # average cumulative ETa (mm)
  perc_tss = perc.tss;                 # average daily percolation (mm)
  perccum_tss = perccum.tss;           # average daily cumulative percolation (mm)
  infcum_tss = infilcum.tss;           # average cumulative interception (mm)
  rocum_tss = runoffcum.tss;           # average cumulative interception (mm)
  theta_tss = theta.tss;               # average daily theta  (-)
  moisture_tss = moisture.tss;         # average daily soil moisture (mm)
  day_tss = day.tss;

areamap
DEM;

timer
 1 365 1;                          # 516 days, January 2010- May 2011 is leap year

initial

 mask = DEM/DEM;
 nrCells = maptotal(mask);         # nr cells in catchment
 dt = 1;                           #timestep 1 day
```

```
####################################
 ###        initial vegetation cover map          ###
 ####################################
 covjan10 = covjan.map;
 covfeb10 = covfeb.map;
 covmar10 = covmar.map;
 covapr10 = covapr.map;
 covmay10 = covmay.map;
 covjun10 = covjun.map;
 covjul10 = covjul.map;
 covaug10 = covaug.map;
 covsep10 = covsep.map;
 covoct10 = covoct.map;
 covnov10 = covnov.map;
 covdec10 = covdec.map;
 covjan11 = covjan.map;
 covfeb11 = covfeb.map;
 covmar11 = covmar.map;
 covapr11 = covapr.map;
 covmay11 = covmay.map;
 jan10 = 1;
 feb10 = 32;
 mar10 = 60;
 apr10 = 91;
 may10 = 121;
 jun10 = 152;
 jul10 = 182;
 aug10 = 213;
 sep10 = 244;
 oct10 = 274;
 nov10 = 305;
 dec10 = 335;
 jan11 = 366;
 feb11 = 397;
 mar11 = 425;
 apr11 = 456;
 may11 = 486;

 #########################
 ###       initial soil data      ###
 #########################
 Ksat1 = lookupscalar(soildata1, 1, soilunit1);
 Ksat = Ksat1 * 24 * mask;
 #convert to mm/day
 theta_s1 = lookupscalar(soildata1, 2, soilunit1);
 theta_s = theta_s1 * mask;
 #porosity (-)
 theta_fc1 = lookupscalar(soildata1, 3, soilunit1);
 theta_fc = theta_fc1 * mask;
 #field capacity (-)
 theta_wp1 = lookupscalar(soildata1, 4, soilunit1);
 theta_wp = theta_wp1 * mask;
 #wilting point (-)
 m_param1 = lookupscalar(soildata1, 5, soilunit1);
 m_param = m_param1 * mask;
 # m parameter (-)
 theta_r = 0.25*theta_wp;
 #residual moisture content (-), set at 25% of wilting point
```

```
############################
###        initialize variables      ###
############################
 theta = 1.5*theta_fc;
# initialize soil moisture theta at 1.5 field capacity (arbitrary in wet season)
GWDepth = soildepth*0.01;
# initial GWDepth is 1% of soildepth
 GWDepth = if (landunit eq 6, 0, GWDepth);
GWDepth = if (landunit eq 7, 0, GWDepth);
# initialize groundwater depth at streams and paddy field are 0 mm
unsatdepth = soildepth - GWDepth;
#depth unsatirated zone (mm)
SoilMoisture = theta*unsatdepth;
# initial soil moisture in mm

############
###  totals ###
############
 ETacum = 0;
 ETpcum = 0;
 Pcum = 0;
 percum = 0;
 intccum = 0;
 infilcum = 0;
 peakcum = 0;
 Tacum = 0;
 Eacum = 0;
 infcum = 0;
 rocum = 0;
 interception = 0*mask;
 Perc = 0*mask;
 FDays = 0*mask;
 baseflow = 0*mask;
 totbase = 0;
 totpeak = 0;

dynamic
 ########################
 ###      meteo data input  ###
 ########################
 P_stat = timeinputscalar(rainfall_tss, stations);
 # get the rainfall values at the stations
 idp = 2;
 Pinterpol = inversedistance(mask gt 0, P_stat, idp, 0, 0);
 # inverse distance interpolation with power 2
 P = Pinterpol*mask;
 # restrict to area mask
 report p_tss = maptotal(P)/nrCells;
 # write a graph of the average daily rainfall
 Pcum = Pcum + P;
 #calculate cumulative P for outut
 report pcum_tss = maptotal(Pcum)/nrCells;
 # write a graph of the average cumulative rainfall
  ETp = timeinputscalar(etp1011.tss, nominal(mask));
 # read potential evapotranspiration from a file and give the whole area that value
 # ETp is the potential evapotranspiration (in mm)  report ETpavg_tss = maptotal(ETp)/nrCells;

 ETpcum = ETpcum + ETp;
 report ETpcum_tss = maptotal(ETpcum)/nrCells;
```

```
# condition post eruption model
  Ksat2 = if(day ge jan11,lookupscalar(soildata2, 1, soilunit2), Ksat1);
  Ksat2 = Ksat2 * 24 * mask;
  theta_s2 = if(day ge jan11,lookupscalar(soildata2, 2, soilunit2), theta_s1);
  theta_s2 = theta_s2 * mask;
  theta_fc2 = if(day ge jan11,lookupscalar(soildata2, 3, soilunit2), theta_fc1);
  theta_fc2 = theta_fc2 * mask;
  theta_wp2 = if(day ge jan11,0.03, theta_wp1);
  theta_wp2 = theta_wp2 * mask;
  m_param2 = if(day ge jan11,0.57, m_param1);
  m_param2 = m_param2 * mask;

  ####################
  ###    Interception    ###
  ####################
  cov = covjan10;
  cov = if(day gt feb10, covfeb10+(day-feb10)/(mar10-feb10+0.0001)*(covmar10-covfeb10), cov);
  cov = if(day gt mar10, covmar10+(day-mar10)/(apr10-mar10+0.0001)*(covapr10-covmar10), cov);
  cov = if(day gt apr10, covapr10+(day-apr10)/(may10-apr10+0.0001)*(covmay10-covapr10), cov);
  cov = if(day gt may10, covmay10+(day-may10)/(jun10-may10+0.0001)*(covjun10-covmay10), cov);
  cov = if(day gt jun10, covjun10+(day-jun10)/(jul10-jun10+0.0001)*(covjul10-covjun10), cov);
  cov = if(day gt jul10, covjul10+(day-jul10)/(aug10-jul10+0.0001)*(covaug10-covjul10), cov);
  cov = if(day gt aug10, covaug10+(day-aug10)/(sep10-aug10+0.0001)*(covsep10-covaug10), cov);
  cov = if(day gt sep10, covsep10+(day-sep10)/(oct10-sep10+0.0001)*(covoct10-covsep10), cov);
  cov = if(day gt oct10, covoct10+(day-oct10)/(nov10-oct10+0.0001)*(covnov10-covoct10), cov);
  cov = if(day gt nov10, covnov10+(day-nov10)/(dec10-nov10+0.0001)*(covdec10-covnov10), cov);
  cov = if(day gt dec10, covdec10+(day-dec10)/(jan11-dec10+0.0001)*(covjan11-covdec10), cov);
  cov = if(day gt jan11, covjan11+(day-jan11)/(feb11-jan11+0.0001)*(covfeb11-covjan11), cov);
  cov = if(day gt feb11, covfeb11+(day-feb11)/(mar11-feb11+0.0001)*(covmar11-covfeb11), cov);
  cov = if(day gt mar11, covmar11+(day-mar11)/(apr11-mar11+0.0001)*(covapr11-covmar11), cov);
  cov = if(day gt apr11, covapr11+(day-apr11)/(may11-apr11+0.0001)*(covmay11-covapr11), cov);
  cov = if(day gt may11, covmay11+(day-may11)/(516-may11+0.0001)*(covjun10-covmay11), cov);

  Coverm = cov/100;
  # make a decimal from percentage
  Coverm = min(Coverm, 0.95);
  # maximize cover fraction to 0.95, to avoid infinite LAI
  LAI = ln(1-Coverm)/-0.4;
  # calculate LAI from Cover using Cover = exp(-0,4*LAI), WOFOST
  Smax = max(0, 0.935+0.498*LAI-0.00575* sqr(LAI));
  Smax = if(landcover.map eq 4, max(0, 0.2856*LAI),Smax);    #evergreen forest
  Smax = if(landcover.map eq 5, max(0, 0.2856*LAI),Smax);    #rangeland
  #calculate smax using Von Hoyningen-Huene equation Smax=0.935+0.498LAI-0.00575*LAI2
  # calculate Smax from LAI and avoid negative values becuse of logarithm
  # formula from Kuriakose (1996), Jetten (2011), Hadi (2011)

  interception = interception + P - ETp;
  # add rainfall and subtract evaporation from interception
  interception = min(Smax, interception);
  # fill up the interception with rain to a max of Smax
  interception = max(0, interception);
  # cannot be less than 0
  Pe = max(P - interception, 0);
  # effective rainfall is rainfall - interception, but larger than 0
  ETp =  if(interception gt ETp, 0, ETp - interception);
  # decrease potential evaporation with interception evaporation
  # if ETp is greater that interception, interception becomes 0
  intccum = intccum + interception;
  report intccum_tss = maptotal(intccum)/nrCells;
```

```
# graph with spatial average cumulative interception (mm)
####################
###    Infiltration      ###
####################
store = unsatdepth*(theta_s2-theta);
# effective storage in mm
a_cal = 0.41;                                   #based on the result calibration
Infilcap = a_cal*Ksat2*mask;
# infil is a fraction of Ksat
 Infilcap = max(min(store, Infilcap),0);
#infiltration in mm, is smallest of storage or rainfall
Infilcap = if (landunit eq 8, 0, Infilcap); # transportation or road

runoff = accuthresholdflux(LDD, Pe, Infilcap);
Infil = accuthresholdstate(LDD, Pe, Infilcap)*mask;
#runoff and infiltration in mm
#NOTE: interception storage above river decreased with rivfrac so
# ER above river cells is direct rainfall
infcum = infcum + Infil;
report infcum_tss = maptotal(infcum)/nrCells;

#################################
###       Actual Evapotranspiration    ###
#################################
# actual evapotranspiration ETa linear with soil moisture content (mm)
ETpoint = theta_wp + (theta_fc - theta_wp)*1/3;
ETfactor = if (theta gt ETpoint, 1.0, 0.0);
ETfactor = if (theta lt ETpoint and theta ge theta_wp,(theta-theta_wp)/(ETpoint-theta_wp), ETfactor);
ETfactor = if (theta lt theta_wp, 0.0, ETfactor);

Kcrop = 1.05;
# FAO crop factor to account for specific crops or vegetation, 1.0 for grass
Ta = ETp * ETfactor * Coverm * Kcrop;
# actual transpiration (mm)
Ea = ETp * theta/theta_s * (1-Coverm);
#actual soil evaporation (mm)
Ea = if(landunit eq 8, 0, Ea);     #transportation (road network)
Ta = if(landunit eq 8, 0, Ta);     #transportation (road network)

ETa = Ea + Ta;
# ETa sum of the Evap and Transp
ETa = min(ETa, SoilMoisture);
# cannot be more than soil moisture present
# graphs with average and cumulative average ETa of all cells
report eta_tss = maptotal(ETa)/nrCells;
ETacum = ETacum + ETa;
report etacum_tss = maptotal(ETacum)/nrCells;


###################
###     Percolation  ###
###################
theta_e = (theta-theta_r)/(theta_s-theta_r);
Perc = if (theta_e gt 0, Ksat2*sqrt(theta_e)*sqr(1-(1-(theta_e**(1/m_param2)))**m_param2), 0);
# assume dH/dz = 1  percolation depends on unsaturated hydr conductivity
# based on Van Genuchten equation
Perc = min(Perc, SoilMoisture);
# cannot have more percolation than soil moisture
Perc = if(landunit eq 8, 0, Perc);
report perc_tss = maptotal(Perc)/nrCells;
```

```
# graph with average spatial percolation
percum = percum + Perc;
report perccum_tss = maptotal(percum)/nrCells;
# cumulative percolation

########################
###     new soil moisture    ###
########################
SoilMoisture = SoilMoisture + (Infil - ETa - Perc) * dt;
SoilMoisture = max(0, SoilMoisture);
SoilMoisture = if(landunit eq 8, 0, SoilMoisture);
# update soil moisture (mm) with rainfall and evapotranspiration
theta = SoilMoisture/unsatdepth;
# average soil moisture content (cm3/cm3) = (-)
theta = if (theta lt theta_r, theta_r, theta);
theta = if (theta gt theta_s2, theta_s2, theta);
# cannot be less than theta_r and more than porosity
# calc new soil moisture based on adjusted theta (mm)
SoilMoisture = theta * unsatdepth;

##########################
###    Groundwater balance   ###
##########################
# Gravity based flow: potential differences
# between GW surface in NS and EW directions
# Total flow in/out cell is:
# Darcy : Q = q*A = K sin(a)*(h*dx)
# A is wet cross section of the flow
# dQ = SUM [ (K * sin(a)*h*dx) ] EW and NS
# dQ is in m3/timestep and is added to the central cell
# Converted to height by division by the cell area
#NOTE: everything is in meters and meters/day

dx = celllength();
# set up basic directions for groundwater movement
ldd2 = ldd(2*mask); #south, row + 1
ldd4 = ldd(4*mask); #west, col - 1
ldd6 = ldd(6*mask); #east, col + 1
ldd8 = ldd(8*mask); #north, row - 1
z = (DEM-mapminimum(DEM)+1) - soildepth/1000;
# gravity potential equals dem of bedrock, soildepth is in mmm, convert to m
# assume more averaged (smooth) subsurface DEM over which GW flows
GWDepth = GWDepth + Perc/(theta_s2-theta+0.01);
GWDepth = min (GWDepth, soildepth);
# add percolation amount to GW depth (convert to height in mm)
h = GWDepth/1000;
# GW depth in mm, h = matric potential in m
H = h + z;
# total hydraulic potential in m
dHdL2 = sin(atan((upstream(ldd2, H)-H)/dx));
dHdL4 = sin(atan((upstream(ldd4, H)-H)/dx));
dHdL6 = sin(atan((upstream(ldd6, H)-H)/dx));
dHdL8 = sin(atan((upstream(ldd8, H)-H)/dx));
# sine of potential differences between central cell
# dH/dx = tan so atan(dH/dx) is angle
# and cells in 4 directions EW ans NS (in m)
h2 = max(h,upstream(ldd2, h));
h4 = max(h,upstream(ldd4, h));
h6 = max(h,upstream(ldd6, h));
h8 = max(h,upstream(ldd8, h));
```

```
  dQ = Ksat2/1000 * dx * (h2*dHdL2 + h8*dHdL8 + h4*dHdL4 + h6*dHdL6);
  # sum of all fluxes in m3/day, ksat in m/day, divide by 1000
  SumGWbefore = maptotal(h);
  # sum GW before movement
  h = h + dQ/(dx*dx);
  # add in/out flow to the cell in m
  h = max(0, min(h, soildepth/1000));
  # h must between 0 and soildepth: 0 < h < soildepth

### mass balance correction ###
  SumGWafter = maptotal(h);    # sum GW after the movement
  errorh = (SumGWbefore - SumGWafter)*mask;
  #total mass balance error in GW depth (before - after)
  wetcells = maptotal(scalar(h gt 0))*mask;
  # calc which cells have GW
  h = h + if(h gt 0, errorh/wetcells, 0);
  # smooth out the error over all wet cells
  h = max(0, min(h, soildepth/1000));
  # correct again: h must between 0 and soildepth: 0 < h < soildepth
  SumGWafter = maptotal(h);
  report error.tss = if (SumGWbefore gt 0.001,(SumGWbefore - SumGWafter)/SumGWbefore,0);
  # report any remaining error in the mass balance

  ########################################
  ###       adjust waterbalance components    ###
  ########################################
  # in the following a small in the top soil is taken that cannot
  # be saturated by the GW to avoid mass balance problems, so the
  # unsaturated zone does not disappear but is always "margin" or more
  # This is completely arbitrary!

    GWDepth = h*1000;
 # convert from m back to mm for comparison with the other fluxesin the model
    margin = 200;      # defined after calibration
   GWDepth = max(0, min(GWDepth, soildepth - margin));
   # confine groundwater between 0 and a dpeth of margin form the surface

   GWloss = if(GWDepth gt 1000, 0.07*GWDepth, 0);
   # subtract a loss when GWDepth is above a threshold
   GWloss = min(GWloss, GWDepth);
   # can not be more than there is
   GWDepth = GWDepth - GWloss/theta_s2;
   # lower the GW with GWloss each timestep
   baseflow = rivfrac*GWDepth*theta_s;
   unsatdepth = max(margin, soildepth - GWDepth);
   # dz is the dry nsoil above the groundwater, unsat zone
    theta = min(theta_s2, SoilMoisture/unsatdepth);
   # adjust the soilmoisture content to the new dry layer size

  ##################
  ###   streamflow    ###
  ##################
  #qpeakflowm3#
  Qpeakm3 = 0.001*(runoff)*cellarea();
  # convert runoff to m3 per day
  Qpeakm3=accuflux(LDD, Qpeakm3);
  report qpeak.tss = timeoutput(outlet, Qpeakm3);
  # output in m3/day to compare to measurements
```

```
baseflowm3 = 0.001*baseflow*cellarea();
# m3/day
fastbasem3 = 0.001*GWloss*cellarea();
# fast groundwater flow in m3/day
Qbasem3=accuflux(LDD, fastbasem3+baseflowm3);
report qbase.tss = timeoutput(outlet, Qbasem3);

totpeak = totpeak + maptotal(if(outlet eq 1,Qpeakm3, 0));
report Qpeakcum.tss = totpeak;
totbase = totbase + maptotal(if(outlet eq 1, Qbasem3, 0));
report Qbasecum.tss = totbase;

report Qsim.tss = timeoutput(outlet, Qpeakm3+Qbasem3);
# Qsim is the total simulated discharge
```

Appendix 2. Rainfall data in Code watershed

(Source : BKMG Stasiun Geofisika Yogyakarta)

Year **2010** Station : **PAKEM**

Date	Month												Yearly
	Jan	Feb	Mar	Apr	May	Jun	Jul	Aug	Sep	Oct	Nov	Dec	
1	25	8	0	0	0	0	10	0	14	0	20	3	
2	2	1	0	0	0	0	0	0	0	0	0	0	
3	0	0	0	0	3	0	2	0	0	0	37	6	
4	0	0	4	0	0	3	0	8	0	0	143	49	
5	0	4	2	0	0	2	0	2	0	10	2	2	
6	0	20	6	0	9	2	0	2	22	7	19	7	
7	0	31	1	3	0	0	0	0	35	1	17	73	
8	49	20	10	2	4	0	52	0	3	3	9	2	
9	51	11	9	3	8	58	51	4	9	55	3	7	
10	6	15	110	10	3	0	2	0	30	3	0	5	
11	50	3	9	22	12	0	0	0	88	0	0	9	
12	13	6	9	8	1	0	3	0	16	0	0	5	
13	16	52	1	3	48	67	4	0	20	0	6	30	
14	0	12	0	0	50	0	0	12	0	0	4	0	
15	49	10	0	0	69	16	0	0	0	10	31	19	
16	25	0	0	0	40	3	0	1	5	19	0	0	
17	10	18	25	0	6	3	0	0	9	5	0	0	
18	16	34	5	3	0	0	0	0	13	75	0	60	
19	52	43	31	2	1	12	0	0	3	15	0	12	
20	20	2	2	0	13	0	0	0	3	12	0	2	
21	11	0	21	0	4	9	0	0	0	2	12	12	
22	0	0	22	3	1	0	0	0	1	12	8	4	
23	20	18	30	0	0	0	0	40	27	9	22	0	
24	2	3	2	5	9	0	0	0	25	2	7	27	
25	39	0	6	7	0	1	0	58	2	17	18	0	
26	53	0	1	11	23	1	0	30	8	0	8	0	
27	14	0	8	0	12	0	13	3	0	34	4	44	
28	2	0	12	17	6	0	6	0	0	3	16	11	
29	40		5	3	12	0	0	0	0	17	4	26	
30	3		2	1	3	2	0	0	0	9	7	3	
31	14		49		2		0	15		6		30	
Maximum	53	52	110	22	69	67	52	58	88	75	143	73	143
Total rainfall	582	311	382	103	339	179	143	175	333	326	397	448	3718
Raindays	24	19	25	16	23	13	9	11	19	22	21	24	226
Rainfall (1-15)	261	193	161	51	207	148	124	28	237	89	291	217	
No data	0	0	0	0	0	0	0	0	0	0	0	0	
Rainfall (16-31)	321	118	221	52	132	31	19	147	96	237	106	231	
No data	0	0	0	0	0	0	0	0	0	0	0	0	

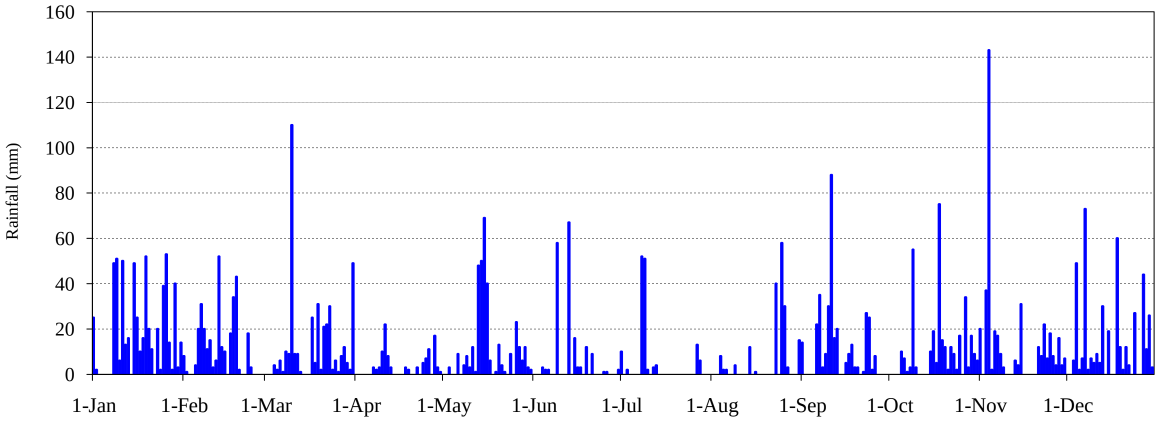

Year **2011** Station : **PAKEM**

Date	Jan	Feb	Mar	Apr	May	Jun	Jul	Aug	Sep	Oct	Nov	Dec	Yearly
	Month												
1	0	0	31	4	160	-	-	-	-	-	-	-	
2	3	1	0	1	7	-	-	-	-	-	-	-	
3	43	22	0	90	0	-	-	-	-	-	-	-	
4	27	13	0	0	98	-	-	-	-	-	-	-	
5	0	19	23	3	3	-	-	-	-	-	-	-	
6	8	6	10	0	90	-	-	-	-	-	-	-	
7	1	1	3	5	12	-	-	-	-	-	-	-	
8	0	6	0	3	3	-	-	-	-	-	-	-	
9	65	0	48	0	0	-	-	-	-	-	-	-	
10	18	11	1	3	0	-	-	-	-	-	-	-	
11	26	3	7	2	0	-	-	-	-	-	-	-	
12	0	5	10	9	0	-	-	-	-	-	-	-	
13	0	2	3	11	0	-	-	-	-	-	-	-	
14	0	0	4	4	40	-	-	-	-	-	-	-	
15	0	87	5	7	8	-	-	-	-	-	-	-	
16	7	3	0	19	22	-	-	-	-	-	-	-	
17	14	20	0	4	0	-	-	-	-	-	-	-	
18	80	15	12	0	10	-	-	-	-	-	-	-	
19	40	1	2	4	4	-	-	-	-	-	-	-	
20	0	0	91	4	23	-	-	-	-	-	-	-	
21	49	15	0	55	0	-	-	-	-	-	-	-	
22	19	1	0	30	0	-	-	-	-	-	-	-	
23	6	26	115	0	0	-	-	-	-	-	-	-	
24	38	0	3	6	0	-	-	-	-	-	-	-	
25	14	39	43	25	0	-	-	-	-	-	-	-	
26	30	19	3	0	0	-	-	-	-	-	-	-	
27	5	46	0	0	0	-	-	-	-	-	-	-	
28	6	11	9	0	0	-	-	-	-	-	-	-	
29	10		0	9	0	-	-	-	-	-	-	-	
30	1		2	15	0	-	-	-	-	-	-	-	
31	0		2		0		-	-		-		-	
Maximum	80	87	115	90	160	-	-	-	-	-	-	-	-
Total rainfall	510	372	427	313	480	-	-	-	-	-	-	-	-
Raindays	22	23	21	22	13	0	0	0	0	0	0	0	-
Rainfall (1-15)	191	176	145	142	421	-	-	-	-	-	-	-	
No data	0	0	0	0	0	15	15	15	15	15	15	15	
Rainfall (16-31)	319	196	282	171	59	-	-	-	-	-	-	-	
No data	0	0	0	0	0	15	16	16	15	16	15	16	

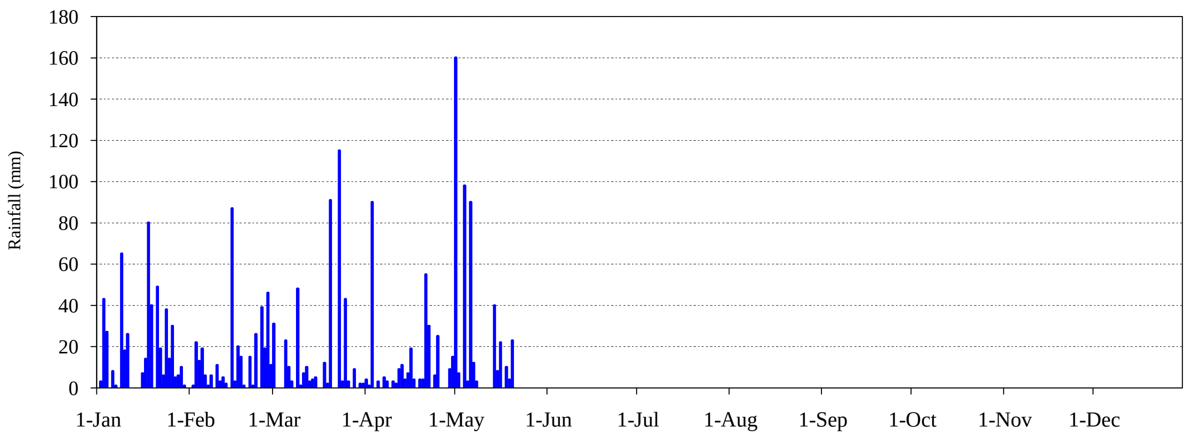

Appendix 3. Temperature, Solar radiation and relative humidity in Code watershed

Temperature in Code watershed of January 2010 – May 2011(oC)

Date	2010												2011				
	Jan	Feb	Mar	Apr	May	Jun	Jul	Aug	Sep	Oct	Nov	Dec	Jan	Feb	Mar	Apr	May
1	25.5	24.5	26.8	25.8	27.5	25.9	25.1	25.9	26.2	25.2	25.2	24.0	25.1	23.9	24.0	24.0	23.0
2	25.7	25.9	26.6	25.9	26.3	26.2	25.7	24.9	25.2	26.9	24.3	24.0	23.7	23.8	25.3	25.0	24.0
3	26.8	26.0	25.0	23.2	26.2	25.5	24.7	24.9	25.6	27.0	24.6	24.0	23.7	25.0	25.8	23.0	26.0
4	26.1	25.9	25.9	25.9	27.1	25.2	24.7	24.9	25.4	26.0	24.0	24.0	24.9	23.9	25.1	24.0	26.0
5	26.3	24.1	25.4	26.0	24.8	25.0	24.8	24.7	25.2	25.8	23.6	24.0	24.8	23.9	23.6	25.0	23.0
6	27.0	23.0	25.5	25.3	26.4	24.8	25.7	23.9	22.6	26.4	24.2	22.1	25.0	24.9	24.4	26.0	24.0
7	24.2	24.3	26.0	24.0	27.1	25.7	24.3	23.7	24.6	24.9	24.8	24.0	24.0	25.0	24.3	25.0	25.0
8	23.1	23.3	24.5	25.6	26.0	23.9	23.9	23.8	23.3	24.0	24.7	24.0	23.1	24.7	22.8	25.0	24.0
9	22.7	24.3	24.5	25.1	24.5	25.1	24.1	24.6	24.2	23.4	23.5	24.5	24.3	25.2	23.8	25.0	24.0
10	23.7	26.1	23.6	24.6	24.8	25.8	24.7	25.6	23.7	23.6	25.8	23.0	24.3	25.0	24.1	25.0	25.0
11	24.9	25.2	25.1	24.5	25.4	27.0	24.7	26.4	23.1	24.3	26.8	23.3	25.6	25.4	24.1	24.0	26.0
12	23.8	24.4	25.4	25.9	24.6	24.1	25.2	26.0	24.7	24.2	25.7	24.0	26.4	24.8	25.4	24.0	26.0
13	25.1	24.1	27.0	26.3	23.9	26.2	25.7	25.3	23.5	25.3	24.6	25.5	24.9	25.6	23.8	24.0	23.0
14	24.9	23.7	26.9	24.7	25.1	24.6	25.6	24.7	25.5	24.5	23.7	24.7	25.5	23.8	23.2	24.0	24.0
15	24.5	25.5	25.6	25.7	24.5	25.2	25.3	24.7	24.4	23.9	26.6	25.3	24.4	23.6	25.6	24.0	24.0
16	24.1	24.2	25.6	25.5	25.4	24.7	25.3	23.9	23.1	24.1	23.5	23.9	24.0	24.3	25.2	24.0	24.0
17	24.9	25.3	24.5	25.3	26.2	24.9	24.8	24.2	23.6	24.2	26.5	24.1	23.7	24.0	23.8	24.0	25.0
18	25.3	24.7	24.9	25.1	25.5	25.4	25.2	24.7	26.6	22.5	26.3	25.4	23.6	24.9	24.7	25.0	24.0
19	24.3	23.0	25.1	25.7	25.9	25.5	25.7	24.8	25.1	23.9	26.4	24.8	25.4	25.3	23.8	24.0	25.0
20	23.7	25.9	26.2	26.5	26.0	25.7	22.2	25.1	25.2	25.7	25.5	23.7	22.9	26.3	25.6	25.0	25.0
21	24.9	26.4	25.0	24.3	26.1	25.0	24.0	24.7	25.2	24.0	25.8	23.5	23.3	26.4	25.6	25.0	25.0
22	24.6	25.1	25.0	26.1	25.6	25.3	23.1	24.2	23.5	24.0	24.1	24.1	23.6	23.7	23.8	25.0	24.0
23	25.1	25.8	26.4	26.0	25.3	24.8	23.2	24.2	23.8	25.2	24.3	23.1	23.5	24.5	24.4	25.0	24.0
24	24.2	25.9	25.7	25.3	25.3	24.8	23.5	22.9	23.9	23.6	24.2	24.3	23.9	26.6	23.1	25.0	24.0
25	23.5	25.1	26.0	23.9	25.4	24.2	24.6	25.4	25.0	25.9	24.0	25.4	23.8	22.1	24.3	24.0	25.0
26	24.3	26.4	24.8	26.2	24.2	24.2	24.3	26.2	25.0	25.6	24.9	23.9	24.4	23.3	24.7	25.0	25.0
27	26.1	26.9	25.8	25.1	25.2	25.1	24.5	25.3	26.8	25.8	24.5	24.2	24.9	24.0	24.2	25.0	25.0
28	24.8	26.8	25.5	25.9	25.6	25.3	24.0	25.3	25.7	24.4	25.3	23.5	24.3	23.0	24.7	26.0	24.0
29	24.5		25.3	26.3	24.8	24.9	25.6	25.7	25.8	26.3	24.7	23.9	25.4		24.5	26.0	26.0
30	24.7		23.6	27.2	25.2	25.6	26.0	25.3	26.3	23.6	25.8	24.2	25.1		25.1	25.0	25.0
31	24.4		25.5		26.2		24.2	24.7		22.9		25.0	24.7		25.1		25.0
T Min	22.7	23.0	23.6	23.2	23.9	23.9	22.2	22.9	22.6	22.5	23.5	22.1	22.9	22.1	22.8	23.0	23.0
T Max	27.0	26.9	27.0	27.2	27.5	27.0	26.0	26.4	26.8	27.0	26.8	25.5	26.4	26.6	25.8	26.0	26.0
Total	768	702	789	763	792	756	764	771	742	767	748	747	756	687	758	740	762

Source : BMKG Stasiun Geofisika Yogyakarta

Solar radiation in Yogyakarta of January 2010 – May 2011(MJ/m2.day)

Date	2010												2011				
	Jan	Feb	Mar	Apr	May	Jun	Jul	Aug	Sep	Oct	Nov	Dec	Jan	Feb	Mar	Apr	May
1	71.1	47.6	67.5	63.4	76.3	50.8	36.0	137.7	56.5	28.7	38.5	34.2	40.9	25.6	34.2	33.9	27.5
2	72.9	78.7	71.7	61.1	59.4	56.5	56.5	51.5	45.1	49.2	33.4	34.2	35.8	33.3	48.4	40.1	26.9
3	71.8	78.9	45.1	4.2	67.5	31.1	30.0	51.5	61.0	60.9	36.2	34.2	46.3	49.2	54.4	22.1	46.7
4	63.9	89.9	46.1	68.7	66.8	44.5	39.8	51.5	42.6	49.9	21.6	34.2	61.4	39.9	47.5	29.6	48.9
5	75.9	52.8	53.7	59.1	27.6	37.5	32.5	48.4	39.6	45.9	0.3	34.2	43.0	25.0	29.6	55.5	16.9
6	143.7	30.8	51.9	7.2	61.6	30.5	38.4	35.7	24.8	49.0	2.0	4.7	46.9	39.2	34.0	54.5	32.1
7	56.4	89.7	68.7	35.4	62.6	32.6	38.0	37.6	40.0	26.4	22.8	37.8	24.4	45.9	41.2	47.5	32.6
8	47.2	9.9	81.2	66.8	47.6	24.9	34.6	39.6	24.0	46.1	29.7	35.3	29.5	38.7	31.8	40.8	19.8
9	45.7	57.3	59.7	44.8	41.5	37.8	41.0	40.5	40.3	36.2	20.4	39.9	38.8	46.4	22.5	35.1	40.6
10	48.3	86.1	36.4	39.6	39.3	49.1	38.4	47.9	35.4	53.0	52.3	27.3	38.3	47.8	37.7	37.7	51.7
11	66.9	51.3	68.0	43.3	36.8	64.1	48.1	48.6	29.0	66.3	58.4	21.8	48.9	51.7	39.7	35.3	28.6
12	54.8	49.5	58.1	52.4	25.0	33.7	52.9	60.1	52.1	63.5	22.5	34.3	63.2	42.8	47.1	34.3	33.7
13	64.8	40.4	83.7	60.9	26.7	56.1	48.5	45.9	34.5	50.5	18.3	44.2	33.7	53.6	28.3	55.9	21.3
14	79.9	38.3	64.1	37.0	40.7	43.6	52.5	35.6	61.3	36.0	29.6	44.1	46.1	32.3	37.5	45.9	22.3
15	77.8	65.8	64.5	58.9	32.2	37.4	42.1	40.3	31.8	28.1	49.7	52.3	54.8	28.2	62.0	42.0	26.9
16	58.5	40.9	54.1	58.2	52.8	34.7	54.5	27.0	39.1	22.9	33.9	35.9	39.8	48.1	56.8	42.9	44.8
17	76.4	63.9	49.3	3.5	46.8	31.5	25.2	35.1	46.1	35.5	55.0	38.4	44.7	51.5	36.1	35.2	48.8
18	85.9	48.5	68.3	49.4	37.2	46.5	41.8	47.0	52.3	24.0	46.0	55.9	43.3	42.0	36.8	56.0	31.4
19	60.3	29.1	59.5	40.7	43.1	43.0	101.4	52.0	31.6	37.8	40.3	48.0	43.5	62.0	46.7	45.4	36.6
20	49.1	81.9	78.7	66.0	53.6	63.4	4.7	54.2	42.7	56.2	46.8	31.2	28.8	62.8	47.2	46.5	41.4
21	49.1	62.4	53.0	38.7	53.1	58.4	45.8	46.8	48.1	33.8	46.4	30.0	41.2	61.7	47.7	49.9	45.0
22	66.8	56.7	70.5	55.8	35.2	64.7	35.6	34.4	32.3	29.0	37.0	34.9	30.0	25.0	36.7	39.7	38.7
23	77.4	71.6	75.9	38.9	36.5	36.3	56.7	24.0	50.2	51.8	25.7	25.4	36.2	29.5	39.4	26.9	49.3
24	58.9	49.6	75.2	35.9	38.3	29.0	50.1	34.6	30.0	33.0	36.8	53.6	41.0	80.1	39.0	28.8	54.6
25	43.9	56.8	80.1	38.8	47.4	28.1	37.7	53.0	48.4	48.5	36.6	56.6	37.8	6.6	44.6	44.4	52.2
26	53.8	65.4	58.7	69.2	27.3	34.1	29.5	50.6	37.5	51.9	34.0	37.9	34.7	27.0	36.5	36.5	40.6
27	81.3	70.3	61.6	46.5	52.8	47.3	36.2	53.6	49.2	45.7	34.8	40.2	36.4	31.4	42.9	41.4	51.1
28	58.3	66.4	68.3	60.7	51.5	40.9	24.0	64.1	48.8	34.1	40.1	31.0	25.6	23.6	39.0	39.8	48.8
29	58.6		51.9	59.7	42.1	39.4	48.0	59.1	55.7	47.0	45.5	23.2	54.2		47.3	41.5	42.6
30	79.2		30.3	72.7	38.8	47.7	64.8	54.2	51.1	5.2	99.8	35.2	44.7		50.3	38.7	26.2
31	62.8		44.5		54.3		47.1	44.0		21.7		39.5	42.0		48.3		40.1
Min	44	10	30	4	25	25	5	24	24	5	0	5	24	7	23	22	17
Max	144	90	84	73	76	65	101	138	61	66	100	57	63	80	62	56	55
Total	2061	1631	1900	1438	1422	1275	1332	1506	1281	1268	1094	1130	1276	1151	1291	1224	1169

Source : BMKG Stasiun Geofisika Yogyakarta

Relative humidity in Yogyakarta of January 2010 – May 2011 (%)

Date	2010												2011				
	Jan	Feb	Mar	Apr	May	Jun	Jul	Aug	Sep	Oct	Nov	Dec	Jan	Feb	Mar	Apr	May
1	77	82	79	80	75	83	84	65	78	82	78	84	82	85	76	86	91
2	76	79	79	77	81	83	79	84	78	69	84	84	91	82	69	79	90
3	75	78	87	88	80	89	86	84	72	71	87	84	89	75	68	88	77
4	78	81	79	79	75	90	84	84	79	78	90	84	84	81	76	81	79
5	76	91	83	81	85	90	84	83	84	84	88	84	86	78	84	79	93
6	70	96	87	81	84	85	82	79	95	78	87	98	85	81	81	75	89
7	87	91	83	87	81	84	90	76	84	85	81	88	88	83	81	81	86
8	93	97	80	83	86	92	91	82	90	86	86	85	90	80	91	82	89
9	95	92	87	84	89	83	88	80	85	86	91	83	84	83	86	86	84
10	90	82	91	93	90	72	91	80	91	77	80	91	89	82	87	81	78
11	84	88	86	91	88	74	88	72	95	70	70	91	80	78	86	85	83
12	90	89	82	84	91	88	87	74	86	71	76	89	74	82	78	84	85
13	80	90	74	82	95	76	81	86	92	77	79	84	81	74	78	84	89
14	76	92	73	89	92	90	81	84	79	84	87	81	78	89	84	86	89
15	81	82	77	85	94	85	80	83	85	88	77	80	78	89	74	87	86
16	87	93	83	86	90	90	79	87	91	87	90	88	78	84	75	85	86
17	80	89	88	87	89	88	83	85	92	88	77	82	85	87	86	87	81
18	80	92	87	84	91	85	80	81	80	92	80	75	91	83	85	80	87
19	90	96	89	81	89	82	75	77	88	88	76	78	79	81	88	84	81
20	91	77	83	75	86	81	85	79	85	80	82	86	91	73	82	83	86
21	83	74	88	89	83	74	77	81	85	86	79	88	89	73	77	85	79
22	85	82	88	80	89	73	78	88	91	91	89	85	87	88	84	88	81
23	84	80	84	85	91	80	73	87	89	84	88	88	87	81	83	87	75
24	89	79	86	86	89	78	76	91	90	89	87	76	82	76	89	86	73
25	91	86	83	89	90	84	81	85	81	79	88	73	86	96	87	86	75
26	88	81	88	80	95	84	87	82	84	81	86	82	84	90	83	84	76
27	73	77	81	87	86	84	91	79	73	84	86	80	84	87	85	81	74
28	87	78	85	82	86	82	92	75	82	87	85	90	87	86	82	79	75
29	86		87	82	91	83	82	74	79	78	88	88	76		82	82	76
30	86		90	80	90	80	78	81	77	89	78	88	74		79	85	80
31	89		79		82		79	86		91		80	76		79		81
Min	70.0	74.0	73.0	75.0	75.0	72.0	73.0	65.0	72.0	69.0	70.0	73.0	74.0	73.0	68.0	75.0	73.0
Max	95.0	97.0	91.0	93.0	95.0	92.0	92.0	91.0	95.0	92.0	91.0	98.0	91.0	96.0	91.0	88.0	93.0
Total	2597	2394	2596	2517	2703	2492	2572	2514	2540	2560	2500	2617	2595	2307	2525	2506	2554

Source : BMKG Stasiun Geofisika Yogyakarta

Appendix 4. Daily discharge data in Pogung

Daily Discharge (m^3/s)

Station	Pogung	River	Code
Station code	2-81-3-6	Area	29.05 km^2
Database number			
South	07°46'19"		
East	110°22'03"		

Rating curve
for H < 1 m , Q = 8.22 (H - -0.05) ^ 2.05
m , Q = 8.22 (H - -0.05) ^ 2.05

Extreme flow in the year

	WL	Q
max	2.44	53.34
min	0.21	0.52

Extreme flow before 2010

	Year	WL	Q
max	2006	2.39	54.40
min	2007	0.04	0.06

Year **2010**

Date	Jan	Feb	Mar	Apr	May	Jun	Jul	Aug	Sep	Oct	Nov	Dec
1	tad	tad	1.39	2.41	1.53	1.07	0.96	1.90	2.88	5.89	4.81	13.85
2	tad	1.39	1.39	2.07	1.39	0.96	1.13	1.83	2.24	5.89	4.07	12.99
3	tad	0.75	1.39	2.07	1.39	0.96	1.26	1.83	2.07	5.75	15.67	18.11
4	tad	0.75	1.32	1.60	1.46	1.07	1.19	2.07	1.98	4.07	43.73	12.57
5	tad	1.07	1.32	1.46	1.83	1.26	0.96	1.98	2.15	4.56	53.34	12.99
6	tad	4.31	1.39	1.53	1.83	0.96	0.96	2.07	9.81	5.61	33.35	14.52
7	tad	4.07	1.67	1.60	1.67	0.96	0.85	2.32	5.34	4.81	30.97	13.42
8	tad	2.07	2.07	1.60	1.67	2.98	1.83	2.15	7.89	4.68	30.64	13.42
9	tad	1.75	6.33	1.67	1.60	5.07	1.53	1.98	5.61	5.20	31.98	12.99
10	tad	1.90	4.19	2.15	1.90	1.32	1.53	1.90	4.19	4.81	31.98	12.57
11	tad	1.98	2.07	2.88	1.83	0.96	1.46	1.90	6.33	3.40	30.97	11.95
12	tad	2.98	1.67	1.83	2.41	3.09	1.39	1.90	8.91	2.98	31.98	11.34
13	tad	3.29	1.60	1.67	3.84	3.19	1.60	1.90	6.18	2.98	21.00	10.95
14	tad	2.60	1.46	1.60	7.24	1.60	1.60	1.90	4.56	2.88	16.87	10.18
15	tad	1.60	1.53	2.24	14.30	1.07	1.67	1.75	3.73	4.07	15.21	10.18
16	tad	1.75	1.83	2.32	4.81	0.85	1.83	1.90	4.56	4.56	15.44	10.56
17	tad	2.41	3.40	1.75	3.73	0.75	1.75	2.24	4.94	4.31	15.21	12.15
18	tad	3.96	2.69	1.60	2.88	0.65	1.83	1.98	3.51	18.36	15.91	10.95
19	tad	3.29	2.98	1.46	2.79	0.56	1.75	1.75	3.40	12.15	15.67	10.18
20	tad	2.41	2.41	1.46	2.69	0.60	1.90	1.75	2.69	6.77	15.67	11.54
21	tad	1.83	2.60	1.60	2.41	0.65	1.90	1.75	2.69	5.34	15.67	11.95
22	tad	1.32	2.60	1.90	1.83	0.65	1.90	1.67	3.51	7.08	11.74	9.81
23	tad	1.19	3.51	1.46	1.90	0.65	1.90	2.69	7.08	5.47	12.15	9.99
24	tad	1.26	2.98	1.39	4.56	0.70	1.90	4.68	7.40	7.72	9.44	8.73
25	tad	1.53	2.69	1.60	3.19	0.85	1.90	4.94	9.44	8.22	8.91	8.39
26	tad	1.46	3.19	1.75	6.77	0.85	2.07	4.19	8.22	5.61	8.39	9.81
27	tad	1.32	2.88	1.60	3.40	0.85	1.98	3.19	7.24	4.81	8.05	9.62
28	tad	1.26	2.79	1.60	2.24	0.85	2.07	2.79	6.47	4.94	8.05	9.08
29	tad		2.98	1.60	3.29	0.90	1.90	2.24	6.18	3.96	16.63	7.89
30	tad		3.29	1.53	2.15	0.96	1.90	2.15	6.03	3.62	24.99	8.39
31	tad		3.29		1.46		1.90	2.98		4.19		7.24
Maximum	tad	4.31	6.33	2.88	14.30	5.07	2.07	4.94	9.81	18.36	53.34	18.11
Monthly average	tad	2.06	2.48	1.77	3.10	1.26	1.62	2.33	5.24	5.64	19.95	11.24
Minimum	tad	0.75	1.32	1.39	1.39	0.56	0.85	1.67	1.98	2.88	4.07	7.24
Average (1-15)	tad	2.18	2.05	1.89	3.06	1.77	1.33	1.96	4.92	4.51	26.44	12.80
no data	15.00	1.00	0.00	0.00	0.00	0.00	0.00	0.00	0.00	0.00	0.00	0.00
Average (16-31)	tad	1.92	2.88	1.64	3.13	0.75	1.90	2.68	5.56	6.69	13.46	9.77
no data	16.00	0.00	0.00	0.00	0.00	0.00	0.00	0.00	0.00	0.00	0.00	0.00

tad : no data
WL : water level (m)
Q : discharge (m^3/s)

Daily Discharge (m^3/s)

Station	Pogung	River	Code
Station code	2-81-3-6	Area	29.05 km^2
Database number			
South	07°46'19"		
East	110°22'03"		

Rating curve
for H < 1 m , Q = 8.22 (H - -0.05) ^ 2.05
m , Q = 8.22 (H - -0.05) ^ 2.05

Extreme flow in the year

	WL	Q
max	4.18	158.08
min	0.21	0.52

Extreme flow before 2011

	Year	WL	Q
max	2006	2.39	54.40
min	2007	0.04	0.06

Year **2011**

Date	Jan	Feb	Mar	Apr	May	Jun	Jul	Aug	Sep	Oct	Nov	Dec
1	tad	1.83	3.29	1.67	tad	0.02	0.02	0.02	0.02	0.02	0.02	0.02
2	tad	2.41	2.24	1.39	tad	0.02	0.02	0.02	0.02	0.02	0.02	0.02
3	tad	2.98	1.67	2.88	1.75	0.02	0.02	0.02	0.02	0.02	0.02	0.02
4	12.15	4.19	1.75	2.69	1.46	0.02	0.02	0.02	0.02	0.02	0.02	0.02
5	8.39	5.07	2.32	1.60	6.93	0.02	0.02	0.02	0.02	0.02	0.02	0.02
6	8.22	4.31	3.96	1.39	2.41	0.02	0.02	0.02	0.02	0.02	0.02	0.02
7	7.08	4.07	2.50	1.32	2.07	0.02	0.02	0.02	0.02	0.02	0.02	0.02
8	10.18	3.96	3.51	1.32	1.46	0.02	0.02	0.02	0.02	0.02	0.02	0.02
9	11.95	3.73	3.62	1.19	1.46	0.02	0.02	0.02	0.02	0.02	0.02	0.02
10	13.42	3.96	2.79	0.90	0.96	0.02	0.02	0.02	0.02	0.02	0.02	0.02
11	8.05	3.84	2.41	0.85	0.75	0.02	0.02	0.02	0.02	0.02	0.02	0.02
12	6.93	4.43	2.32	1.01	0.65	0.02	0.02	0.02	0.02	0.02	0.02	0.02
13	6.33	3.29	1.83	1.32	1.19	0.02	0.02	0.02	0.02	0.02	0.02	0.02
14	6.18	3.62	2.15	1.60	1.83	0.02	0.02	0.02	0.02	0.02	0.02	0.02
15	6.18	4.07	2.15	2.15	1.53	0.02	0.02	0.02	0.02	0.02	0.02	0.02
16	7.40	5.34	1.90	1.53	0.02	0.02	0.02	0.02	0.02	0.02	0.02	0.02
17	7.24	4.31	2.41	1.32	0.02	0.02	0.02	0.02	0.02	0.02	0.02	0.02
18	7.08	4.31	2.60	1.39	0.02	0.02	0.02	0.02	0.02	0.02	0.02	0.02
19	5.07	4.07	7.40	1.39	0.02	0.02	0.02	0.02	0.02	0.02	0.02	0.02
20	6.77	4.07	5.75	1.53	0.02	0.02	0.02	0.02	0.02	0.02	0.02	0.02
21	5.75	4.07	3.96	2.24	0.02	0.02	0.02	0.02	0.02	0.02	0.02	0.02
22	3.96	3.51	8.73	1.83	0.02	0.02	0.02	0.02	0.02	0.02	0.02	0.02
23	4.81	2.24	4.19	1.53	0.02	0.02	0.02	0.02	0.02	0.02	0.02	0.02
24	4.56	1.90	5.20	1.53	0.02	0.02	0.02	0.02	0.02	0.02	0.02	0.02
25	4.94	2.69	3.84	tad	0.02	0.02	0.02	0.02	0.02	0.02	0.02	0.02
26	3.73	2.88	2.32	tad	0.02	0.02	0.02	0.02	0.02	0.02	0.02	0.02
27	3.09	2.41	2.07	tad	0.02	0.02	0.02	0.02	0.02	0.02	0.02	0.02
28	2.60	3.51	1.83	tad	0.02	0.02	0.02	0.02	0.02	0.02	0.02	0.02
29	2.32		1.67	tad	0.02	0.02	0.02	0.02	0.02	0.02	0.02	0.02
30	2.24		1.67	tad	0.02	0.02	0.02	0.02	0.02	0.02	0.02	0.02
31	1.98		1.60		0.02		0.02	0.02		0.02		0.02
Maximum	13.42	5.34	8.73	tad	6.93	0.02	0.02	0.02	0.02	0.02	0.02	0.02
Monthly average	6.38	3.61	3.09	tad	0.85	0.02	0.02	0.02	0.02	0.02	0.02	0.02
Minimum	1.98	1.83	1.60	tad	0.02	0.02	0.02	0.02	0.02	0.02	0.02	0.02
Average (1-15)	8.75	3.72	2.57	1.55	1.88	0.02	0.02	0.02	0.02	0.02	0.02	0.02
no data	3.00	0.00	0.00	0.00	2.00	0.00	0.00	0.00	0.00	0.00	0.00	0.00
Average (16-31)	4.60	3.49	3.57	tad	0.02	0.02	0.02	0.02	0.02	0.02	0.02	0.02
no data	0.00	0.00	0.00	6.00	0.00	0.00	0.00	0.00	0.00	0.00	0.00	0.00

tad : no data
WL : water level (m)
Q : discharge (m^3/s)
0.02 means that the discharge unmeasured at the moment

Appendix 5. Distribution Fitting Test using EasyFit 5.5 on Rainfall Data 1984 -2010

#	Distribution	Kolmogorov Smirnov		Anderson Darling		Chi-Squared	
		Statistic	Rank	Statistic	Rank	Statistic	Rank
1	Chi-Squared	0.27197	25	12.08	29	17.067	27
2	Chi-Squared (2P)	0.14388	15	0.36433	13	0.58092	17
3	Exponential	0.40321	28	4.867	27	1.323	24
4	Exponential (2P)	0.34609	26	4.5898	25	9.1372	26
5	Gamma	0.12203	6	0.30791	8	0.11476	4
6	Gamma (3P)	0.13231	13	0.28328	6	0.18198	6
7	Gen. Extreme Value	0.12202	5	0.27124	3	0.33963	11
8	Gen. Gamma	0.12335	7	0.3252	11	0.10916	2
9	Gen. Gamma (4P)	0.13096	12	0.28455	7	0.18364	7
10	Gen. Pareto	0.15382	18	4.3099	23	N/A	
11	**Gumbel Max**	**0.10168**	**1**	**0.31663**	**9**	**0.09633**	**1**
12	Gumbel Min	0.19378	24	1.6828	22	0.95248	21
13	Inv. Gaussian	0.10417	3	0.45292	16	0.60824	19
14	Inv. Gaussian (3P)	0.15751	20	0.36338	12	1.2139	22
15	Log-Gamma	0.13405	14	0.62302	19	0.38603	14
16	Log-Logistic	0.16543	22	0.74318	20	0.36895	13
17	Log-Logistic (3P)	0.10333	2	0.20112	1	0.3548	12
18	Log-Pearson 3	0.16965	23	4.4729	24	N/A	
19	Lognormal	0.12632	8	0.49662	17	0.58125	18
20	Lognormal (3P)	0.12995	10	0.27286	4	0.18617	8
21	Normal	0.15563	19	0.42123	15	0.52755	16
22	Pareto	0.44851	29	7.9886	28	2.2348	25
23	Pareto 2	0.40049	27	4.8229	26	1.2504	23
24	Pearson 5	0.16223	21	0.94212	21	0.90442	20
25	Pearson 5 (3P)	0.12906	9	0.26908	2	0.1877	10
26	Pearson 6	0.12196	4	0.32114	10	0.11178	3
27	Pearson 6 (4P)	0.1302	11	0.27545	5	0.18712	9
28	Student's t	0.9992	30	210.89	30	N/A	
29	Weibull	0.14938	17	0.50331	18	0.40171	15
30	Weibull (3P)	0.14756	16	0.38678	14	0.17482	5

Appendix 6. Bankfull Discharge in Code watershed

No. Sta	Bankfull Discharge (m3) 2011	2007	No. Sta	Bankfull Discharge (m3) 2011	2007
1	61.31	118.01	26	304.6	534.1
2	163.58	212.06	27	112	313.1
3	14.5	60.1	28	53.61	99.14
4	38.48	111.36	29	128.26	241.88
5	87.61	240.1	30	120.95	280.94
6	2.51	16.55	31	76.5	209.37
7	187.9	440.72	32	48.77	181.16
8	46.82	95.03	33	45.87	201.18
9	79.22	95.87	34	86.05	415.92
10	77.38	165.3	35	47.92	127.01
11	238.75	293.67	36	38.49	177.61
12	117.24	175.92	37	14.91	149.15
13	94.71	227.1	38	94.77	148.87
14	87.43	175.76	39	139.38	441.98
15	70.24	77.69	40	111.73	270.92
16	33.73	59.18	41	58.91	107.81
17	388.99	417.14	42	7.69	55.38
18	165.59	229.31	43	14.84	47.97
19	48.91	151.11	44	4.19	21.59
20	57.57	145.41	45	277.66	621.93
21	195.89	203.67	46	681.86	813.22
22	207.32	642.71	47	382.97	651.28
23	246.27	517.11	48	337.78	598.04
24	34.09	182.38	49	274.2	391.76
25	83.33	168.71	50	275.49	542.14

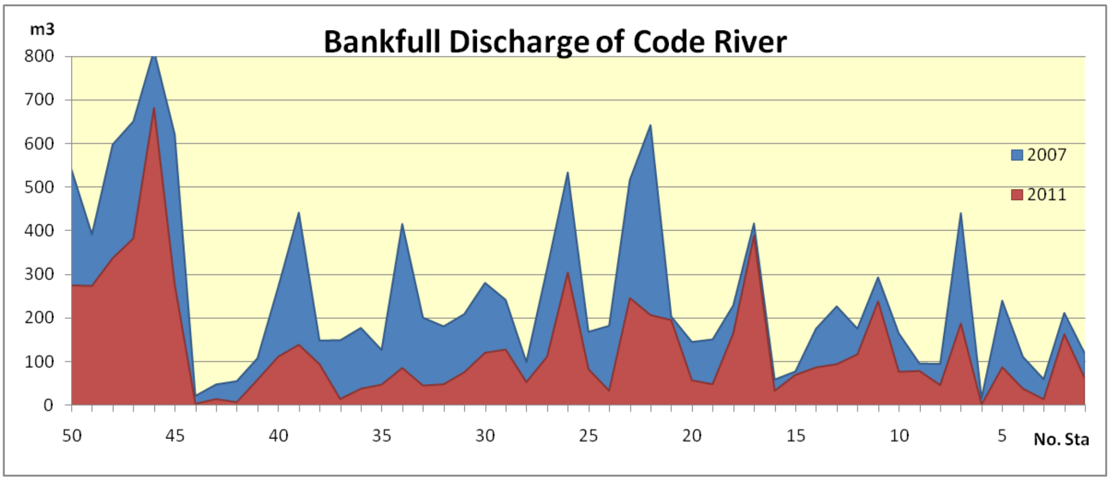

Source : Widiyanto (2007) and Rahayu (2011)

Appendix 7. Calculation of natural unit hydrograph

Hour	Water Level (m)				Discharge (m3/s)			
	3-Jan-11	9-Jan-11	19-Mar-11	22-Mar-11	3-Jan-11	9-Jan-11	19-Mar-11	22-Mar-11
1st	1.10	0.80	0.46	0.71	9.085	4.558	1.322	3.507
2nd	1.14	0.85	0.58	0.85	9.808	5.202	2.237	5.202
3rd	1.19	0.90	0.80	1.00	10.753	5.891	4.558	7.400
4th	1.29	0.92	1.34	1.50	12.776	6.179	13.854	17.607
5th	1.40	1.00	2.15	2.05	15.207	7.400	37.620	34.040
6th	1.70	1.05	2.88	1.85	22.946	8.220	69.348	27.427
7th	2.96	1.10	2.40	1.65	73.426	9.085	47.376	21.544
8th	2.10	1.44	2.00	1.50	35.807	16.146	32.318	17.607
9th	1.70	2.46	1.60	1.30	22.946	49.889	20.186	12.988
10th	1.50	2.00	1.20	1.10	17.607	32.318	10.947	9.085
11th	1.40	1.70	1.10	0.95	15.207	22.946	9.085	6.623
12th	1.35	1.38	1.05	0.91	14.075	14.749	8.220	6.034
13th	1.30	1.34	1.00	0.85	12.988	13.854	7.400	5.202
14th	1.25	1.29	0.95	0.83	11.945	12.776	6.623	4.939
15th	1.24	1.24	0.90	0.78	11.742	11.742	5.891	4.312
16th	1.23	1.19	0.87	0.75	11.541	10.753	5.473	3.957
17th	1.21	1.14	0.84	0.72	11.143	9.808	5.070	3.617
18th	1.20	1.12	0.83	0.70	10.947	9.443	4.875	3.399
19th	1.19	1.10	0.80	0.68	10.753	9.085	4.558	3.188
20th	1.17	1.08	0.78	0.65	10.370	8.733	4.312	2.885
21st	1.16	1.06	0.75	0.62	10.181	8.389	3.957	2.597
22nd	1.15	1.04	0.72	0.60	9.994	8.052	3.617	2.413
23rd	1.14	1.02			9.864	7.722		
24th	1.14				9.808			
25th	1.14				9.753			

Hour	3-Jan-11	9-Jan-11	19-Mar-11	22-Mar-11	Average
1st		4.5577			1.1394
2nd		5.2024			1.3006
3rd	9.0847	5.8909	1.3215		4.0743
4th	9.8084	6.1785	2.2369		4.5559
5th	10.7529	7.3995	4.5577	3.5070	6.5543
6th	12.7757	8.2200	13.8542	5.2024	10.0131
7th	15.2074	9.0847	37.6202	7.3995	17.3280
8th	22.9464	16.1455	69.3480	17.6066	31.5116
9th	73.4264	49.8892	47.3763	34.0395	51.1829
10th	35.8069	32.3179	32.3179	27.4271	31.9675
11th	22.9464	22.9464	20.1861	21.5436	21.9056
12th	17.6066	14.7492	10.9472	17.6066	15.2274
13th	15.2074	13.8542	9.0847	12.9879	12.7835
14th	14.0752	12.7757	8.2200	9.0847	11.0389
15th	12.9879	11.7420	7.3995	6.6232	9.6882
16th	11.9452	10.7529	6.6232	6.0338	8.8388
17th	11.7420	9.8084	5.8909	5.2024	8.1609
18th	11.5406	9.4430	5.4726	4.9393	7.8489
19th	11.1432	9.0847	5.0700	4.3120	7.4025
20th	10.9472	8.7335	4.8746	3.9566	7.1280
21st	10.7529	8.3894	4.5577	3.6168	6.8292
22nd	10.3698	8.0524	4.3120	3.3989	6.5333
23rd	10.1808	7.7224	3.9566	3.1880	6.2620
24th	9.9937		3.6168	2.8846	4.1238
25th	9.8638			2.5967	3.1151
26th	9.8084			2.4133	3.0554
27th	9.7531				2.4383

Appendix 8. Infiltration rate of post eruption in Code watershed

Code	Lat	Long	Landcover	Texture			Texture	BOD	COD	Infiltration rate	FC (%)	WP (%)
				Sand	Silt	Clay						
A	431039	9143756	Built-up land	86	11	3	Loamy Sand	0.52	0.30	0.360	6.5	1.4
B	432091	9145333	Built-up land	78	17	4	Loamy Sand	2.32	1.34	0.859	10.2	3.3
C	432532	9145134	Mixed rangeland	74	22	4	Loamy Sand	0.88	0.51	0.580	9.9	2.5
D	432453	9144879	Built-up land	74	22	4	Loamy Sand	0.88	0.51	0.320	9.9	2.5
E	431775	9145793	Cropsland and pasture	82	12	6	Loamy Sand	1.22	0.71	0.228	9.5	3.7
F	433024	9146145	Mixed rangeland	79	19	2	Loamy Sand	1.36	0.79	0.449	8.1	1.4
G	433274	9146732	Built-up land	82	16	2	Loamy Sand	0.89	0.52	0.424	7.1	1.1
H	432271	9147787	Built-up land	61	37	2	Sandy Loam	0.50	2.03	0.680	14.3	3.1
I	433220	9148375	Cropsland and pasture	71	24	5	Sandy Loam	1.98	1.15	0.168	12.1	3.9
J	432877	9150174	Built-up land	69	27	4	Sandy Loam	1.88	1.09	0.140	12	3.2
K	433829	9150663	Cropsland and pasture	48	38	14	Loam	2.07	1.20	0.420	22	9.4
L	433313	9151661	Mixed rangeland	76	20	4	Loamy Sand	2.60	1.51	0.500	10.9	3.5
M	433244	9152616	Mixed rangeland	83	12	5	Loamy Sand	3.87	2.25	0.907	11.1	4.9
N	434197	9152682	Built-up land	77	21	2	Loamy Sand	0.94	0.55	0.560	8.2	1.2
O	434249	9152940	Cropsland and pasture	83	12	5	Loamy Sand	3.87	2.25	0.079	11.1	4.9
P	434717	9153214	Cropsland and pasture	81	14	5	Loamy Sand	1.88	1.09	1.559	9.7	3.6
Q	434881	9154673	Mixed rangeland	69	26	5	Sandy Loam	2.20	1.27	0.879	12.8	4
R	436270	9156195	Cropsland and pasture	62	31	7	Sandy Loam	2.40	1.39	0.480	15.5	5.4
S	433518	9154379	Cropsland and pasture	63	32	5	Sandy Loam	3.87	2.24	1.079	15.5	5
T	434080	9153326	Built-up land	77	21	2	Loamy Sand	0.94	0.55	1.159	8.2	1.2
U	434801	9157022	Mixed rangeland	80	17	3	Loamy Sand	2.28	1.32	0.100	9.2	2.6
V	435308	9158404	Mixed rangeland	74	24	2	Loamy Sand	4.07	2.36	0.999	11.8	3.3
W	435991	9160801	Evergreen forest land	56	39	5	Sandy Loam	4.64	2.69	0.247	18	5.5
X	435654	9160186	Evergreen forest land	81	18	1	Loamy Sand	4.12	2.39	0.700	11.7	5
Y	436763	9160995	Evergreen forest land	77	22	1	Loamy Sand	4.45	2.58	1.299	12.8	5.2
Z	438597	9161624	Built-up land	78	19	3	Loamy Sand	0.34	0.20	0.879	8.1	1.5
AA	436750	9161014	Evergreen forest land	56	39	5	Sandy Loam	4.64	2.69	0.402	18	5.5
AB	436573	9160774	Mixed rangeland	77	22	1	Loamy Sand	4.45	2.58	0.140	12.8	5.2
AC	436186	9158965	Mixed rangeland	81	18	1	Loamy Sand	4.12	2.39	0.939	11.7	5

Source : Field measurement and Laboratory analysis by BPTP Yogyakarta

Appendix 9. Infiltration rate on near Code watershed (Noordianto, 2005)

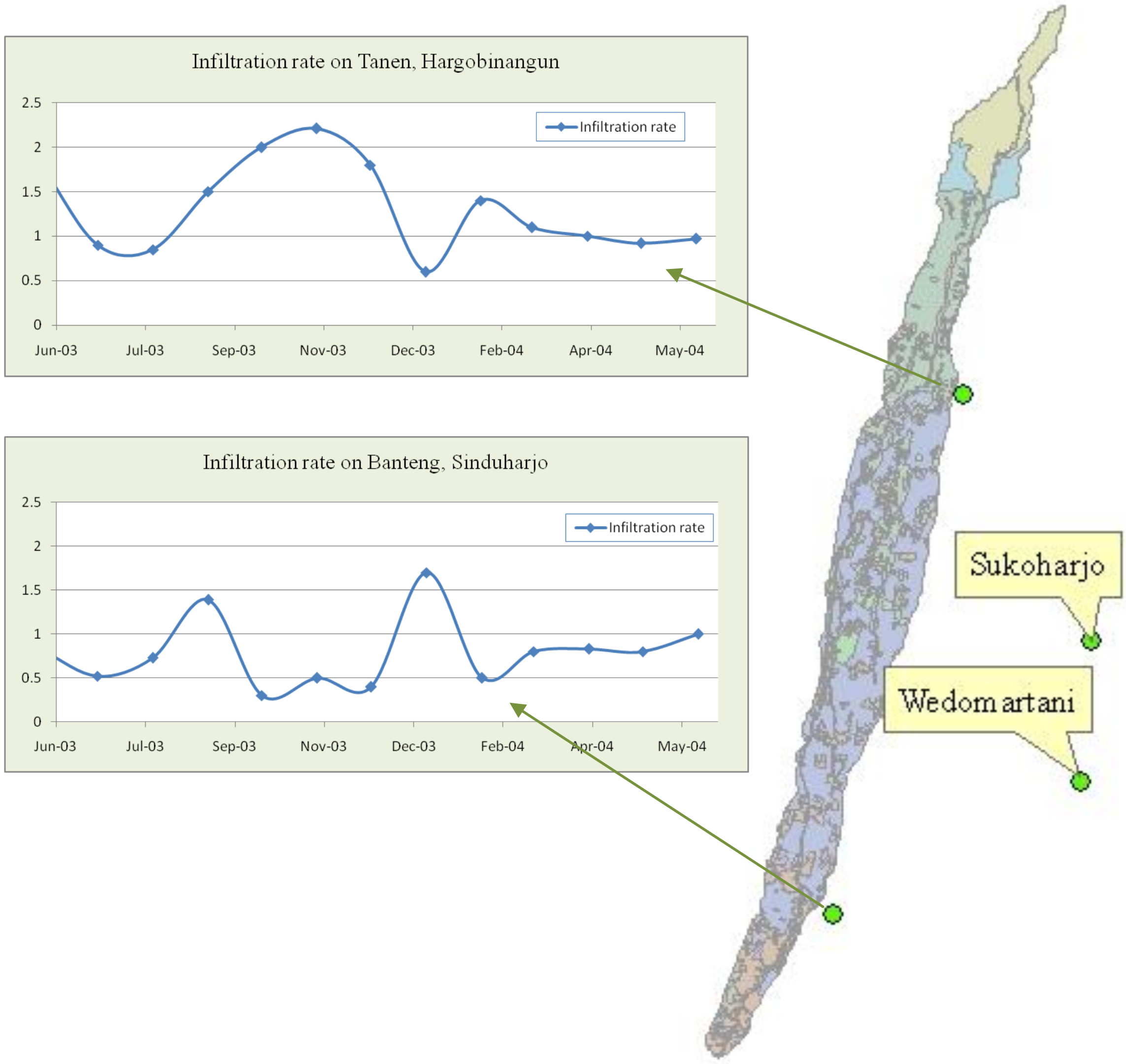

Infiltration Rate (cm/min)	Location			
	Tanen*	Banteng*	Sukoharjo	Wedomartani
Maximum Infiltration rate	2.21	1.70	2.26	1.23
Minimum Infiltration rate	0.94	0.38	0.214	0.58
Average Infiltration rate	1.38	0.79	0.67	0.81

*) the infiltration rate near Code watershed (Noordianto, 2005)

Infiltration rates were measured every three weeks during July 2003 – June 2004. Double ring infiltrometer was employed to measure the rate and calculation using Horton method. the objectives of the research is to determine groundwater recharge (Noordianto, 2005).

Appendix 10. Student t-test for soil properties of pre and post eruption

Paired Samples Statistics

		Mean	N	Std. Deviation	Std. Error Mean
Pair 1	Pre_Pore	43.26	6	7.19	2.94
	Post_Pore	43.46	6	1.55	0.63
Pair 2	Pre_Ksat	22.94	6	13.84	5.65
	Post_Ksat	94.02	6	7.09	2.89
Pair 3	Pre_FC	21.55	6	3.06	1.25
	Post_FC	11.82	6	2.05	0.84
Pair 4	Pre_WP	11.75	6	2.59	1.06
	Post_WP	3.69	6	0.98	0.40

Paired Samples Correlations

		N	Correlation	Sig.
Pair 1	Pre_Pore & Post_Pore	6	.487	.327
Pair 2	Pre_Ksat & Post_Ksat	6	-.441	.381
Pair 3	Pre_FC & Post_FC	6	-.077	.885
Pair 4	Pre_WP & Post_WP	6	.167	.752

Paired Samples Test

		Paired Differences					t	df	Sig. (2-tailed)
		Mean	Std. Deviation	Std. Error Mean	95% Confidence Interval of the Difference				
					Lower	Upper			
Pair 1	Pre_Pore - Post_Pore	-0.19	6.58	2.69	-7.10	6.71	-0.07	5	.950
Pair 2	Pre_Ksat - Post_Ksat	-71.07	18.12	7.40	-90.10	-52.06	-9.61	5	.000
Pair 3	Pre_FC - Post_FC	9.73	3.81	1.56	5.73	13.73	6.25	5	.002
Pair 4	Pre_WP - Post_WP	8.06	2.61	1.07	5.32	10.81	7.53	5	.001

Pair 1 --> Ho: The difference between the means is equal to 0.
Ha: The difference between the means is different from 0.
As the computed p-value is greater than the significance level alpha=0.05,
one cannot reject the null hypothesis Ho.

Pair 2,3,4 --> Ho: The difference between the means is equal to 0.
Ha: The difference between the means is different from 0.
As the computed p-value is lower than the significance level alpha=0.05,
one should reject the null hypothesis Ho, and accept the alternative hypothesis Ha.

Appendix 11. Statistical test of calibrated model using XLSTAT 2011, 5.01

- Model Pre-eruption (February – December 2010)

Summary statistics:

Variable	Observations	Obs. with missing data	Minimum	Maximum	Mean	Std. deviation
model_pre	333	0	37521.400	2956920.000	332113.985	360386.389
Measure_pre	333	0	48493.248	4608867.487	446395.629	576311.743

t-test for two independent samples / Two-tailed test:
95% confidence interval on the difference between the means:
] -187420.08 , -41143.20 [

Difference	-114281.64
t (Observed value)	-3.07
|t| (Critical value)	1.96
DF	664
p-value (Two-tailed)	0.002
Alpha	0.05

Test interpretation:
Ho: The difference between the means is equal to 0.
Ha: The difference between the means is different from 0.
As the computed p-value is lower than the significance level alpha=0.05,
one should reject the null hypothesis Ho, and accept the alternative hypothesis Ha.
The risk to reject the null hypothesis Ho while it is true is lower than 0.22%.

- Model Pre-eruption (February – October 2010)

Summary statistics:

Variable	Observations	Obs. with missing data	Minimum	Maximum	Mean	Std. deviation
model_pre	269	0	37521.400	1701530.000	286287.221	311160.848
Measure_pre	269	0	48493.248	1586434.247	244723.399	192876.358

t-test for two independent samples / Two-tailed test:
95% confidence interval on the difference between the means:
] -2283.42 , 85411.07 [

Difference	41563.82
t (Observed value)	1.86
|t| (Critical value)	1.96
DF	536
p-value (Two-tailed)	0.06
alpha	0.05

Test interpretation:
Ho: The difference between the means is equal to 0.
Ha: The difference between the means is different from 0.
As the computed p-value is greater than the significance level alpha=0.05,
one cannot reject the null hypothesis Ho.
The risk to reject the null hypothesis Ho while it is true is 6.31%.

- Model Post-eruption (January – May 2011)

Summary statistics:

Variable	Observations	Obs. with missing data	Minimum	Maximum	Mean	Std. deviation
model_post	124	0	82325.1	1319350.0	323433.086	268278.779
measure_post	124	0	56143.7	1159266.2	304724.476	213283.406

t-test for two independent samples / Two-tailed test:
95% confidence interval on the difference between the means:
] -41913.39 , 79330.61 [

Difference	18708.61
t (Observed value)	0.61
|t| (Critical value)	1.97
DF	246
p-value (Two-tailed)	0.54
alpha	0.05

Test interpretation:
Ho: The difference between the means is equal to 0.
Ha: The difference between the means is different from 0.
As the computed p-value is greater than the significance level alpha=0.05,
one cannot reject the null hypothesis Ho.
The risk to reject the null hypothesis Ho while it is true is 54.38%.